Enhanced transcription of the IFN-alpha inducible gene IFITM3 by means of dynamic promoter demethylation in the presence of the TGF-beta inducible small calcium binding protein S100A2

Inauguraldissertation

zur

Erlangung der Würde eines Doktors der Philosophie

vorgelegt der

Philosophisch-Naturwissenschaftlichen Fakultät

der Universität Basel

von

RACHEL WOODWARD SCOTT

aus

Widnau, SG

Basel, 2010

Genehmigt von der Philosophisch-Naturwissenschaftlichen Fakultät

auf Antrag von

Prof. Dr. Ulrich Certa

Prof. Dr. Christoph Dehio

Prof. Dr. Primo Schär

Basel, den 25. Mai 2010

Prof. Dr. Eberhard Parlow

Dekan

“Quidquam recipitur ad modum recipientis recipitur.”

Thomas von Aquin

i. Acknowledgements

First of all I want to express my gratefulness to the country I live in. Never before has it been possible for a woman to pursue her passion exploring the depths of knowledge and never before has it been so affordable to contribute to the world of science as it has today and here. Thanks to all the pioneers in this field of improvement of the right of every person to attend schools and universities.

My warmest thanks to Prof. Dr. Ulrich Certa who has guided me through the valleys and hills of the last couple of years. Having an open door at all times he encouraged my explorative work and cheered me up in times of trouble. His introduction into science both in performance as well as in writing has left a high impact with me. Since he thoroughly attached great importance to the professional handling of GCP thinking out of the box became even more substantial in working with him and extended my horizon way beyond the laboratory. Thank you very much for you mentorship.

My appreciation goes to Dr. Stefan Foser who initiated this work.

Thanks also to Dr. Thomas Singer for his encouragement throughout my work and thanks to F. Hoffmann-La Roche Ltd. for funding my work over the last four years.

Let me also thank Prof. Dr. Christoph Dehio for his support as the faculty member and his chaperonage of my thesis and special thanks to Prof. Dr. Primo Leo Schär for his valuable scientific inputs at all times.

Without her competent guidance in the laboratory throughout the first couple of month of my work and her patience in answering any open question I most likely would have spent an extra couple of years on my work. My upmost thank to Yvonne Burki.

Special thanks goes to Fredy Siegrist who somehow always knew everything about anything one can imagine. Without our scientific and non-scientific conversations life in 90/ 519 would have been completely secluded.

Upmost thank to Dr. Laura Burleigh and Dr. Sylvia Kiese for proofreading my manuscript and teaching me the ways of the English language.

Of course all my thanks to the whole Certa laboratory both the MML and the NCS. Dr. Sylvia Schreiber, Adriana Ille, Ursula Nelboeck-Hochstetter, Inga Redwanz, Monika Wilhelm-Seiler, Alexandra Gerber, Sonja Fellert, Erich Kueng, Judith Knehr,

Morgane Ravon, Susanne Fischer, Peter Noy, Dr. Cristina Bertinetti-Lapatki, Dr. Jean-Christophe Hoflack, Monika Haiker and Nicholas Flint. Also special thanks to everyone else at F. Hoffmann-La Roche Ltd. and outside the company, Dr. Laura Suter-Dick, Dr. Stefan Platz, Dr. Christian Czech, Dr. Adrian Roth, Christine Zihlmann, Karen Schad, Dr. Radina Kostadinova, Dr. Stefan Kustermann, Dr. Markus Schmitz, Michel Erhart, Julie Vargas, Alain Lautenschlager, Yolande Lang, Dr. Claas Meyer, Dr. Daniel Breustedt, Dr. Antonio Iglesias, Krisztina Oroszlan-Szovik, Dr. Bernd Bohrmann, Dr. Heather Hinton, Dr. Tobias Manigold, Dr. Michelle Browner, Prof. Dr. Claudia Taubenberger, Prof. Dr. Christoph Moroni, Stefan Weis, Dr. Patrick Urfer, Dr. Christoph Kunz, Sylvia Hoffmann, Prof. Dr. Peter Miny and many more. Please rest assure, I thank every single one of you, for the one good idea in order to successfully perform an experiment, for the coffee break and the lunch we spent together, for the proof reading of a manuscript, the suggestions in designing experiments, the good laugh and once in a while even the consolation. Thanks for your companionship throughout this amazing time.

And of course my deepest gratitude goes to my Mom and Dad who always encouraged me to reach for the highest. Thanks for their trust in me their support and their love for me.

Thanks to my family and friends, so many of them who always supported me at all times. Even when I got cranky and upset, or simply just almost too occupied; thanks for being there for me.

And at last thanks to my heavenly Father for his guidance in every step I take.

Dedicated to Life.

ii. Abstract

In human melanoma cell lines, the calcium binding protein S100A2 augments the antiproliferative activity of interferon-alpha (IFNα) by an unknown mechanism. I show by microarray profiling that recombinant over-expression of S100A2 upregulates the expression of a subset of IFNα response genes beyond the maximal cytokine inducible level including IFITM3, a gene with documented antiproliferative activity. I have chosen IFITM3 as chromosomal IFNα response reporter gene in a model system consisting of two human melanoma cell lines ME15 and D10 described previously (Brem, Oraszlan-Szovik et al. 2003). In ME15 cells IFITM3 expression is strictly IFNα dependent whilst it is constitutively expressed in the IFNα resistant D10 cells. It was shown that S100A2 is sufficient to restore IFNα sensitivity in D10 (Foser, Redwanz et al. 2006) and I show by indirect immunofluorescence cytoplasmic localization of S100A2, which eliminates a direct function as a transcriptional enhancer of IFITM3 expression and other antiproliferative genes. I show that treatment of ME15 melanoma cells with the demethylating agent 5-aza-2'deoxycytidine (DAC) results in a significant increase of IFITM3 expression following IFNα stimulation suggesting a DNA methylation mediated mechanism. Based on bisulfite sequencing of the IFITM3 core promoter, I show that D10 cells exhibit hypomethylation and I demonstrate that S100A2 is required for kinetic and reversible IFNα induced CpG demethylation in ME15 cells. Since p53 signaling is not functional in D10 cells I propose an indirect mechanism of methylation that involves p53 controlled signaling pathways.

Table of Contents

1. INTRODUCTION

1.1. INTERFERON

1.1.1. History of Interferon

Interferon was discovered 50 years ago as a host-derived interference activity induced by heat-inactivated viral particles (Isaacs and Lindenmann 1957). The advent of a novel technique termed “high performance liquid chromatography” enabled purification of interferon from virus-infected leukocytes 20 years after its discovery (Rubinstein, Rubinstein et al. 1978). In the 1980s advances in technology provided new possibilities in research but gene cloning was a difficult task compared to today. A combination of peptide sequencing and differential cloning finally allowed isolation of the first recombinant gene encoding the human interferon-α (Maeda, McCandliss et al. 1980; Borden, Sen et al. 2007). Since then, several additional interferons have been discovered and are classified in two categories, namely type I and type II interferons, that signal through distinct pathways but induce similar responses such as immune defense or antiviral activity (Stark, Kerr et al. 1998).

1.1.2. Type I And Type II Interferons

A hallmark of interferon type I and type II activity is the induction of anti-proliferative activity coupled to transcriptional activation of target genes. The major role of type I and type II interferons in the cell, as well as upon excretion into the extracellular lumen, is their antiviral activity. Interferons are induced upon viral infection but it was also noticed that interferon can be induced by bacteria and protozoa (Akira, Uematsu et al. 2006). Therefore interferons execute vital activities in the maintenance of the healthy organism.

The type I interferons are made up of the IFNαs and IFNβs, both located on chromosome 9 in the human genome, in addition to IFNω, IFNε, IFNκ, IFNδ and IFNτ. All these interferons share structural similarities (helical cytokine family) (Decker, Muller et al. 2005), contain 165 to 200 amino acids and are mostly non-glycosylated (Borden, Sen et al. 2007). The IFNα protein family consists of 13 functional homologues and one pseudogene. Members of the type I interferon family are involved not only in viral combat but also in cell differentiation and proliferation control (Henco, Brosius et al. 1985).

The only type II interferon is IFNγ, which is located on chromosome 12 (Henco, Brosius et al. 1985). This interferon is produced in natural killer cells or in activated T cells upon viral and bacterial assault. IFNγ is conserved throughout many species and loss of IFNγ has been shown to provoke autoimmune disorders. The pleiotropic functions that IFNγ exhibits made it difficult to introduce in clinical treatments, nevertheless IFNγ is absolutely indispensible in the innate and adaptive immune responses (Miller, Maher et al. 2009).

Interleukin 28 and interleukin 29 have recently been recognized as a third class of interferons: the lambda interferons (Borden, Sen et al. 2007). In contrast to type I and II these interferons have introns and up to five exons (Uze and Monneron 2007). Located on chromosome 19, the IFNλs activate similar pathways to IFNα and IFNβ but use a different set of receptors (Uze and Monneron 2007). IFNλ receptors exhibit selective expression, in contrast to the IFNα/β receptors which are constitutively expressed to guarantee immediate signal transduction upon viral threat.

1.1.3. Interferon-alpha Signaling

The interferon pathway is one of the most studied signaling pathways (figure 1). Following virus-induced expression of IFNα the cytokine is excreted and binds to the type I interferon receptor 1 (IFNAR1), promoting heterodimerization with the type I interferon receptor 2 (IFNAR2). Thereafter a tyrosine phosphorylation cascade is initiated inside the cell. The tyrosine kinase TYK2 associated with the IFNAR1 and the Janus kinase JAK1 permanently bound to the IFNAR2 reciprocally phosphorylate the intracellular receptor subunits and each other (Borden, Sen et al. 2007). Next, signal transducer and activator of transcription 1 and 2 (STAT1 and STAT2) are recruited to the receptors where JAK2 phosphorylates the tyrosine subunits of STAT1 and STAT2, which subsequently associate with another subunit, the interferon response factor 9 (IRF9; also named p48), to form the interferon stimulated gene factor 3 (ISGF3) complex. In a last step, this ISGF3 complex translocates to the nucleus where it stimulates gene expression classically by means of the interferon stimulated response element (ISRE) (Decker, Muller et al. 2005). The STAT1 are also able to homodimerize to form the AAF (alpha-interferon activation factor) factor and upon nuclear translocation they bind to the GAS element (interferon-gamma activated site) to induce alternative interferon gene transcription (Taniguchi and Takaoka 2001).

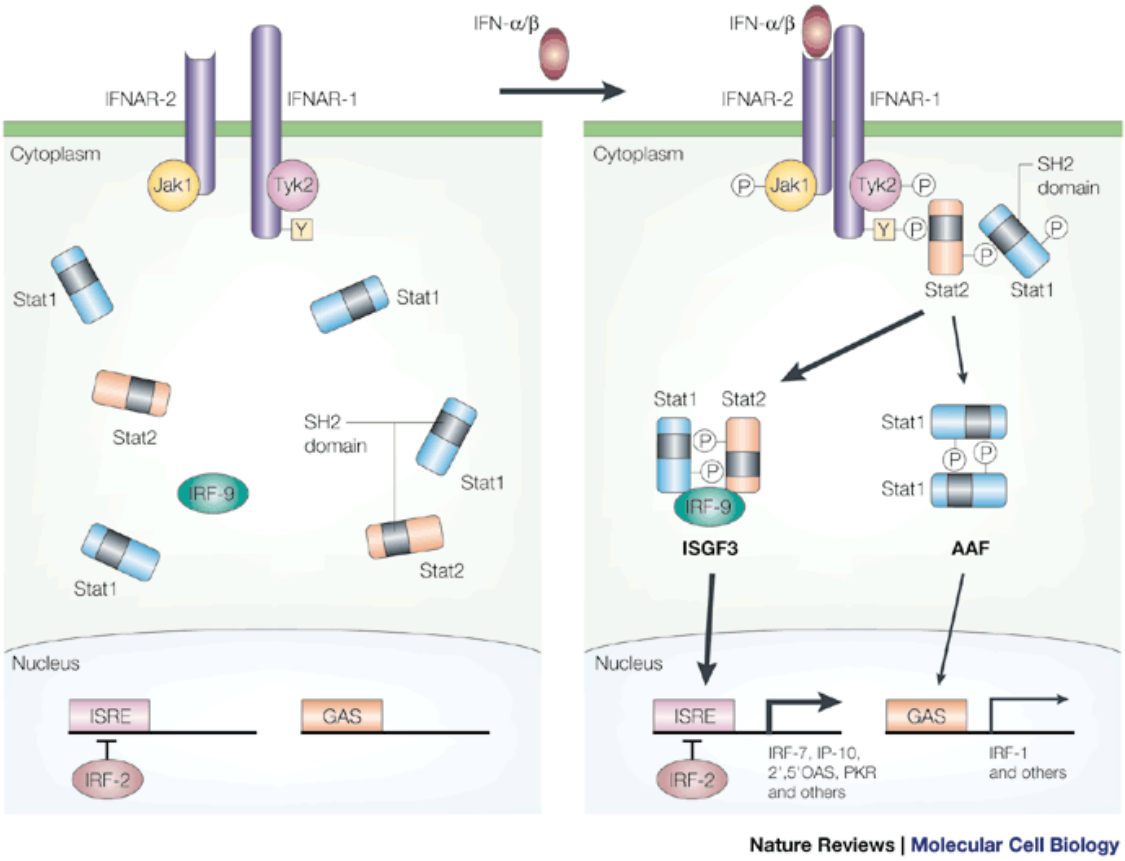

Figure 1

Figure 1. Main features of the IFN-α/β signalling pathway. On the other hand, another IRF-family member, IRF-2, is a nuclear factor that also binds to ISRE, and this factor interferes with ISGF3 action, thereby functioning as atranscriptional attenuator. **Taniguchi, T. and A. Takaoka (2001). "A weak signal for strong responses: interferon-alpha/beta revisited." Nat Rev Mol Cell Biol 2(5): 378-86.** (Taniguchi and Takaoka 2001)

It is crucial for the cell to shutdown interferon signaling therefore the IFNα inducible SOCS proteins are expressed also. SOCS1 binds to the IFNR receptors and inhibits binding of JAKs and TYKs by sterical hindrance as well as by receptor dephosphorylation. Another way to close down IFNα signaling is by promotion of phosphorylases which act on the receptors as well as on STATs to inactivate them. PIAS binds to the STATs and inhibits their transciptionnal activity therefore interfering with the IFNα pathway also (Greenhalgh and Hilton 2001; Naka, Fujimoto et al. 2005).

1.1.4. The Interferon Induced Transmembrane Protein IFITM3

The interferon-induced transmembrane protein (IFITM3) is a small (17 kDa) antiproliferative protein. It belongs to a family consisting of three functional IFTIM proteins, 1-8U (IFITM3), 1-8D (IFITM2) and 9-27 (IFITM1) as well as one pseudogene (Lewin, Reid et al. 1991). IFITM3 belongs to the early response genes, has two ISRE elements and is inducible by IFNα in the human melanoma cell lines ME15 and D10 (Certa, Seiler et al. 2001; Brem, Oraszlan-Szovik et al. 2003) with protein expression peaking at around 6 hours post- IFNα stimulus. IFITM3 seems to be deregulated in cells classified as interferon resistant, therefore does not exert its antiproliferative properties (Deblandre, Marinx et al. 1995). Additionally, studies have shown that over-expression of recombinant IFITM3 leads to proliferation inhibition in IFNα-sensitive cell lines (Brem, Oraszlan-Szovik et al. 2003). IFITM3 is therefore considered a marker for interferon resistance and it has also been identified as an early carcinogenesis biomarker of colon tumors (Fan, Peng et al. 2008).

1.1.5. Interferon-alpha – Clinical Relevance

Recombinant IFNα became the first protein based drug in the 1980s and even though treatment of hepatitis C virus (HCV) infected patients is a predominant use of IFNα, this cytokine is also used to treat other diseases such as schizophrenia (Hurlock 2001), multiple sclerosis and melanoma (Kirkwood 1998). In 1987 Spiegel noted that IFNα was a potent drug in hematologic malignancies, since IFNα normalized blood cell counts upon treatment. (Spiegel 1987). Seven years later Guttermann reviewed various diseases successfully treated with IFNα either alone or in combination with other substances such as retinoids or interleukins: hairy cell leukemia, chronic myelogenous leukemia, angiogenic diseases, viral diseases (HCV, herpes virus, hepatitis B virus, papilloma virus and HIV) and fibrosis. Gutterman concludes that IFNα is potent drug but that it needs further research on the mechanisms of action (Gutterman 1994). Furthermore type I interferons feature tumor suppressing activities and therefore widen their clinical application spectrum to various pathophysiologies (Pestka 2003).

The pleiotropic functions of interferons validate them as a potential drug (figure 2) and understanding of the underlying molecular mechanism involved in the interferon signaling will contribute to improved possibilities in successful treatment of patients suffering from virus infection, cancer and other diseases.

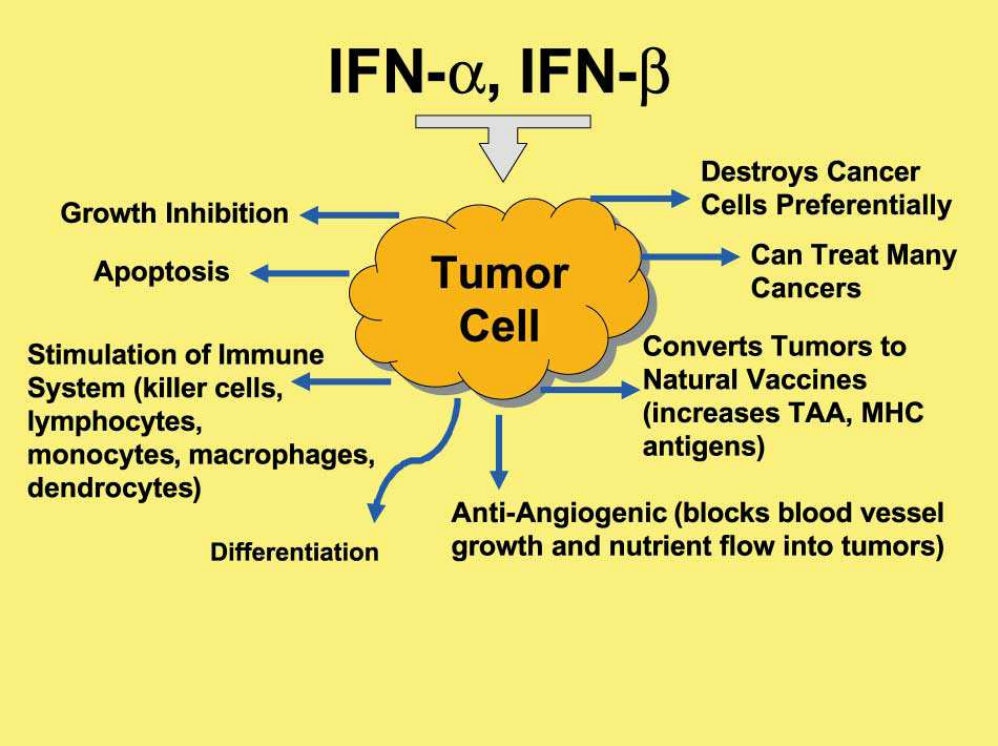

Figure 2

Figure 2. Antitumor actions of IFNα and IFNβ. **Pestka, S. (2003). "A dance between interferon-alpha/beta and p53 demonstrates collaborations in tumor suppression and antiviral activities." Cancer Cell 4(2): 85-7.** (Pestka 2003)

1.1.6. Interferon-alpha Resistance

Unfortunately, features like partial responses, side effects and especially drug resistance currently limit therapeutic efficacy of IFNα treatment. This holds true for hepatitis C virus infected patients also which currently are being treated with a combination of a viral RNA polymerase inhibitor gold standard and pegylated recombinant IFNα and has improved their convalescence from 20% to 50% (Duong, Christen et al. 2006). Resistance to interferons can be mediated by different means. Chadha et al. present four resitance mechanisms affecting the interferon molecule inactivation of intererons either by freely circulating interferon receptor capture or by inhibitory proteins thet are still under investigation and interference with IFNα synthesis either through elevated leves of prostaglandin E_2 or by cAMP phosphodiesterase mediated cAMP reduction which is necessary for IFNα synthesis (Chadha, Ambrus et al. 2004). There are though other ways to develop resistance to IFNα and the most evident causes are chromosome aberrations and mutations in the IFNα signaling pathways. Interestingly, although resistance by mutation does occur, it is not the most prevalent method for cells to develop resistance. More often it was observed that there is lack of diligence in the IFNα signaling pathway (Pansky, Hildebrand et al. 2000). It has been shown, that IFNα resistance can be induced in human melanoma cells with high doses of IFNα (Brem, Oraszlan-Szovik et al. 2003) and genes upregulated in resistant cell lines imply possible active mechanisms of IFNα resistance (Certa, Seiler et al. 2001). Additionally, microarray analysis comparing gene expression of the human melanoma celll lines ME15 and D10 upon IFNα administration revealed that the JAK/STAT pathway is delayed but not defective in the resistant cell line D10 proposing an alternative resistance mechanism involving secondary signaling pathways rather than the JAK/STAT pathway (Certa, Wilhelm-Seiler et al. 2003).

Another level of signaling interference occurs in the modulation of signaling proteins by means of methylation or defects in the same. These modulations are essential in maintaining accurate IFNα signaling. Interestingly, HCV infected patients have been treated successfully with S-adenosylmethionine (SAM) the substrate for methylation (Duong, Christen et al. 2006; Li, Chen et al. 2010).

IFNα resistance strikingly demonstrates how crucial this signaling pathway is when it comes to the combat of virus infections, cancer and other diseases. To this point a vast variety of IFNα response inhibition has been described and this fact underlines the crucial function of the importance of a diligent IFNα signaling.

1.2. EPIGENETICS

1.2.1. History of Epigenetics

The first biologist known to propose an epigenetic model according to his research was Paul Kammerer in the early 1920. Kammerer supposedly showed that toads were able to aquire features namely the nuptial pads and propagate them to their offspring (Pennisi 2009). Lamarque had postulated a plastic model of inheritance around 1800 which was widely accepted until the early 20th century. Anyhow, around that time the deterministic genetic model prevailed and the Lamarckien model was set aside. Unfortunately the story concerning Kammerer took a turn when he embellished his results and as a consequence was excluded from the scientific community (Pennisi 2009). When Muller reported his findings of the position effect variegation in the 30's the ground was set for a new direction in the biological concepts (Muller and Tyler 1930). One of the major contributors in the exploration of epigenetics is Barabara Mc Clintock. In 1951 she had observed a the chromosomal position-effect variegation in maize (Mc Clintock 1951) and when she introduced her findings on movable genetic elements (Yarmolinsky 1981) the scientific community started to assume that these effects observed most likely promoted genetic variability (Campbell 1981). During those 20 to 30 years many suggestions had been proposed and some puzzling effects not congruent with the deterministic genetic code were acknowledged as epigenetics. According to Gottschling epigenetics is defined as "a change in phenotype that is heritable but does not involve DNA mutation" (Gottschling 2007) and others as for example Feinbergs definition conforms with the mentioned, setting the focus on inherited features that are not transducted by the genetic code (Feinberg and Tycko 2004).

1.2.2. Basics of Epigenetics

The idea that all somatic cells contain the complete genome was not proven and accepted until the 1970s when the famous cloning experiment with Xenopus skin was performed (Gurdon and Laskey 1970; Laskey and Gurdon 1970). With this insight it became clear that the differentiated somatic cells did not involve genetic mutations or loss of genes but that the genes themselves must be regulated in a more complex manner. X-chromosome inactivation observed a while earlier provided one mechanistic cellular strategy to modulate its somatic phenotype (Ohno, Kaplan et al. 1959) and it was clear that DNA associated proteins, e.g. histones, must be

involved in gene expression regulation (Stedman 1950). Until 1964 it was not clear how histones were able to exhibit regulatory effects and Alfrey et al. introduced the concept of gene activation by histone acetylation (Allfrey, Faulkner et al. 1964). Along with the occurrence of acetylated histones there was soon also the finding of the according proteins, histone acetyltransferases (HATs). It took quite a while to find enzymes promoting deacteylation but finally these HDACs were also discovered (reviewed in (Losick 1998)). Furthermore histones are subject to specific histone methylation leading to heterochromatin recruitment and propagation of silenced DNA (Bannister, Zegerman et al. 2001). Additional players in the regulation of gene expression are the small RNAs which can be involved in proper heterochromatin formation and RNA interference adds another layer to epigenetic gene expression regulation through DNA methylation (Mathieu and Bender 2004). Many different modifications can be observed and DNA methylation is probably one of the most exciting modulations of the language of life.

1.2.3. DNA Methylation

In the 1970's Holliday doing quite some work on DNA replication realized that CpG methylaltion would administer a sound explanation how DNA repair mechanisms are able to distinguish daughter from parental DNA strands when proofreading the replicated double helix (Holliday and Pugh 1975). Bird et al. introduced methylation sensitive restriction enzymes and were able to demonstrate that CpG sites were either completely methylated or demethylated thus confirming the model Holliday had proposed earlier (Bird and Southern 1978). Years later Bird discovered the first methyl binding protein MeCP1 (Bird 1993) that directly was involved in CpG methylation gene suppression. Later on MeCP2 was identified and since then a variety of DNA methylation binding proteins have been discovered (Wade, Jones et al. 1998).

In mammals, DNA methylation occurs at the cytosine base followed by an adjactent guanosine base through covalent binding thus the termination CpG methylation. Statistically the CpG content of the DNA various between 4 and 6% and usually three courters of all CpGs are methylated (Ehrlich, Gama-Sosa et al. 1982). Interestingly there are sites that exhibit either lower or higher contents of CpG. Very often seen throughout the DNA is the suppressed CpG content of under one percent. Whenever a stretch of 200 bases contains more than 55% CpG base combinations it is considered a CpG island. In general these are encountered in the promoter regions of genes (McKeon, Ohkubo et al. 1982) and they have even served as

markers in the search for novel genes since two thirds of all genes feature these CpG islands. Unfortunately it is a bit more complicated to map DNA methylation patterns. Unwittingly, Bird et al. started an approach by using restriction enzymes particular to DNA unmethylated CpG sites (Bird and Southern 1978). The so obtained fragments were originally called “HpaII tiny fragments” but soon the preferred applied terminology shifted to CpG islands (Gardiner-Garden and Frommer 1987; Bird 2009). In contrast to the normally methylated CpG sites these island are often not methylated at all especially in germ cells (Bird, Taggart et al. 1985). Frommer et al. introduced the bisulfite conversion where every unmethylated cytotosine is deaminated resulting in a thymidine instead of the original cytidine. This means, that every cytosine that has survived the bisulfite treatment was originally methylated and when the strands are sequenced or hybridized to a microarray chip these methylated cytosines can be easily identified (Frommer, McDonald et al. 1992).

In order to maintain sound CpG methylation cells are dependant on their methyltransferases. To date five different DNA methyltransferases are known two of which are definitely expressed and functional in humans: the de novo DNA methyltransferase DNMT3b and the maintenance DNA methyltransferase DNMT1 both of which use S-adenosyl-methionine (SAM) as a substrate. It is still not quite clear how the *de novo* DNA methyltransferase recognizes the CpGs that are not supposed to be methylated and the effect seen in germ cells, when all CpG sites are completely demethylated is still puzzling the scientific community (Rougier, Bourc'his et al. 1998). Mutations in the DNMTs have fatal consequences, lethal in mice, lack of DNA methyltransferase in humans lead to a disease called ICF syndrome (immunodeficiency, centromeric instability, facial abnormalities) which is associated with reduced methylation in the pericentric regions of the chromosome (Ehrlich 2003).

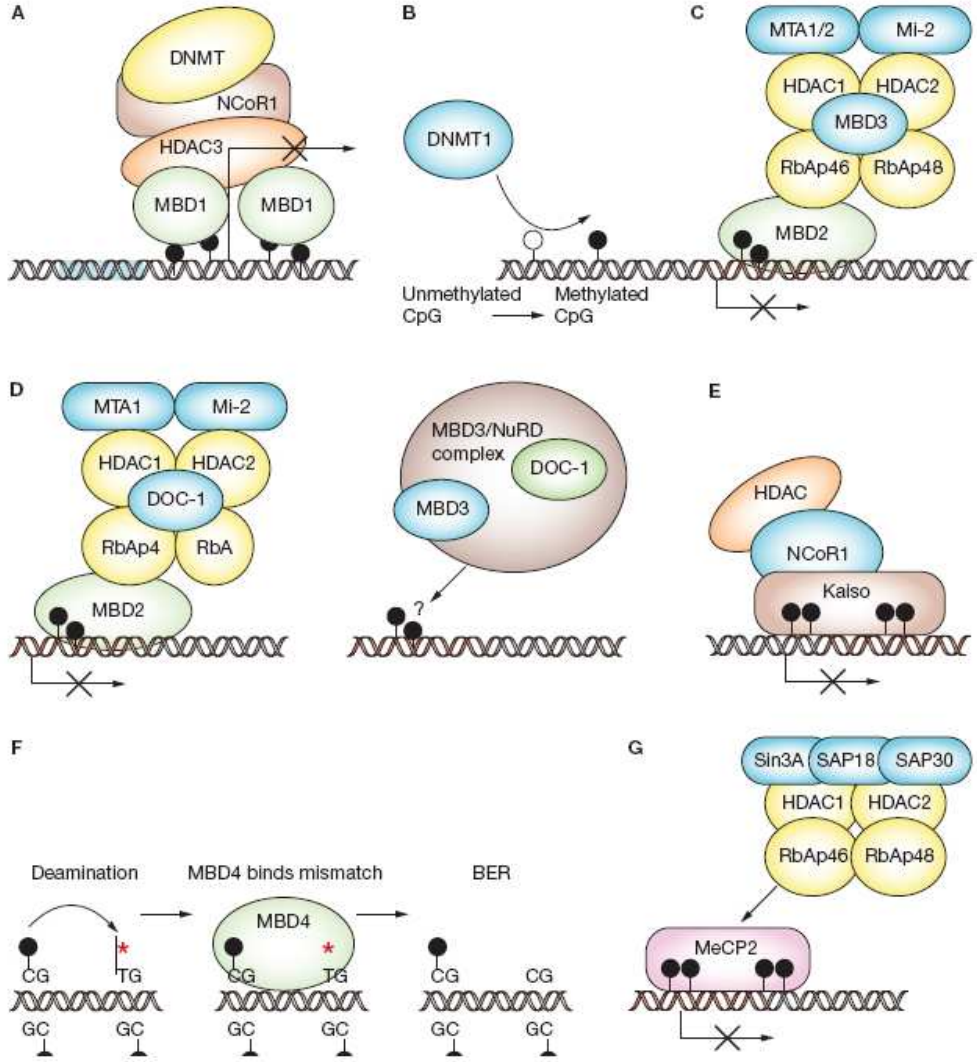

Figure 3

Figure 3. Modes of action of DNMT1, MBD2, MBD3, MBD4, MeCP2 and Kaiso. (A) MBD1 binds to methylated CpGs and mediates repression (B) DNMT1 is responsible for the DNA methylation (C) MBD2 is a component of the Mi-2/NuRD complex and binds to methylated CpGs to mediate repression. (D) MBD2 and MBD3 do not coexist in the same Mi-2/NuRD like complexes. MBD3 does not bind methylated DNA. (E) Kaiso binds methylated CpGs through a zinc finger motif and mediates both sequence-specific as well as methylation-dependent suppression. (F) MBD4 repairs mismatches and may also function as a repressor. (G) MeCP2 seems to bind the Sin3A repressor complex, which acts to remodel chromatin. **Sansom, O. J., K. Maddison, et al. (2007). "Mechanisms of disease: methyl-binding domain proteins as potential therapeutic targets in cancer." Nat Clin Pract Oncol 4(5): 305-15.** (Sansom, Maddison et al. 2007)

Another group of proteins involved in the methylated CpG sites and regions are the methyl binding proteins. Most of them exhibit a methyl binding domain hence their names: MBD1, MBD2, MBD3 and MBD4. As introduced earlier MeCP2 is also a known methyl binding protein (Bogdanovic and Veenstra 2009). MeCP1 turned out to be a protein complex rather than a single protein containing MBD2 along with different histone acetylases (Feng and Zhang 2001). Another methyl binding complex is termed Mi-2/NURD complex which contains MBD3 (Wade, Gegonne et al. 1999) and it exerts nucleosome remodeling as well as histone deacetylase activities (Esteller 2005). The methyl binding proteins share up to 70 % homology and they are crucial in maintaining accurate transcriptional regulation. There is a further protein, Kaiso, which itself does not contain an MBD binding site but embodies a zinc finger domain to bind DNA. These proteins interact with eachother and the methylated or nonmethylated DNA to maintain truthful transcription regulation (see figure 3) and disruptions of the MBDs, MECP2 and Kaiso cause fatal diseases.

As described above mutations in proteins involved in DNA methylation maintenance (DNMTs) and binding (MBDs) leads to different diseases such as ICF syndrome and the disruption of MeCP2 is known to cause Rett syndrome (Amir, Van den Veyver et al. 1999). It is furthermore known that DNA methylation aberrations are involved in cancer development. This happens through either hypermethylation of tumor suppressor genes or hypomethylation of oncogenes therefore leading to inactivation or activation of gene expression, respectively (depicted in figure 4) (Sansom, Maddison et al. 2007). Interestingly, in the mouse multistage skin cancer progression model it has been found that the degree of tumor development correlates well with DNA hypomethylation (Fraga, Herranz et al. 2004). Furthermore DNA hypomethylation is being used as a potent marker of some cancers (Esteller, Corn et al. 2001). Esteller outlines different CpG methylation affected mechanisms in the development of cancer: Cell cycle proteins, DNA repair machinery, hormonal response, p53 network and cytokine signaling are all subject to DNA methylation and loss or aberrations of DNA methylation cause fatal derangement (Esteller 2005). A powerful tool in the discovery of aberrant gene expressions and X-chromosome silencings as well as cancer treatment is the cytosine analog 5’-aza-2’-deoxycytidine (DAC). This substance is incorperated into the DNA but unlike the original cytosine DAC is not subject to methylation but instead binds DNMTs covalently therefore also exhibiting DNMT inhibitory effects (Jones and Taylor 1980).

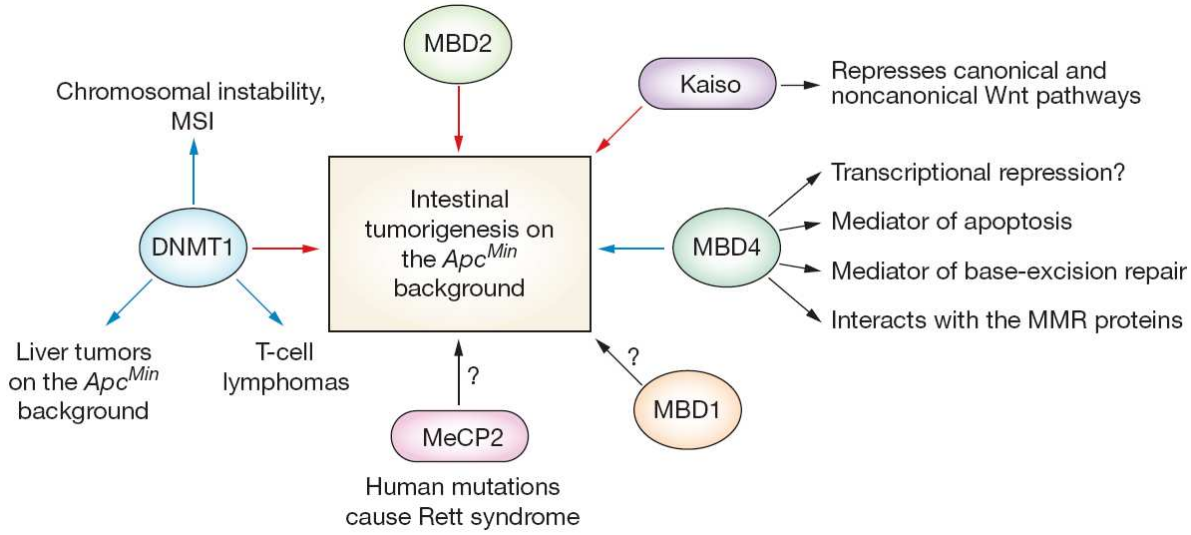

Figure 4

Figure 4. The MBD proteins and neoplasia. Red arrows indicate that the protein has a tumor augmenting effect, and blue arrows indicate that the indicated protein has a protective effect against tumor formation. **Sansom, O. J., K. Maddison, et al. (2007). "Mechanisms of disease: methyl-binding domain proteins as potential therapeutic targets in cancer." Nat Clin Pract Oncol 4(5): 305-15.** (Sansom, Maddison et al. 2007)

1.2.4. DNA Methylation and Interferon Resistance

Epigenetics is known to be involved in silencing of genes (Epstein, Smith et al. 1978) and aberrations in DNA methylation lead to changes in the expression of tumor suppressor genes as well as oncogenes and therefore promote cancer development (Jones and Laird 1999). Senescence can be induced in the immortalized Li-Fraumeni syndrome cells by treatment with the DNA demethylating and DNA methyltransferase (DNMT) inhibitory agent DAC and interestingly IFNα treatment exhibits a similar effect in these cells (Fridman, Rosati et al. 2007). Additionally treatment of human pancreatic cancer with DAC leads to activation of the interferon signaling pathway (Missiaglia, Donadelli et al. 2005). In mice, suppression of endogenous IFNs enhances development of metastases (Reid, Minato et al. 1981) and microarray studies with DAC treated immortalized cells revealed expression of a significant number of IFN pathway genes (Kulaeva, Draghici et al. 2003). Resistance to IFNα in renal carcinoma as well as melanoma cells can be overcome either by means of DAC or DNMT1 depletion by using its antisense (Reu, Bae et al. 2006). IFNα resistant HCV replicant harbouring cells exhibit sensitivity to IFNα upon treatment with DAC (Naka, Abe et al. 2006) again implicating a strong relationship between IFNα and DNA methylation. Evidence is obviously arising that the mechanisms behind IFNα resistance also involve aberrations in the biology of Epigenetics such as DNA methylation.

Treatment	System	Effect	Reference
DAC or IFNα	Li-Fraumeni syndrome cells	induction of senescence	(Fridman, Rosati et al. 2007)
DAC or DNMT1depletion	renal carcinoma as well as melanoma cells	resistance to IFNα is overcome	(Reu, Bae et al. 2006)
DAC	resistant HCV replicant harbouring cells	resistance to IFNα is overcome	(Naka, Abe et al. 2006)
DAC	human pancreatic cancer	activation of the interferon signaling pathway	(Missiaglia, Donadelli et al. 2005)
DAC	immortalized cells	enhances IFN pathway gene expression	(Kulaeva, Draghici et al. 2003)
suppression of endogenous IFNs	mouse	enhances development of metastases	(Reid, Minato et al. 1981)

Table 1. Overcoming interferon resistance by means of DNA methylation modulation

1.3. BACKGROUND

1.3.1. The Human Melanoma Cell Lines ME15 and D10

The ME15 and D10 cell lines are derived from human melanomas and the D10 cells exhibit IFNα resistance in that proliferation does not decrease upon IFNα stimulus (Figure 5) (Certa, Seiler et al. 2001). Both cell lines have been thoroughly characterized over the past years and therefore constitute an elaborate model to investigate mechanisms of IFNα resistance. Interestingly the resistance seen in D10 cells was thought to be resulting from a defect in the JAK/STAT pathway, since no chromosomal aberrations nor muations had been found (Pansky, Hildebrand et al. 2000). Anyhow, coregulation of many IFNα-inducible genes in ME15 and D10 cells propose that IFNα resistance of the D10 cell line is caused by abnormal signaling or delay downstream of the IFNα response therefore not involving the JAK/ STAT signaling cascade (Certa, Wilhelm-Seiler et al. 2003). Certa et al. have furthermore identified differently regulated gene-clusters and they highlighted a set of genes one of which is the imprinted maternally expressed transcript H19. This gene is upregulated in the IFNα sensitive cell line ME15 and known to be involved in DNA methylation and imprinting (Brannan, Dees et al. 1990). Another gene was found to be upregulated solely in D10 cells namely the DSS1 and loss of the same is associated with DNA damage (Li, Zou et al. 2006). These findings support the notion that alternative mechanisms are involved in the development of IFNα resistance. Crosstalk between pathways have been suggested as an additional layer of complexity in signaling (Certa, Wilhelm-Seiler et al. 2003). Elevated levels of transforming growth factor beta (TGFβ) have been observed in IFNα resistant HCV patients (Vidigal, Germer et al. 2002) and a similar effect might be partially responsible for the delayed gene expression response to IFNα seen in D10 cells. In conclusion IFNα resistance observed in D10 cells involves secondary effects apart from the primary IFNα response or the JAK/STAT signaling cascade, and alternative signaling pathways have been proposed in transmodulation of the IFNα stimulus.

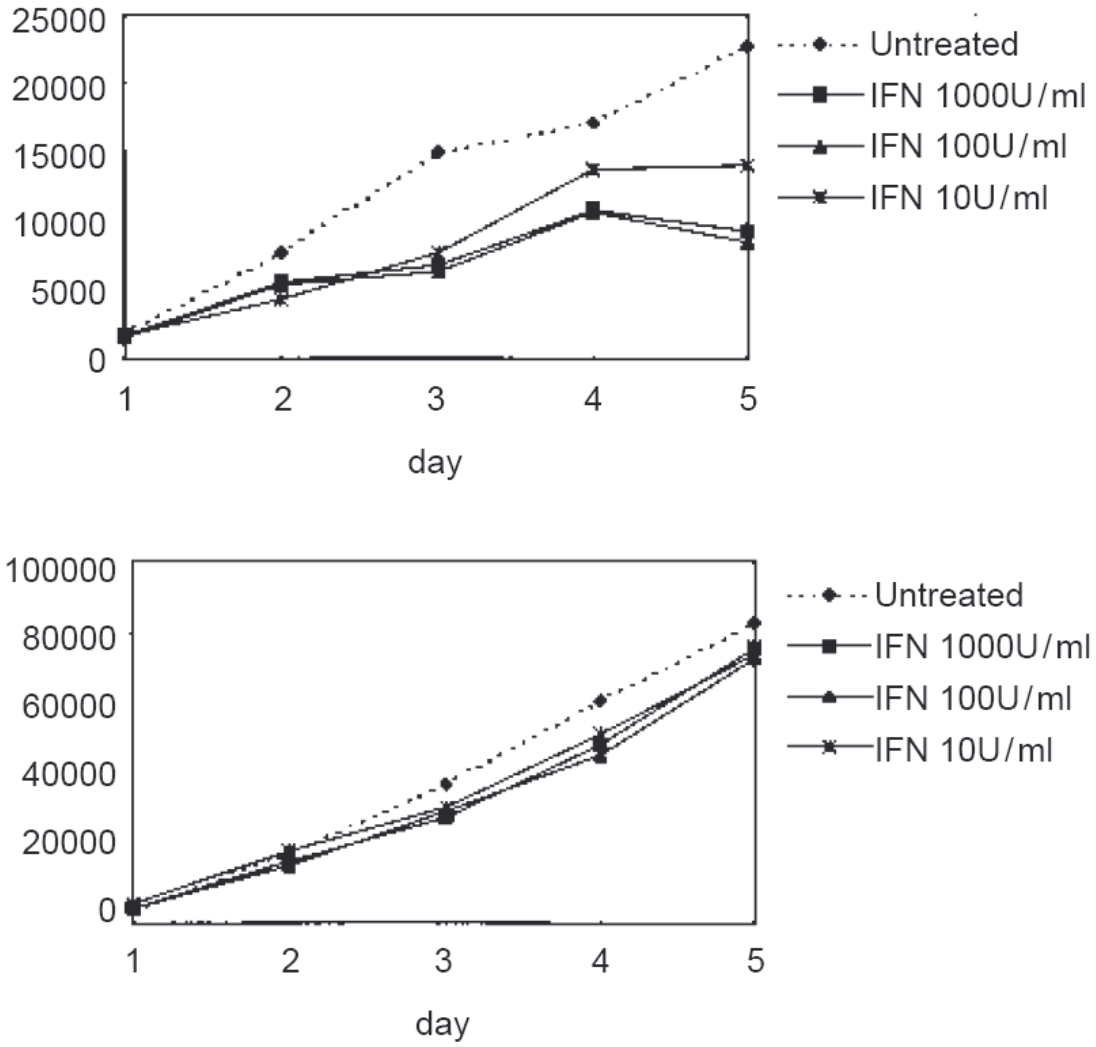

Figure 5

Figure 5. Proliferatiion of ME15 and D10 cells. DNA synthesis was measured by 3H-thymidine incorporation in the absence or presence IFNα. **Certa, U., M. Seiler, et al. (2001). "High density oligonucleotide array analysis of interferon- alpha2a sensitivity and transcriptional response in melanoma cells." Br J Cancer 85(1): 109**. (Certa, Seiler et al. 2001).

1.3.2. S100A2 Restores Interferon-alpha Sensitivity

In order to investigate previously proposed pathway crosstalks in IFNα signaling TGFβ stimulus was combined with the IFNα treatment. Foser et al. demonstrated that co-stimulation with IFNα and TGFβ restores antiproliferative activity in the resistant human melanoma cell line D10 (Figure 7, middle) (Foser, Redwanz et al. 2006). Furthermore, co-stimulation induces the cooperative activation of 28 genes including the insulin growth factor binding protein 3, IGFBP3, and the small calcium binding protein, S100A2 (figure 6) (Foser, Redwanz et al. 2006).

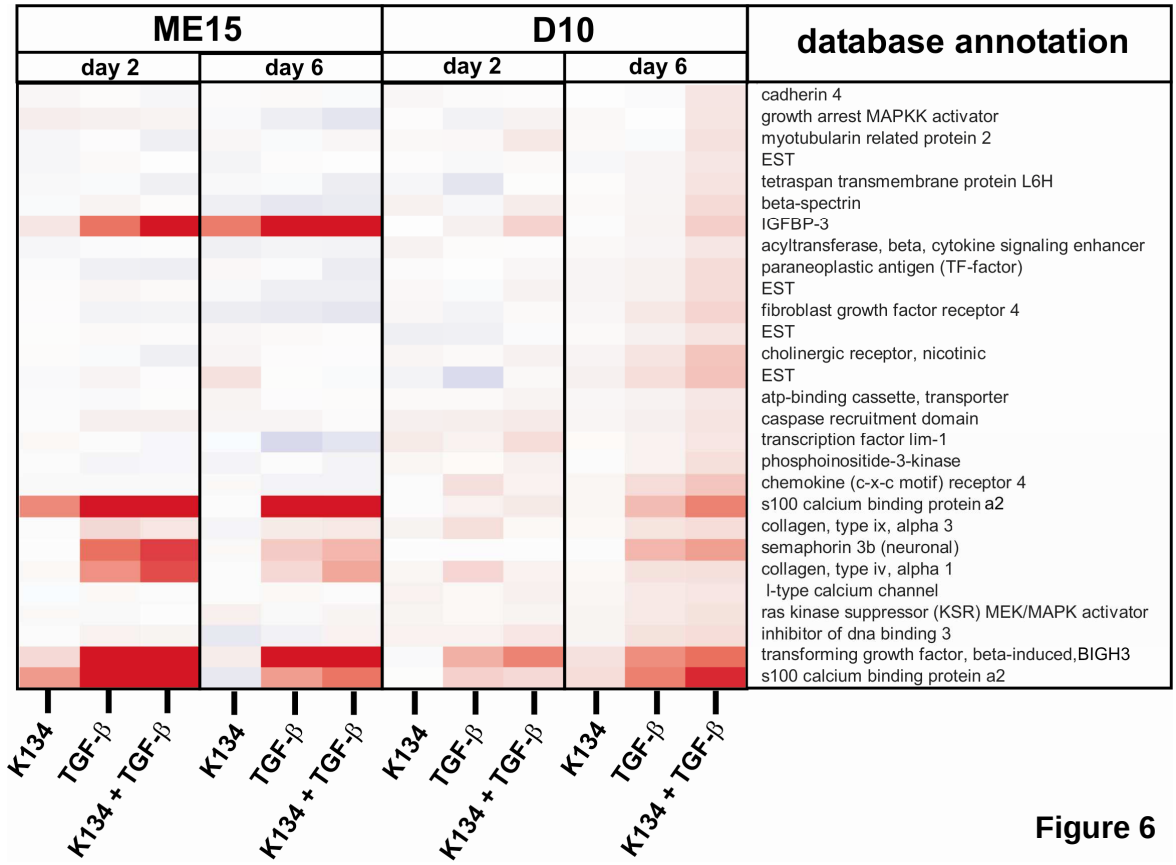

Figure 6

Figure 6. Proliferation control genes with additive induction by IFNα^{K134} and TGFβ. Up-regulated transcripts are displayed in blue. **Foser, S., I. Redwanz, et al. (2006). "Interferon-alpha and transforming growth factor-beta co-induce growth inhibition of human tumor cells." Cell Mol Life Sci 63(19-20): 2390**. (Foser, Redwanz et al. 2006)

Stable over-expression of S100A2 but not IGFBP3 in melanoma cells leads to a marked inhibition of cell proliferation in the presence of Ca^{2+} ions in response to IFNα stimulation (Figure 7). It has been suggested that calcium signaling as well as

the calcium protein S100 is involved in the interferon pathway (Naeim, Hoon et al. 1987; Gutterman 1994). Therefore, the combined activity of the upregulated calcium binding protein S100A2 along with the calcium efflux induced by IFNα plots a plausible correlation of the TGFβ and the IFNα signaling pathways. Nevertheless, the issue of IFNα resistance in D10 cells persists unsolved and continuing investigations of possible malfunctions in the cell response to cytokines remains subject of thorough research.

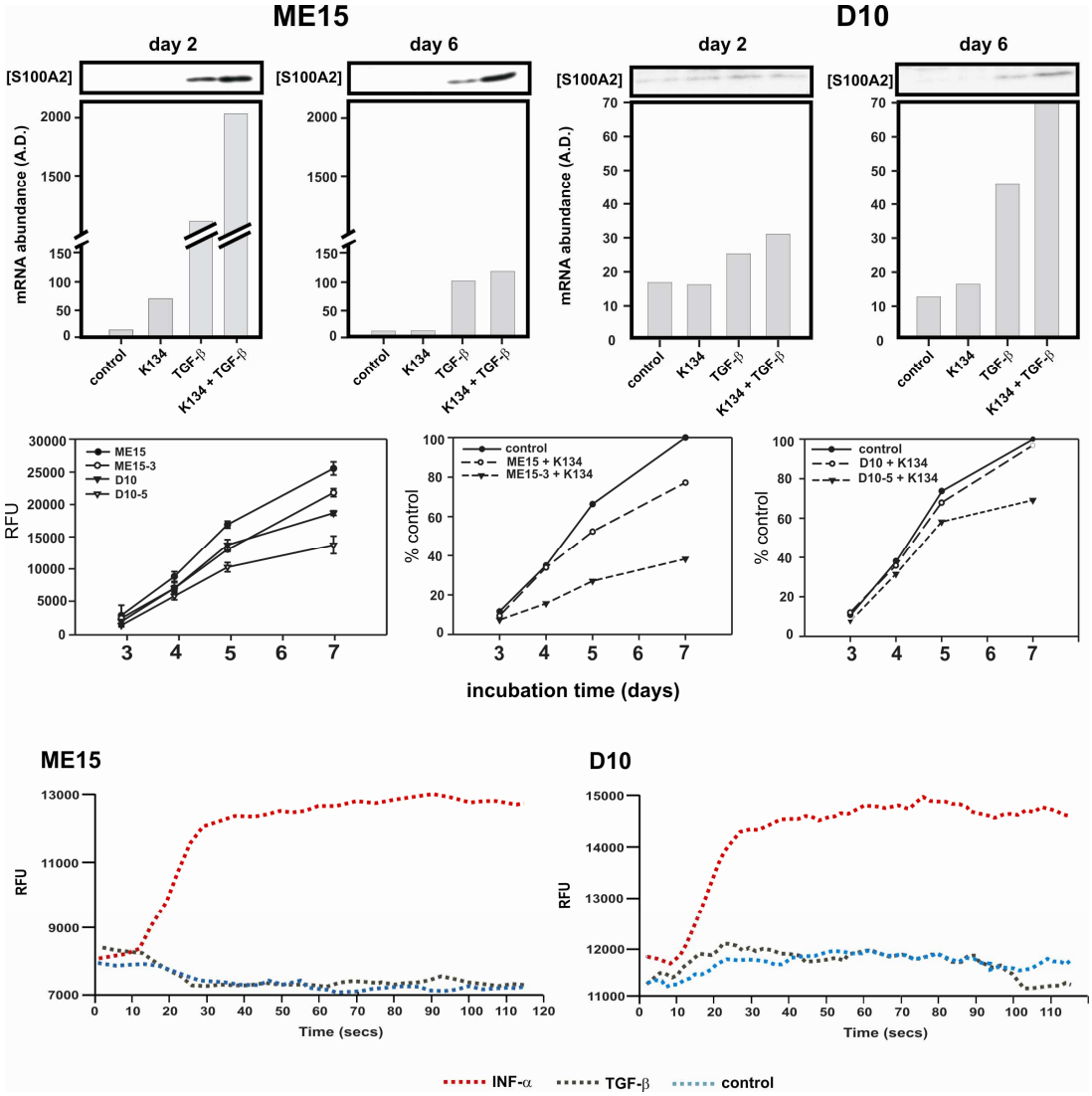

Figure 7

Figure 7. IFNα enhances antiproliferative activity of S100A2. S100A2 protein expression correlates with mRNA abundance (top). Growth rates of ME15 and D10 cells stably transfected with S100A2 (middle). IFNα induces intracellular calcium release (bottom). **Foser, S., I. Redwanz, et al. (2006). "Interferon-alpha and transforming growth factor-beta co-induce growth inhibition of human tumor cells." Cell Mol Life Sci 63(19-20): 2390**. (Foser, Redwanz et al. 2006)

1.3.3. The Small Calcium Binding Protein S100A2

The family of S100 type calcium binding proteins consist of as many as 21 members with pleiotropic functions (Eckert, Broome et al. 2004). Shared feature of all S100 proteins is the so called EF-hand motif which binds calcium and this leads subsequently to dimerization and activation (Donato 2001). It is commonly known that calcium plays crucial roles in a wide range of different cellular functions (Berridge, Lipp et al. 2000). Unlike the universally expressed Ca^{2+} binding protein calbindin S100 proteins exhibit differential expression throughout various cell types and therefore provide cell type specific Ca^{2+} signaling (Zimmer, Wright Sadosky et al. 2003). They work as modulators of signal transduction through phosphorylation or by acting as Ca^{2+} level sensors. They change their subcellular distribution, interact directly with transcription and even trigger Ca^{2+} signals themselves (Schafer and Heizmann 1996; Mandinova, Atar et al. 1998). S100 proteins are known to be crucial in stress response, epidermal wound repair and differentiation and aberrations of S100 expression often result in carcinogenicity (Eckert, Broome et al. 2004).

Interestingly, S100A2 is often downregulated in melanomas or breast tumors (Pedrocchi, Schafer et al. 1994; Maelandsmo, Florenes et al. 1997), which is consistent with a putative role in cell cycle control. In ME15 cells S100A2 expression is induced by TGFβ and further boosted by IFNα co-stimulation, which links these two signaling pathways at a transcriptional level (Foser, Redwanz et al. 2006). Since S100A2 is known to be hypermethylated upon others in mammary cancer (Lee, Tomasetto et al. 1992; Wicki, Franz et al. 1997) and prostate cancer (Rehman, Cross et al. 2005) the implication is close to suggest a possible epigenetic link in the co-regulating effect of TGFβ and IFNα on IFNα inducible genes.

1.4. AIM OF THE STUDY

Since S100A2 in contrast to other TGFβ-inducible genes (like the insulin growth factor binding protein 3; IGFBP3) leads to restoration of IFNα sensitivity in D10 cells, I am addressing the modulatory effect of S100A2 on the gene expression of the IFNα-inducible transmembrane protein IFITM3. I have chosen IFITM3 as chromosomal IFNα-response reporter gene in a model system consisting of the two human melanoma cell lines ME15 and D10. In the IFNα-sensitive ME15 cells IFITM3 expression is strictly IFNα dependent whilst it is constitutively expressed in the IFNα-resistant D10 cells. Since IFNα resistance is known to involve epigenetic mechanisms and since the IFNα pathway is functional in D10 cells, I decided to investigate DNA methylation of the core promoter of IFITM3 along with the potential modulatory effect of S100A2.

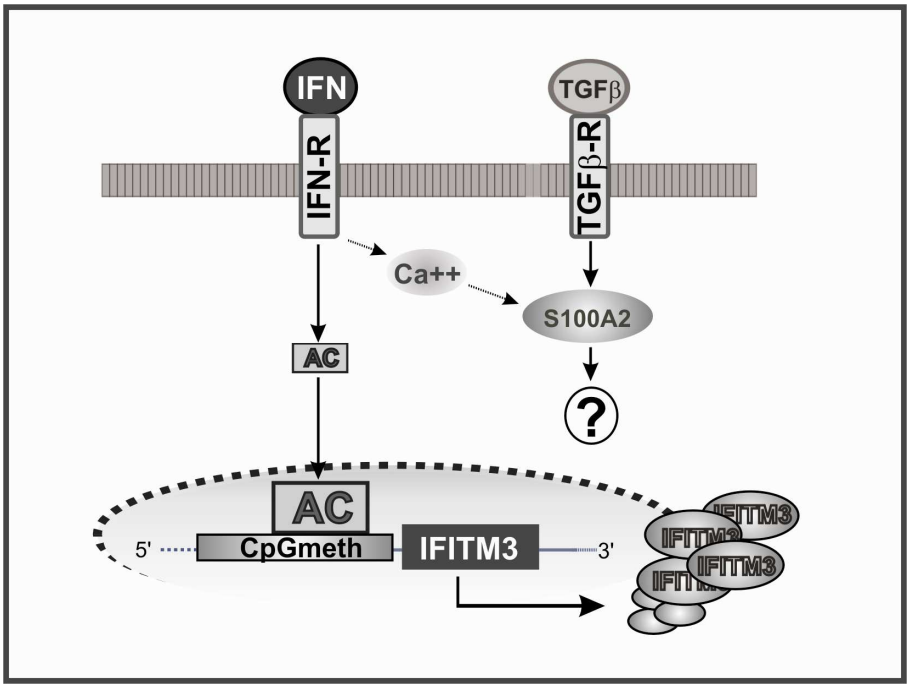

Figure 8

Figure 8. Key players of my thesis. The antiproliferative IFITM3 protein is IFNα-inducible and has been used as a marker for IFNα-resistance (Brem, Oraszlan-Szovik et al. 2003). The TGFβ-inducible S100A2 is a small calcium binding protein and it was seen in previously published work that S100A2 is sufficient to restore IFNα-sensitivity in D10 cells (Foser, Redwanz et al. 2006).

2. MATERIAL AND METHODS

2.1. Cell Lines

ME15, D10, ME15^{S100A2} and D10^{S100A2} have been described elsewhere (Luscher, Filgueira et al. 1994; Pansky, Hildebrand et al. 2000; Brem, Oraszlan-Szovik et al. 2003; Foser, Redwanz et al. 2006). Puromycin and blasticidin resistant cell lines ME15fPuro, ME15fBla, D10fPuro and D10fBla were generated in the course of this work and are described below along with the pluriploid cell line MDbla.

2.2. Cell Culture

All cell lines were cultured at 37℃ in a 5% CO_2 atmosphere in RPMI 1640 medium (GIBCO Life Sciences, Paisley, U.K.) supplemented with 10% fetal bovine serum (FBS), L-glutamine (2 mM), sodium pyruvate (1 mM), nonessential amino acids, antibiotics, and 10 mM HEPES buffer (Certa, Wilhelm-Seiler et al. 2003).

2.3. Antibodies, Cytokines and Reagents

Antibody against IFITM3 (1-8U) has been described previously (Brem, Oraszlan-Szovik et al. 2003). Anti-IFITM3 was diluted 1:2000 for western blotting. Anti-S100A2 was kindly provided by Prof. Dr. Claus W. Heizmann and diluted 1:1000 and 1:500 for western blotting and immunofluorescence, respectively. Anti-p21 Waf1/ Cip1 was purchased from Bioconcept (Allschwil, Switzerland) and used at a dilution of approximately 1:200 (Cell Signaling Technology®, catalog number 2946). Goat anti-rabbit and goat anti-mouse IgG (H+L) horseradish peroxidase (HRP) conjugate were obtained from BioRad (Basel, Switzerland) and used at a dilution of 1:5000. Alexa Fluor 555 goat anti-rabbit IgG (H+L) was purchased from Invitrogen (Basel, Switzerland) and diluted 1:100. IFNα (IFNα2a, Roferon®-A) and its monopegylated isomer K134 (IFNα^{K134} (Foser, Schacher et al. 2003; Foser, Weyer et al. 2003; Foser, Redwanz et al. 2006)) was provided by F. Hoffmann-La Roche Ltd. (Basel, Switzerland). TGFβ has been purchased from Calobiochem (Germany). Concentrations used were 1000 U/ml IFNα and 2 ng/ml TGFβ unless indicated otherwise. 5-aza-2'-deoxycytidine (DAC) from Sigma (Basel, Switzerland) was used at a concentration of 2 ug/ml. Puromycin (a kind gift from Prof. Dr. Christoph Moroni, University of Basel, Switzerland) was used at a concentration of 0.5 mg/ml and 1

mg/ml and blasticidin (Alexis Biochemicals, Lausen, Switzerland) a concentration of 3.75 mg/ml and 7.5 mg/ml for the ME15 and D10 cell line, respectively. Propidium Iodide was purchased from Sigma (Basel, Switzerland) and RNase was provided by F. Hoffmann-La Roche Ltd. (Basel, Switzerland).

2.4. Cell Treatments

Proliferation assays as well as protein detection assays were performed using the standard IFNα treatment of 1000 U/ml (figures 10 and 11A). For oligonucleotide array analysis ME15, ME15^{S100A2}, D10 and D10^{S100A2} melanoma cell lines were grown in triplicate cultures for 2 days with either IFNα^{K134} (1000 U/ml), TGFβ (2 ng/ml) or a combination of both cytokines (figure 11B). For cell fractionation either ME15 as well as ME15^{S100A2} cells were treated with IFNα (1000 U/ml), TGFβ (2 ng/ml) or a combination of both cytokines for 2 days or ME15 cells were transfected with SNAP-S100A2-Bam and SNAP-S100A2-Eco vectors for 6 and 20 hours (figure 12). In the S100A2 immunofluorescence localization assay cells were incubated with both IFNα (1000 U/ml) and TGFβ (2 ng/ml) or either the SNAP-S100A2-Bam or the SNAP-S100A2-Eco recombinant vector for two days (figure 12). To promote genome wide demethylation the cell lines were treated with 5- aza-2'-deoxycytidine (DAC) (2 μg/ml) or a control along with IFNα (1000 U/ml, 100 U/ml or 10 U/ml), TGFβ (1μg/ml) or a combination of both cytokines with incubation times depicted in figures 13 and 23 and the concentration of SAM supplementation was 160 mM (figure 14). Luciferase assays were performed using 1 μg of plasmid (figures 15 and 22) The standard IFNα concentration of 1000 U/ml were used in figures 15, 16, 18 and 19. For the IFITM3 promoter methylation analysis ME15, ME15^{S100A2}, D10 and D10^{S100A2} cells were stimulated with IFNα (1000 U/ml) according to figure 20 and to induce S100A2 expression ME15 and D10 cells were incubated with TGFβ (2 ng/ml) for 2 days. The p53 luciferase reporter assays were performed using 5-fluoruracil (5-FU, 10 μg/ml, in DMSO dilution), lipopolysaccharide (LPS, 100 μg/ml, in DMSO dilution), 0.1% DMSO alone or DAC (2 μg/ml) treatment for 24h in ME15 and D10 cells previously transfected with the outlined luciferase reporter plasmids figure 22.

2.5. Proliferation Assays

In order characterize growth respond to IFNα of ME15 and D10 standard proliferation assays have been performed previously using CellTiter Aequeous One Solution Cell Proliferation Assay (Promega, Madison, USA) (Foser, Redwanz et al. 2006). Here, proliferation rates have been assessed using the RT-CES® System from ACEA Biosciences. ME15 and D10 cells were seeded in a gold coated 96-well plate at concentrations 5000, 2500, 1250 and 650 cells per well. After an incubation time of 8 hours cells were treated with the standard concentration of 1000 U/ml IFNα. Impedance was measured every three minutes over the course of a week monitoring cell growth in real time.

2.6. Oligonucleotide Array Analysis

Oligonucleotide array analysis has been described in detail previously (Foser, Redwanz et al. 2006). In this study RNA levels were measured 2 days after cytokine treatment. Genes considered had to exhibit a maximum mean of 50 and a changefactor (CHF) threshold of +/- 2. These experiments have been performed by the group of Stefan Foser ante inceptum operam meam.

2.7. Transfections and Plasmids

All transfections were performed using either FuGENE® from F. Hoffmann-La Roche Ltd. (Basel, Switzerland), Optifect or LipofectAMINE 2000 reagents from Invitrogen (Basel, Switzerland) according to the manufacturer's protocol.

PcDNA3 -S100A2 and PGL3-PA2 (S100A2 luciferase reporter plasmid) were kindly provided by Prof. Dr. Claus W. Heizmann (University of Zürich). The IFITM3 Neo/N686 (IFITM3 luciferase reporter plasmid) and the 6-16 Neo/N686 (6-16 luciferase reporter plasmid) have been described previously (Brem, Oraszlan-Szovik et al. 2003). PSirBGLoBla and pSirBGLoPuro carrying a blasticidin or a puromycin resistance, respectively, were kindly provided by Prof. Dr. Giulio Moroni (University of Basel). The firefly, pGL3-tk-luc, and the renilla, phRL tkluc, luciferase plasmids were purchased from Promega (Dübendorf, Switzerland). The p53 reporter plasmid was constructed by insertion of two p53 consensus sequences of GADD45 'tggtacaGAACATGTCTAAGCATGCTGgggactg' between the NotI / SacI and the NheI / Xho restriction sites of the pGL3 vector (Promega, Madison, USA) multiple cloning

site, resulting in a 5'-gagctcttacgcgtgctagc-3' spacer sequence in front of the herpes simplex virus (HSV) thymidine kinase (tk) promoter sequence and was a kind gift from Karen Schad from the laboratory of Dr. Adrian Roth (F. Hoffmann-La Roche Ltd., Basel, Switzerland).

2.8. Cloning of SNAP-tagged S100A2

For subcloning S100A2 from pcDNA3 into the pSEMS-26m vector from Covalys (Witterswil, Switzerland), S100A2 was amplified by PCR using primers with internal EcoRI and BamHI restriction sites to obtain a C-terminal SNAP-tag construct and a N-terminal SNAP-tag construct, respectively. Primers used for the C-terminal construct were (forward) 5'- CCT GGT CTG CCA CGA ATT CAT GAT GTG CAG TTCT and (reverse) 3'- GTT CTG AAT TCG GGT CGG TCT GGG CAG CCC. For the N-terminal construct following primers were used: (forward) 5'- CCT GGT CTG CCA CGG ATC CAT GAT GTG CAG TTCT and (reverse) 3'- AAG TGG ATC CTC AGG GTC GGT CTG GGC AGCC (Microsynth, Balgach, Switzerland). All sequences were verified by standard automated sequencing.

2.9. Cell Fractionation

ME15, D10, ME15^{S100A2} and D10^{S100A2} cells were lysed and fractionated using a commercial kit according to the instructions supplied (Qiagen Qproteome Cell Compartment Kit, Qiagen, Hombrechtikon, Switzerland).

2.10. Immunoblotting

Immunoblots were performed with total protein extracts or cell fractions. Protein amounts were normalized by standard BCA assays. SDS PAGE was performed with 4-12% Bis-Tris gels and nitrocellulose membranes using the XCell SureLock^{TM} system from Invitrogen (Basel, Switzerland). Proteins were detected using 1° antibodies against IFITM3 or S100A2, HRP-conjugated 2° antibody and a chemiluminescent substrate (SuperSignal West Pico Chemiluminescent; Pierce Chemical Co., Thermo Fisher Scientific Inc., Rockford, IL, USA).

2.11. Immunofluorescence

Approximately 2000 ME15 cells and 4000 cells of each ME15^{S100A2}, D10 and D10^{S100A2} were seeded on 4-well Lab-Tek® II Chamber Slides™ (LabTek, Nunc Inc., Langenselbold, Germany). The following day, cells were treated with a combination of IFNα (1000 U/ml) and TGFβ (2 ng/ml) or a control, followed by an incubation time of 2 days. All subsequent cell manipulations were performed on ice. Cells were washed twice with ice-cold OptiMEM from Invitrogen (Basel, Switzerland) and fixed for 2 minutes using 70% acetone kept at -20º C. After two additional washes with ice-cold PBS the samples were treated with Image-iT® FX signal enhancer from Invitrogen (Basel, Switzerland) for 30 minutes and blocked for 1.5 hours in PBS containing 1% Bovine Serum Albumin (BSA) (Sigma, Basel, Switzerland), 1% Normal Goat Serum (NSG) (Sigma, Basel, Switzerland) and 1‰ Ova Albumin (OVA) (Fluka, Basel, Switzerland). Cells were incubated for 1 hour with anti-S100A2 serum at a dilution of 1:500 in blocking solution. After washing twice with PBS containing 1% BSA for 5 minutes, cells were stained with Alexa Fluor 555 diluted 1:100 in PBS containing 1% BSA for 1 hour. Cells were washed twice for 5 minutes with PBS. Images were recorded with a Zeiss Axiovert 135 microscope using Axiocam software (Zeiss, Feldbach, Switzerland).

2.12. DNA Wide Demethylation by 5-Aza-2'-deoxycytidine Treatment

Approximately 10'000 ME15 cells and 20'000 ME15^{S100A2}, D10 and D10^{S100A2} cells were seeded in 6-well plates. Cells were grown for three days following stimulation with TGFβ (1 μg/ml), IFNα (1000 U/ml) or a combination of both cytokines, in the presence or absence of 5-Aza-2'-deoxycytidine (DAC) (2 μg/ml). After 6, 12, 24 and 51 hours cells were washed twice with PBS, resuspended in standard lysis buffer and the whole protein extract was thereafter used for immunoblot analysis. The same procedure was applied for the IFNα sensitivity experiment with 100 U/ml or 10 U/ml IFNα treatment in the presence or absence of DAC (2 μg/ml).

2.13. IFITM3 Protein Expression Upon S-Adenosyl-methionine Supplementation

ME15 and D10 cells were grown in 6 well plates for two days. Cells were then stimulated with TGFβ (1 μg/ml), IFNα (1000 U/ml) or a combination of both cytokines

in the presence or absence of S-adenosyl methionine (SAM; 160 mM). After 6, 25 and 50 hours cells were washed twice with PBS, resuspended in standard lysis buffer and the whole protein extract was thereafter used for immunoblot analysis.

2.14. CpG Methyltransferase Mediated *In Vitro* Methylation

PGL3-PA2 (S100A2 luciferase reporter plasmid), IFITM3 Neo/N686 (IFITM3 luciferase reporter plasmid) and the 6-16 Neo/N686 were incubated with the CpG methyltransferase M. SssI (New England BioLabs Inc., Ipswich, USA) supplemented with methylgroup donor S-adenosyl methionine (SAM; New England BioLabs Inc., Ipswich, USA) according to the manufacturers protocol for 1 hour at 37℃. To control for successful methylation plasmids were digested for 1 hour at 37℃ using the methyl-sensitive restriction enzyme AVA I (New England BioLabs Inc., Ipswich, USA), DNA was purified by precipitation and analyzed using gel electrophoresis.

2.15. Luciferase Reporter Assays with the *In Vitro* Methylated Promoters IFI6, IFITM3 and S100A2

ME15 and D10 cells were seeded into 24-well plates at a 70% confluence. One day later cells were transfected with either methylated or unmethylated PGL3-PA2, IFITM3 Neo/N686 or 6-16 Neo/N686 using 1 μg of plasmid DNA according to standard transfection procedures and serum was added after 7 hours. Another day later cells were incubated with the standard concentration of 1000 U/ml IFNα and luciferase activity was measured 6 hours later using the Berthold Lumat (Berthold Technologies, Regensdorf, Switzerland).

2.16. Generation of the ME15-D10 Hybrid Cell Line MDbla

2.16.1. Generation of Stable Cell Lines

After optimal antibiotic concentrations were determined, ME15 and D10 cells were transfected with 4 µg of either PSirBGLoBla or pSirBGLoPuro plasmid DNA (kindly provided by Prof. Dr. Christoph Moroni, University of Basel) according to standard transfecion procedures. Cells were then grown under according antibiotic pressure to yield the puromycin and blasticidin resistant cell lines ME15fPuro, ME15fBla, D10fPuro and D10fBla.

2.16.2. Fusion of Cell Lines

The newly generated cell lines ME15fPuro and D10fBla as well as ME15fBla and D10fPuro were mixed 1:1 and washed twice in RPMI. The cell pellet was collected in a cuvette and given a pulse of 220 V and 900 µF. The cell pellet was incubated at 37°C for 30 minutes and thereafter res uspended in a standard culture flask. Fusioned cells were incubated for one day and then grown in selection media containing the adequate concentrations of antibiotics. Unfortunately only one clone survived, namely the MDbla which is the fusion cell line from the combined ME15fPuro and the D10fBla cell line.

2.16.3. Evaluation by FACS

ME15, D10 and MDbla cells were first fixed in 70% ethanol and thereafter labeled with propidium iodide purchased at Sigma (Basel, Switzerland) (0.05 mg/ml in PBS containing 0.1 mg/ml RNase provided by F. Hoffmann-La Roche Ltd. (Basel, Switzerland)) for one hour under standard cell culture conditions. Cells were kept on ice until cellcount was measured using a standard FACS analyzer.

2.16.4. Evaluation by Karyotyping

The karyotyping of the ME15, D10 and MDbla cell lines was kindly performed in the laboratory of Prof. Dr. Peter Miny at the UKBB (Universitäts-Kinderspital Beider Basel), Switzerland.

2.17. Isolation of Genomic DNA

Cells were harvested using trypsin and genomic DNA was either isolated using the PureLink™ Genomic DNA Mini Kit from Invitrogen (Basel, Switzerland) or the MagNA Pure DNA Isolation Kit from Roche Applied Science (F. Hoffmann-La Roche Ltd., Basel, Switzerland) following manufacturers isolation protocol.

2.18. DNA Wide Methylation Analysis Using the Illumina Infinium Methylation Assay

ME15 cells were grown in T75 culture plates. After one hour of stimulation with IFNα (1000 U/ml), cells were harvested and genomic DNA was isolated. Bisulfite treatment for this assay was kindly performed by Dr. Patrick Urfer using the Zymo EZ DNA Methylation™ Kit (Orange, CA, USA) according to the manufactures protocol with 2μg of genomic DNA input. Bisulphited genomic DNA was processed further according to the instructions of the Infinium® Methylation Assay protocol (Illumina, San Diego, USA) and hybridization to the Illumina BeadChip. Scanning was performed using the Illumina BeadArray™ ReaderScanner. Data was imported into Illumina's own methylation analysis software, Beadstudio, undergoing a preanalysis where the methylation ratios are internally calculated and displayed as beta values.

2.19. Promoter Methylation Analysis by Bisulfite Sequencing

ME15, ME15^{S100A2}, D10 and D10^{S100A2} melanoma cell lines were treated with IFNα (1000 U/ml) for 1, 6 and 24 hours. In order to promote S100A2 expression in ME15 cells they were pretreated with TGFβ (2 ng/ml) for 2 days. Isolated genomic DNA was bisulfite treated using the Zymo EZ DNA Methylation™ Kit (Orange, CA, USA) according to the manufactures protocol with 2μg of DNA input. The bottom strand of the IFITM3 promoter was amplified to yield an 820 bp fragment using bisulfite adjusted primers designed to cover 19 CpG sites adjacent to the translation initiation site (ATG) (forward primer (Chromosome 11: 311612) 5'-ATA ATC CAA CTA CCT AAA CAC CATA and backward primer (Chromosome 11: 310793) 5'–GGT TTG GAT AGT GTG ATT TAT GG TGT TTA–3' (Even though this primer encloses a mismatch this does not influence specific binding to the target sequence in silico.) The PCR program consists of following parameters: initial incubation time of 10 minutes at 95℃, 40 cycles with 1 minute at 94℃, 1 minute at 58℃ and 1 minute at 72℃ and an additional 10 minutes at 72℃ for final elongation. Amplified fragments

were cloned into the pCR®2.1-TOPO® vector (Invitrogen, Basel, Switzerland) and transformed into XL1-blue (Stratagene, La Jolla, CA, USA) or TOP10 (Invitrogen, Basel, Switzerland) competent cells and plated on IPTG/ X-gal containing agar plates. Plasmids from white colonies were isolated and sequenced using an ABI 3730xl DNA analyzer instrument and generic vector based primers using standard procedures. Following computer assisted alignment with the clustalw GCG-program the methylation state of CpG sites was determined.

Bisulfite treated genomic DNA from healthy mucosa and colon cancer tissue samples of patients were a gift from Prof. P. Schär (University of Basel).

2.20. P53 Luciferase Reporter Assay

ME15 and D10 cells were transfected with a mix of a p53 negative firefly and a control renilla luciferase plasmid or the p53 reporter plasmid firefly mix ('2 x p53 in pGl3-tk-luc' and phRL tkluc') at a confluency of approximately 50% in 24 wells. To ensure efficient transfection reaction cells were incubated for 6 hours whereupon medium was replaced with culture medium containing either LPS (100 ug/mL, in DMSO dilution), 0.1% DMSO alone or DAC at the standard concentration. Cells were further incubated for 48 hours before luciferase activity was measured by Dual Luciferase Reporter Assay System (Promega, Dübendorf, Switzerland). Transfection and measurements were performed by Karen Schad (F. Hoffmann-La Roche Ltd., Basel, Switzerland) and Fredy Siegrist (F. Hoffmann-La Roche Ltd., Basel, Switzerland) analyzed data using the statistical program R.

3. RESULTS

3.1. ME15 Cells Respond to Interferon by Decrease in Proliferation Rate Whereas D10 Cells Exhibit Resistance

Previous research has established a model system to investigate IFNα-resistance using two different melanoma cell lines. The ME15 cell line, considered sensitive to IFNα, markedly decreases its proliferation rate when exposed to IFNα. The other melanoma cell line, D10 is known to exhibit resistance to IFNα in that proliferation is not affected by cytokine treatment (Foser, Redwanz et al. 2006). In order to verify sensitivity of ME15 cells and resistance of D10 cells to IFNα we decided to verify the expected proliferation behaviour.

There are three standard methods for assessing proliferation rate: either by cell-count, by detection of DNA synthesis or measurement of metabolic activity (Cunningham 2001). Each method reflects a different property of the cell line and it is advisable to investigate cell proliferation using different techniques. Certa et al. have used the thymidine incorporation to investigate DNA content in ME15 and D10 cells (Certa, Wilhelm-Seiler et al. 2003) and Foser et al. addressed cell proliferation by applying the CellTiter™ Assay (Promega) to measure metabolites in ME15, D10, $ME15^{S100A2}$ and $D10^{S100A2}$ cells (Foser, Redwanz et al. 2006). One main limitation of these methods is that cells must be harvested necessitating large amounts of starting material in order to investigate several time points. This issue can be circumvented by impedance measurement where proliferation is monitored in real time. The technique uses gold-coated wells that are attached to a low electrical circuit. Once a cell attaches to that surface, the resistance of the alternating current (e.g. the impedance) is measured and a Cell Index is calculated

$CI = (Z_i - Z_0)/ 15\ \Omega$ Z = impedance, i = measured time point, 0 = time point zero, Ω = resistance

reflecting both individual cell growth and population proliferation (xCELLigence**,** Roche Applied Science and ACEA Biosciences, figure 9).

We seeded different ME15 and D10 cell concentrations into xCELLigence's gold-coated 96 well plates and stimulated with IFNα after an incubation of eight hours. Impedance measurements were acquired every three minutes over the time-course of seven days (174 hours).

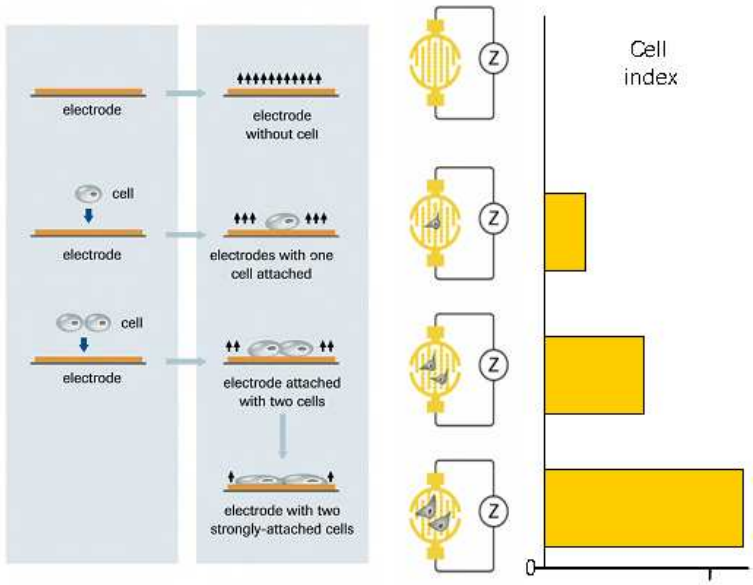

Figure 9

Figure 9. Principle of the xCELLigence System. Gold coated 96 well plates are connected to an electrical circuit and upon attachment of cells, impedance increases therefore measuring cell growth and proliferation (**xCELLigence, Roche Applied Science and ACEA Biosciences, 2010** (Sciences 2010)).

Interestingly, ME15 cells seemed to exhibit a marked sensitivity to the seeding concentration. Only a concentration of 1250 cells per well allowed exponential growth (figure 10A); neither the higher nor the lower cell densities showed detectable proliferation with this method. ME15 cells exhibit a considerable downshift in the proliferation curve when exposed to IFNα indicating slower growth (figure 10A). Proliferation of untreated cells peaked at around 100 hours and then decreased, most likely due to detachment of the cells. For the IFNα-treated cells, peak levels are reached 45 hours later than in untreated cells and the cell index does not reach comparable levels. D10 cells, however, grow proportionally to their seeding concentration (figure 10B). Furthermore, it is clearly demonstrated that D10 does not exhibit sensitivity to IFNα.

These findings are consistent with our previously published results (Certa, Wilhelm-Seiler et al. 2003; Foser, Redwanz et al. 2006) and we additionally conclude that cell density is a critical factor in determining proliferation rates of ME15 but not D10 cells.

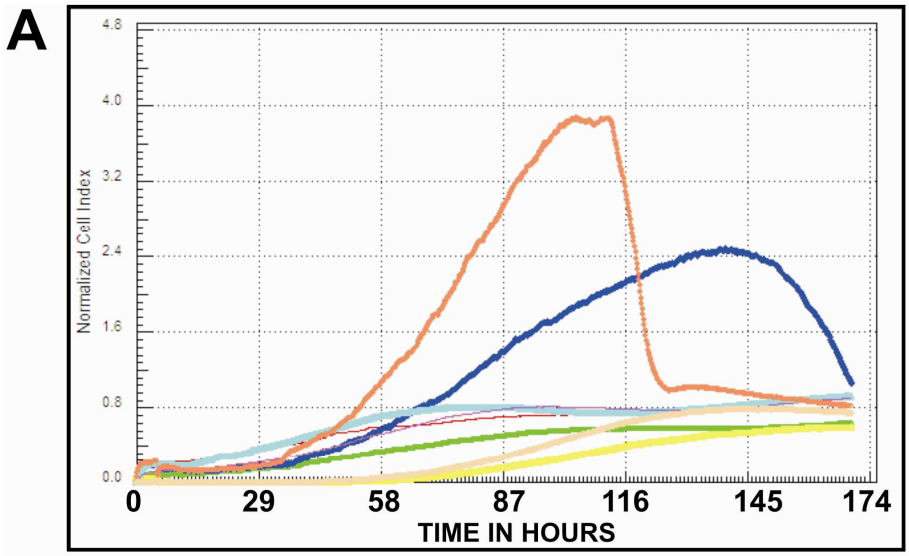

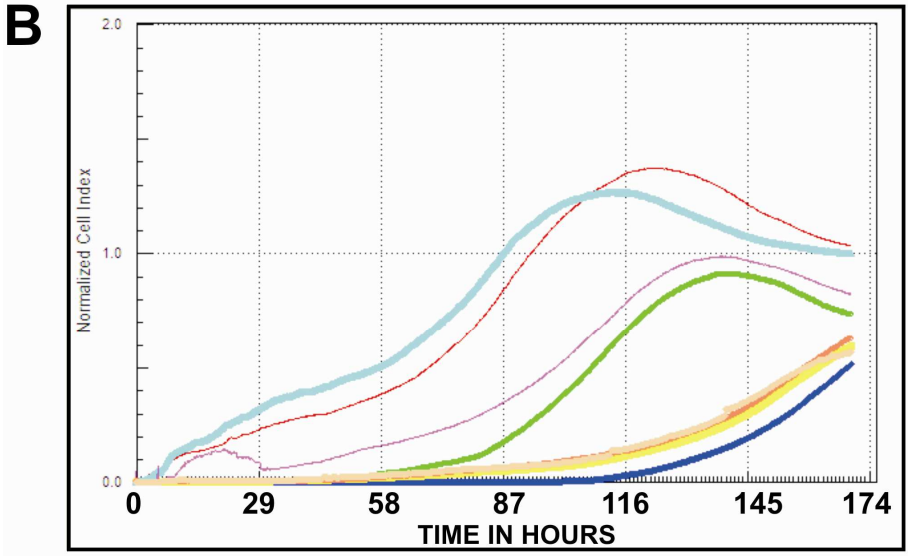

cells densitiy	5000		2500		1250		625	
IFNα	-	+	-	+	-	+	-	+
color code								

Figure 10

Figure 10. Proliferation is inhibited by IFNα in ME15 but not in the IFNα-resistant cell line D10. ME15 and D10 cells were seeded in gold-coated 96 well plates at the indicated concentrations. Cell density refers to number of cells seeded per well in 100µl media. Eight hours after seeding cells were stimulated with IFNα (1000 U/ml). Real-time proliferation was monitored by measurement of impedance every three minutes over a time range of 174 hours. Cells were normalized ($NCI_{\tau i} = CI_{\tau i}/CI_{nrm\text{-}time}$) at time-point 8 hours post seeding using the ACEA Biosciences' internal software. A. ME15 cells grow best at an initial seeding density of 1250 cells per well and exhibit a marked decrease in proliferation upon IFNα stimulation. B. In contrast, D10 cells exhibit insensitivity to IFNα treatment and the proliferation rate is proportional to the initial cell density.

3.2. Restricted Enhancement of Interferon-alpha Response Gene Induction by S100A2

We have shown previously that the TGFβ-inducible calcium binding protein S100A2 inhibits growth of stably transfected human melanoma cell lines (Foser, Redwanz et al. 2006). The antiproliferative activity however is potentiated by co-stimulation with IFNα, which induces calcium release required for the activation of all calcium binding proteins. Since co-stimulation of cell lines with IFNα and TGFβ further reduces cell growth, we tested whether constitutive expression of S100A2 modulates the induction of IFNα-inducible genes. Thus, we first measured the levels of IFITM3 protein in transgenic lines under conditions of single or combined treatment with TGFβ and IFNα. We observed a significant IFNα-dependent upregulation of IFITM3 protein in the S100A2 transfectants as compared to the precursor cells (figure 11A), which points to transcriptional enhancement. Interestingly, IFITM3 has marked antiproliferative activity and further upregulation could explain the synergistic activity of IFNα and TGFβ on cell growth in non-transfected cells.

We next asked whether constitutive S100A2 expression enhances the transcriptional IFNα response in general and we performed an mRNA expression microarray analysis of S100A2-transfected human ME15 melanoma cells, with untransfected cells as control (figure 11B). Apart from IFNα stimulation, we included TGFβ and the combination of both cytokines in order to detect possible interactions of S100A2 with the TGFβ signaling pathway. In $ME15^{S100A2}$ cells, two clusters of genes are significantly upregulated by over-expression of S100A2 (figure 11B, clusters 1 and 3, table 2). Genes in cluster one do not respond to IFNα in untransfected cells and S100A2 over-expression renders them sensitive. Interestingly, this cluster contains two probes for S100A2 which suggests autoregulation and perhaps an autocrine amplification loop under natural conditions. Apart from apolipoprotein E, β-actin and a dehydrogenase this particular cluster includes mitogen-activated protein kinase kinase 5 (MAP2K5) which is known to stimulate cell cycle progression and its induction is probably required to antagonize complete cycle arrest and apoptosis. The second group of genes (figure 11B, cluster 3) contains IFITM3 and other known IFNα inducible genes like p27, 9-27 or 2-5 oligoadenylate cyclase, as expected. Others, such as ISG15, STAT1 or MHC class 1, are part of a third cluster and insensitive to S100A2 over-expression (figure 11B, cluster 2, and table 2). In contrast to the second cluster (figure 11B, cluster 3), none of these genes has documented antiproliferative activity. In conclusion, S100A2

exhibits a specific modulatory effect on particular gene expression in ME15 cells provided administration of IFNα is given.

We also included the IFNα unresponsive cell line D10 in our analysis in order to detect possible correlations with drug resistance (figure 11B). In these cells, IFNα responses are not impaired but are in general delayed (Certa, Wilhelm-Seiler et al. 2003) which might explain the obvious lack of significant S100A2 mediated enhancement of gene expression. Thus, S100A2 alone does not restore responsiveness to IFNα but requires TGFβ-inducible proteins (Foser, Redwanz et al. 2006).

TGFβ or combined IFNα/ TGFβ responses are in general not modified by recombinant S100A2 expression in ME15 or D10 cells, although certain genes appear moderately downregulated. In summary, this analysis shows interactions of S100A2 with the induction of subsets of IFNα inducible genes in ME15. In addition, the chromosomal copy of S100A2 becomes IFNα responsive in the transgenic ME15 line and S100A2 hence has properties of a cis-acting transcriptional enhancer.

Figure 11. S100A2 modulates transcriptional responses to IFNα and TGFβ. A. Immunoblot detection of IFITM3 in whole cell extracts of ME15 and ME15^{S100A2} (stably over-expressing S100A2) cells stimulated with IFNα (1000 U/ml) for 8 hours. B. Primary cell lines (ME15 and D10) indicated as *P* and transgenic cell lines (ME15^{S100A2} and D10^{S100A2}) indicated as *TG* were treated with IFNα (1000 U/ml), TGFβ (2 ng/ml) or a combination of both cytokines. After 2 days, total RNA was extracted, processed and hybridized to commercial DNA microarrays. The heat map indicates change of gene expression in stimulated *P* vs. non-stimulated *P* cell lines as well as in stimulated *TG* vs. non-stimulated *TG* cell lines. Blue bands indicate down-regulated genes, the red ones show up-regulated genes. Maximum mean was set to 50 and change-factor (CHF) cut off was +/- 2. Maximum blue and red intensities correspond to a range of 10 (indicated as CHF). Clustering was performed using hierarchical clustering including the t-test. Note the clusters of up-regulated genes in ME15^{S100A2} vs. ME15 cells stimulated with IFNα (boxed: cluster 1-3).

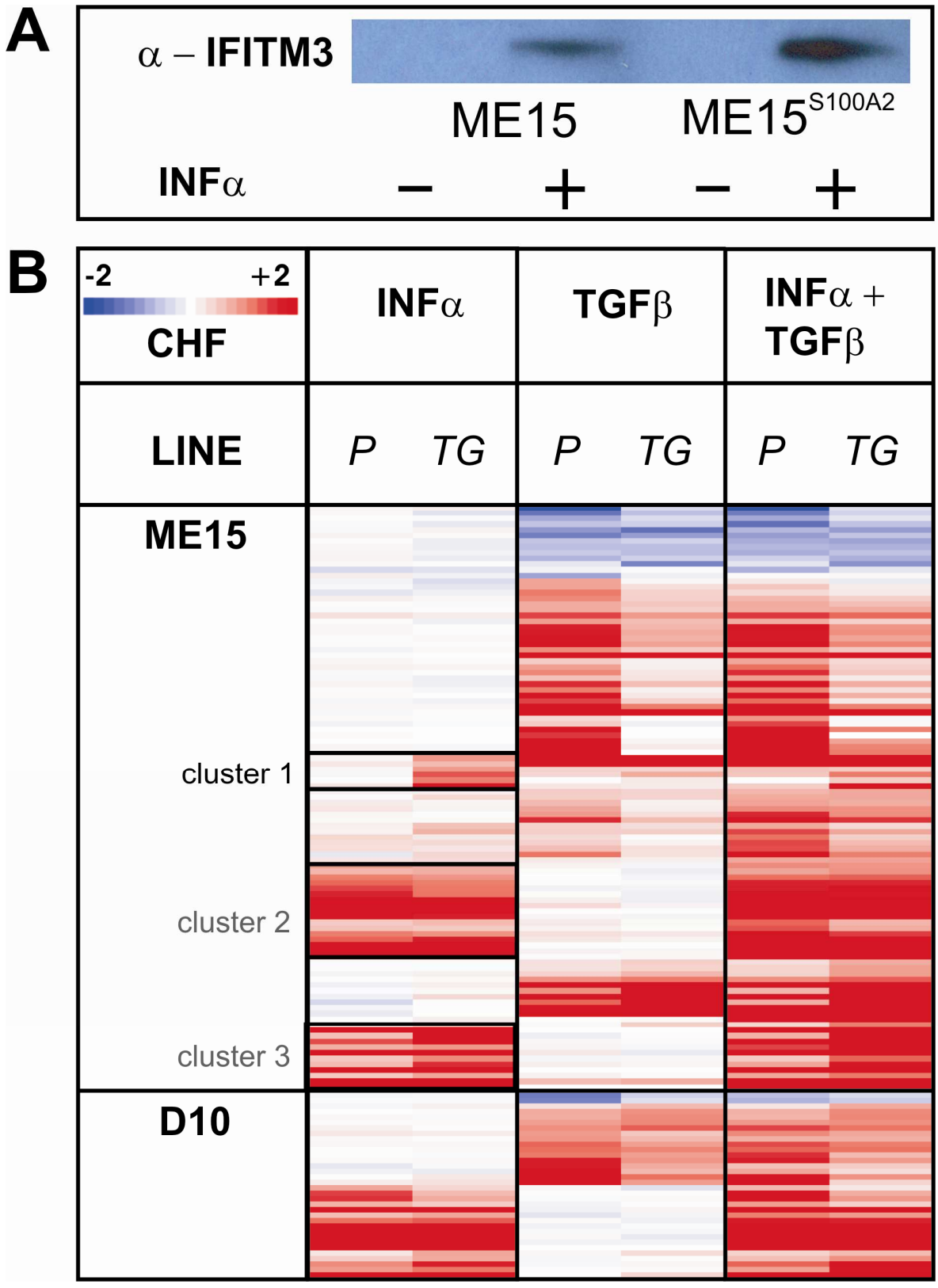
A
α – IFITM3
ME15
ME15S100A2
INFα
–
+
–
+
B
-2
+2
CHF
INFα
TGFβ
INFα + TGFβ
LINE
P
TG
P
TG
P
TG
ME15
cluster 1
cluster 2
cluster 3
D10

Figure 11

Table 2. List of genes in clusters 1 to 3 including change factors (CHGF)

DESCRIPTION	SYMBOL	CHGF ME15	CHGF ME15^{S100A2}
cluster 1			
s100 calcium binding protein a2	S100A2	0.22	2.45
s100 calcium binding protein a2	S100A2	0.63	1.72
apolipoprotein e	APOE	0.17	2.42
actin, beta	ACTB	0.13	3.53
mitogen-activated protein kinase kinase 5	MAP2K5	0.1	2.9
dehydrogenase/reductase (sdr family) member 2	DHRS2	0.64	6.22
cluster 2			
beta-2-microglobulin	B2M	3.3	2.94
interferon-induced protein 35	IFI35	1.83	1.98
beta-2-microglobulin	B2M	2.93	2.51
beta-2-microglobulin	B2M	2.38	2.1
signal transducer and activator of transcription 1, 91kda	STAT1	3.72	3.07
signal transducer and activator of transcription 1, 91kda	STAT1	4.28	3.1
interferon-induced protein with tetratricopeptide repeats 1	IFIT1	11.78	6.35
signal transducer and activator of transcription 1, 91kda	STAT1	16.79	11.77
interferon-induced protein with tetratricopeptide repeats 1	IFIT1	8.59	5.27
ubiquitin-conjugating enzyme e2l 6	UBE2L6	7.78	4.42
lectin, galactoside-binding, soluble, 3 binding protein	LGALS3	1.4	1.71
major histocompatibility complex, class i, f	HLA-F	1.55	1.4
major histocompatibility complex, class i, f	HLA-F	2.96	2.57
major histocompatibility complex, class i, b	HLA-B	3.35	4.37
isg15 ubiquitin-like modifier	ISG15	14.84	14.17
interferon, alpha-inducible protein 6	IFI6	9.09	13.12
isg15 ubiquitin-like modifier	ISG15	18.43	22.7
cluster 3			
small proline-rich protein 2d	SPRR2D	0.5	1.37
interferon-induced protein 44-like	IFI44L	5.89	8.86
interferon induced transmembrane protein 3 (1-8u)	IFITM3	1.6	6.52
interferon induced transmembrane protein 1 (9-27)	IFITM1	9.73	27.19
proteasome (prosome, macropain) subunit, beta type, 9	PSMB9	1.97	2.46
interferon induced transmembrane protein 1 (9-27)	IFITM1	3.62	19.79
interferon-induced protein 35	IFI35	1.43	2.69
interferon-stimulated transcription factor 3, gamma 48kda	IRF9	1.71	4.07
2`,5`-oligoadenylate synthetase 1, 40/46kda	OAS1	5.75	13.62
2`-5`-oligoadenylate synthetase 2, 69/71kda	OAS2	1.42	2.19
bone marrow stromal cell antigen 2	BST2	41.07	62.6
interferon, alpha-inducible protein 27	IFI27	65.94	111.36

Table 3. List of genes regulated in ME15 and ME15^{S100A2} cells clustered in figure 11

dopachrome tautomerase
heat shock protein 90kda alpha (cytosolic), class a member 1
gtpase activating protein (sh3 domain) binding protein 2
glycoprotein m6b
human endogenous retrovirus herv-k22 pol and envelope orf region
dopachrome tautomerase
melan-a
myelin basic protein
chromosome 11 open reading frame 72
tubulin, beta 4
human endogenous retrovirus herv-k22 pol and envelope orf region
histone cluster 1, h4c
asparagine synthetase
tubulin, alpha 1a
dihydropyrimidinase-like 2
cd59 molecule, complement regulatory protein
discoidin domain receptor family, member 1
ae binding protein 1
inhibitor of dna binding 1, dominant negative helix-loop-helix protein
immediate early response 3
collagen, type ix, alpha 3
collagen, type iv, alpha 2
fibronectin 1
fibronectin 1
fibronectin, alt. splice 1
Zyxin
insulin-like growth factor binding protein 5
plasminogen activator, tissue
eukaryotic translation elongation factor 1 alpha 2
plasminogen activator, urokinase receptor
milk fat globule-egf factor 8 protein
jun b proto-oncogene
solute carrier family 20 (phosphate transporter), member 1
tenascin c (hexabrachion)
s100 calcium binding protein a1
s100 calcium binding protein a13
transforming growth factor, beta-induced, 68kda
insulin-like growth factor binding protein 3
insulin-like growth factor binding protein 3
interleukin 1, beta
Galanin
tyrosine kinase, receptor axl, alt. splice 2
calbindin 2, 29kda (calretinin)
axl receptor tyrosine kinase
s100 calcium binding protein a2
s100 calcium binding protein a2
apolipoprotein e
actin, beta
mitogen-activated protein kinase kinase 5
dehydrogenase/reductase (sdr family) member 2

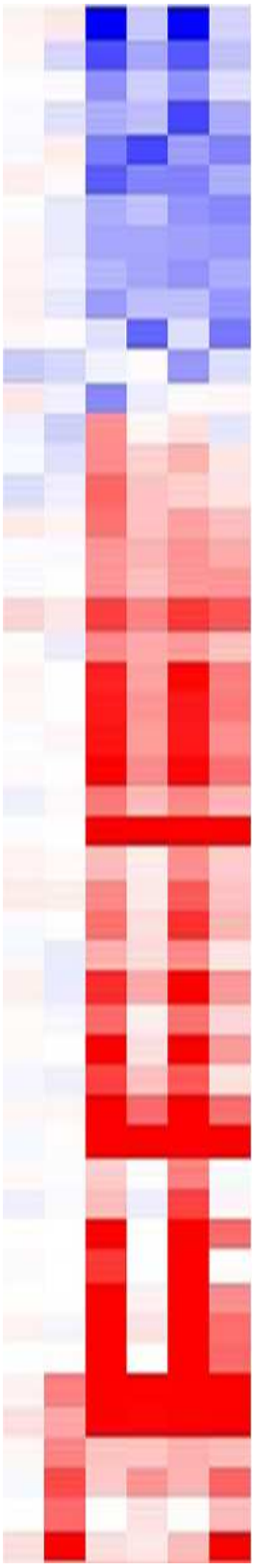

v-erb-b2 erythroblastic leukemia viral oncogene homolog 3 (avian)
udp-gal:betaglcnac beta 1,4- galactosyltransferase, polypeptide 1
secreted phosphoprotein 1 (osteopontin)
secreted phosphoprotein 1 (osteopontin)
prion protein (p27-30)
collagen, type iv, alpha 1
glyceraldehyde-3-phosphate dehydrogenase
2`,3`-cyclic nucleotide 3` phosphodiesterase
major histocompatibility complex, class i, a
tap binding protein (tapasin)
tryptophanyl-trna synthetase
interleukin 1, beta
neuroblastoma breakpoint family, member 14
beta-2-microglobulin
interferon-induced protein 35
beta-2-microglobulin
beta-2-microglobulin
signal transducer and activator of transcription 1, 91kda
signal transducer and activator of transcription 1, 91kda
interferon-induced protein with tetratricopeptide repeats 1
signal transducer and activator of transcription 1, 91kda
interferon-induced protein with tetratricopeptide repeats 1
ubiquitin-conjugating enzyme e2l 6
lectin, galactoside-binding, soluble, 3 binding protein
major histocompatibility complex, class i, f
major histocompatibility complex, class i, f
major histocompatibility complex, class i, b
isg15 ubiquitin-like modifier
interferon, alpha-inducible protein 6
isg15 ubiquitin-like modifier
cyclin d1
cyclin d1
dehydrogenase/reductase (sdr family) member 3
ectodermal-neural cortex (with btb-like domain)
podocalyxin-like
lymphoid enhancer-binding factor 1
serpin peptidase inhibitor, clade a, member 3
nicotinamide n-methyltransferase
insulin-like growth factor binding protein 5
insulin-like growth factor binding protein 5
keratin 81
small proline-rich protein 2d
interferon-induced protein 44-like
interferon induced transmembrane protein 3 (1-8u)
interferon induced transmembrane protein 1 (9-27)
proteasome (prosome, macropain) subunit, beta type, 9
interferon induced transmembrane protein 1 (9-27)
interferon-induced protein 35
interferon-stimulated transcription factor 3, gamma 48kda
2`,5`-oligoadenylate synthetase 1, 40/46kda
2`-5`-oligoadenylate synthetase 2, 69/71kda
bone marrow stromal cell antigen 2
interferon, alpha-inducible protein 27

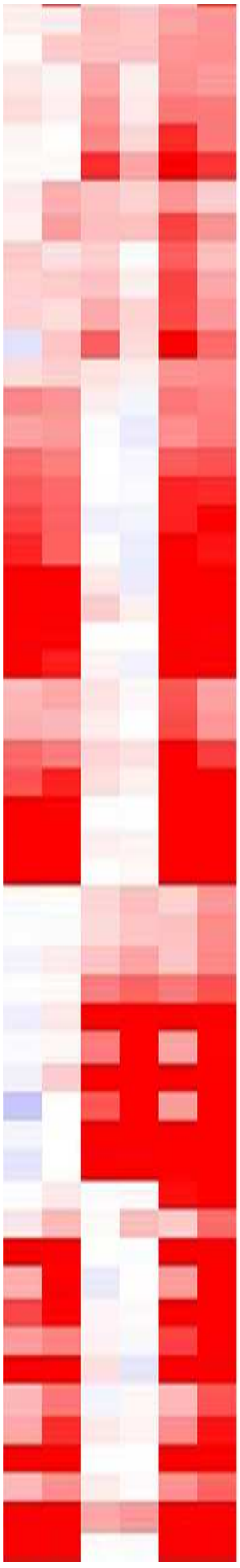

Table 4. List of genes regulated in D10 and D10^{S100A2} cells clustered in figure 11

dopachrome tautomerase
dopachrome tautomerase
ectodermal-neural cortex (with btb-like domain)
fibronectin 1
fibronectin, alt. splice 1
fibronectin 1
collagen, type iv, alpha 1
immediate early response 3
s100 calcium binding protein a13
serpin peptidase inhibitor, clade e, member 2
tenascin c (hexabrachion)
prion protein (p27-30)
insulin-like growth factor binding protein 7
crystallin, alpha b
crystallin, alpha b
s100 calcium binding protein a2
s100 calcium binding protein a2
proteasome (prosome, macropain) subunit, beta type, 8
interferon induced transmembrane protein 1 (9-27)
interferon induced transmembrane protein 3 (1-8u)
2`-5`-oligoadenylate synthetase 2, 69/71kda
interferon, alpha-inducible protein 6
signal transducer and activator of transcription 1, 91kda
signal transducer and activator of transcription 1, 91kda
isg15 ubiquitin-like modifier
isg15 ubiquitin-like modifier
bone marrow stromal cell antigen 2
interferon-stimulated transcription factor 3, gamma 48kda
interferon, alpha-inducible protein 27
2`,3`-cyclic nucleotide 3` phosphodiesterase
major histocompatibility complex, class i, f
major histocompatibility complex, class i, b
major histocompatibility complex, class i, f
interferon induced transmembrane protein 1 (9-27)

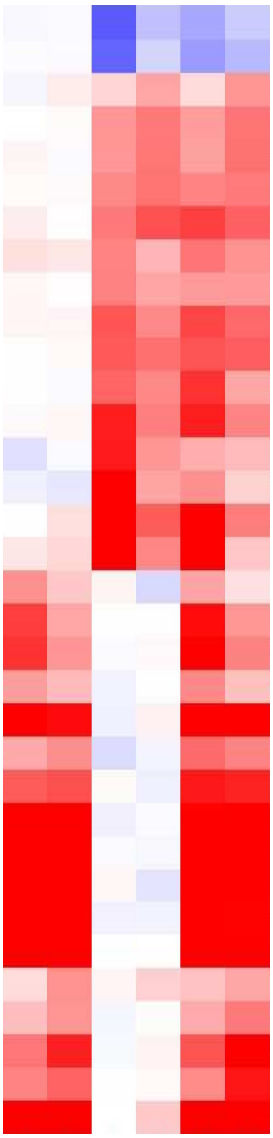

3.3. Cellular Localization of Native and Recombinant S100A2

The S100A2 mediated enhancement of transcription suggests that the molecule is localized in the nucleus where it might function as transcription factor or enhancer. The class of S100 calcium binding proteins contains EF-hand motifs which are required for calcium binding and subsequent activation (reviewed in (Schafer and Heizmann 1996)). Like S100A2, they are quite abundant and frequently associated with tumorigenic disorders where they function presumably as inhibitors of proliferation (Salama, Malone et al. 2008). In particular, S100A2 has been detected in the cytoplasm and nucleus from lung, kidney and corneal epithelium (Nielsen, Heegaard et al. 2005) or predominantly in the nucleus of keratinocytes and breast cancer cells (Mueller, Bachi et al. 1999; Deshpande, Woods et al. 2000) or exclusively in the cytoplasm of epithelial cells (Gimona, Lando et al. 1997). We thus wished to determine the subcellular localization of S100A2 in human melanoma ME15 and D10 cells in order to elucidate a mechanism of action. We included IFNα and TGFβ cytokine stimulation of cells because this may trigger shuttling of the protein between cellular compartments.

Figure 12. S100A2 is localized in the cytoplasm. A. Localization of S100A2 upon cytokine treatment. Upper panel: Immunoblot detection of S100A2 in cell fractions of ME15 and ME15^{S100A2} (stably over-expressing S100A2) cells stimulated with TGFβ (2 ng/ml), IFNα (1000 U/ml) or a combination of both cytokines for 2 days. Lower panel: S100A2 detection by immunofluorescence. ME15, ME15^{S100A2}, D10 and D10^{S100A2} cells were seeded on chamber-slides, treated with both IFNα (1000 U/ml) and TGFβ (2 ng/ml) one day later and fixed and stained after a further two days. B. Localization of over-expressed S100A2-SNAP-tag fusion protein. SNAP-tag was fused either to the N-terminus (3') or the C-terminus (5') of S100A2. Upper panel: Immunoblot detection of S100A2-SNAP fusion proteins in fractions of ME15 cells transiently transfected with S100A2-SNAP-tag. Cell-fractioning was performed 6 and 20 hours post transfection. Lower panel: Localization of S100A2-SNAP fusion proteins in ME15 and D10 cells three days post transfection. Left panel: Unfixed cells were stained with SNAP-cell TMR-star labeling reagents and visualized 3 hours thereafter. Right panel: Fixed cells were stained with S100A2 antibody.

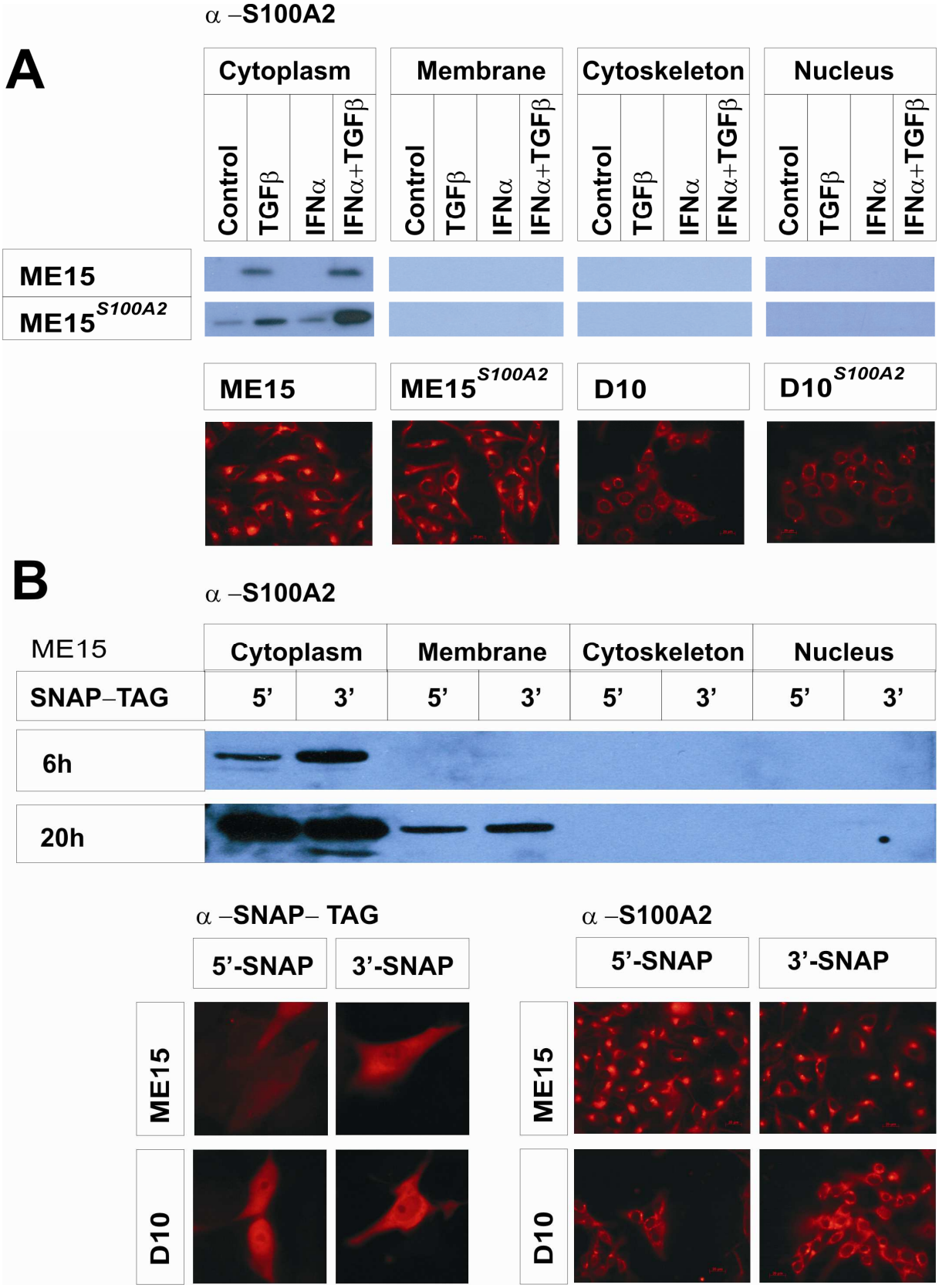
α –S100A2
A
Cytoplasm
Membrane
Cytoskeleton
Nucleus
Control
TGFβ
IFNα
IFNα+TGFβ
ME15
ME15S100A2
ME15
ME15S100A2
D10
D10S100A2
B
α –S100A2
ME15
Cytoplasm
Membrane
Cytoskeleton
Nucleus
SNAP–TAG
5'
3'
6h
20h
α –SNAP– TAG
α –S100A2
5'-SNAP
3'-SNAP
ME15
D10

Figure 12

First, we prepared subcellular fractions of ME15 and ME15^{S100A2} cells by differential centrifugation and probed them with rabbit antibodies to S100A2 in immunoblots (figure 12A, top). In both lines, S100A2 is exclusively detected in the cytoplasm and is virtually absent in the membrane, cytoskeletal or nuclear fractions regardless of cytokine treatment. Even a boost of expression in the S100A2 transgenic line by TGFβ/ IFNα co-stimulation did not induce any translocation into the nucleus. We confirmed this finding by immunofluorescence in IFNα-treated tumor cell lines ME15 and D10 that are either stably transfected with S100A2 or alternatively TGFβ stimulated. In general, the protein is evenly distributed in the cytoplasm. Although in some cells we noted weak punctate staining in the nucleus and enhanced peri-nuclear fluorescence.

As the cellular localization of S100A2 is important for the interpretation of the transcriptional results and possible mode of action, we engineered N- or C-terminal fusion proteins of S100A2 with the SNAP-tag. The SNAP-tag is based on the DNA repair protein AGT and can be post-translationally labeled by fluorescent nucleotide analogs. These bind with high affinity and sensitivity (Keppler, Gendreizig et al. 2003). In contrast to other tags, such as green fluorescent protein, SNAP fusion proteins preserve the subcellular localization of the native polypeptide. Indeed, the S100A2 fusion proteins are predominantly detected in the cytoplasmic fraction of transiently transfected ME15 and D10 cells, regardless of the tag attachment site. In samples analyzed 20 hours after transfection some fusion protein is present in the membrane fraction but is undetectable in nuclei (figure 12B).

Next, we labeled the fusion protein with TMR-Star and inspected the cells microscopically. This resulted in bright, homogeneous fluorescence in the cytoplasm and somewhat reduced in the nucleus, which was in disagreement with the immunoblotting results above (figure 12B, bottom, left panels). We therefore detected the S100A2 domain in the fusion protein with antibodies and obtained virtually the same staining pattern as with native or recombinant S100A2 (figure 12B**,** bottom, right panels). Consistent with previous findings S100A2 in contrast to other S100 proteins does not relocalize to different compartiments of the cell upon calcium elevation in the cytoplasm (Mueller, Bachi et al. 1999). We conclude that S100A2 is predominantly localized in the cytoplasm of human melanoma cells, which eliminates to a large extent the possibility that S100A2 is a component of transcriptional activator complexes operating in the nucleus.

3.4. Core Promoter Methylation Modulates Expression Levels of S100A2 and IFITM3

The cytoplasmic location of S100A2 excludes a direct involvement in transcriptional regulation, so we addressed the question of S100A2-mediated transcriptional enhancement on an epigenetic level. The S100A2 promoter is known to be methylated (Rehman, Cross et al. 2005) and this suggests a possible link between S100A2 and DNA methylation. We stimulated cells with the cytokines as above but included incubation with the cytosine analog 5-aza-2'-deoxycytidine (DAC), which cannot be methylated after incorporation into chromatin, and also actively inhibits DNA methyltransferases (DNMTs). We observed a significant upregulation of S100A2 expression in DAC-treated ME15 cells as compared to cells that were stimulated with TGFβ alone (figure 13A). As expected, IFNα did not induce this gene and co-stimulation with both cytokines boosted expression in untreated cells as previously shown (Foser, Redwanz et al. 2006). Interestingly, the levels of S100A2 in stably transfected cells were not modified by either treatment, including TGFβ, suggesting a certain expression threshold that cannot be exceeded without cell damage or proliferation arrest. Consistent with previous microarray data (Foser, Redwanz et al. 2006), S100A2 is inducible in untreated D10 cells but here the impact of DAC is less pronounced. The overall levels of S100A2 in stably transfected cells are higher and D10 may be less sensitive to S100A2 over-expression due to an epigenetic malfunction of D10 cells. In conclusion, DAC treatment increases the response of the S100A2 gene to TGFβ stimulation in ME15 cells suggesting a methylation dependency, as has been described before (Lee, Tomasetto et al. 1992; Wicki, Franz et al. 1997).

We next analyzed expression of the IFNα-inducible gene IFITM3 in the same samples, because stable over-expression of S100A2 boosts IFITM3 protein levels (figure 11). Interferon-inducible genes have been shown to be silenced epigenetically (Naka, Abe et al. 2006) and we suggested a deterioration in the methylation pattern of the IFITM3 promoter as an additional layer of gene expression control. In untransformed ME15 cells, IFITM3 protein expression is detectable after 12 hours of IFNα exposure and as expected TGFβ does not activate this gene (figure 13B, left blot). Analogous to protein expression of the TGFβ-induced S100A2, treatment with DAC results in a clear, time dependent upregulation of IFITM3 protein by IFNα. Expression levels were even more enhanced after 51 hours. In addition, protein expression commences at earlier time points in DAC-treated cells. We noted that DAC treatment alone is sufficient to trigger IFITM3 expression in the absence of IFNα

(figure 13B**,** left blot, arrowhead). Consistent with the S100A2 expression mode described above, DAC treatment does not alter expression levels of IFITM3. IFITM3 is however clearly upregulated by S100A2 expression (figure 13B, second blot from left), when compared to induction in control ME15 cells under comparable blotting and exposure conditions (figure 13B, left blot). As above, the detected levels of IFITM3 are probably at maximal tolerated levels before complete cell cycle arrest occurs. At 51 hours though, IFITM3 expression levels drop in the absence of DAC, indicating a natural mechanism of gene silencing in the presence of endogenous S100A2.

In D10 cells, IFITM3 is deregulated for unknown reasons (figure 13B, third blot from left) (Certa, Wilhelm-Seiler et al. 2003). As previously shown, IFNα stimulation further upregulates IFITM3 levels and we note here that D10 cells lack IFNα-inducible antiproliferative activity. (Certa, Seiler et al. 2001). This IFITM3 upregulation is entirely DAC-insensitive which suggests a methylation-related defect in these cells. In $D10^{S100A2}$ cells, expression is further boosted so that maximal levels are already achieved 6 hours after stimulation. In contrast to untransfected D10 cells, IFITM3 expression drops back to baseline levels after 24 hours under all conditions (figure 13B, right blot). Together, these results suggest that DAC treatment increases promoter sensitivity in ME15 cells resulting in an earlier onset of induction and higher as well as more persistent protein levels in comparison to non-treated cells. Stable S100A2 expression upregulates IFITM3 in both ME15 and D10 cell lines in a similar manner to the DAC treatment, but by a mechanism which is largely DAC insensitive.

In order to verify our suggestion that DAC increases promoter sensitivity to IFNα, ME15 and $ME15^{S100A2}$ cells were treated with DAC and thereafter with low doses of IFNα (100U and 10U instead of 1000U) (figure 13C). As expected, cells exhibited high sensitivity to even very low levels of IFNα in the presence of DAC. Note that IFITM3 is upregulated with DAC treatment even in the absence of administered IFNα (figure 13B, star). This finding correlates well with the constitutive expression of IFITM3 in D10 cells and the DAC treatment insensitivity that D10 cells exhibit.

In summary, DAC-mediated demethylation of CpG sites enhances the responsiveness of the IFITM3 and S100A2 promoters to IFNα or TGFβ in ME15 cells, whilst no significant DAC-mediated modulation occurs in the IFNα-resistant cell line D10. This strongly suggests that CpG methylation is involved in the regulation of the IFITM3 core promoter, particularly in ME15 cells.

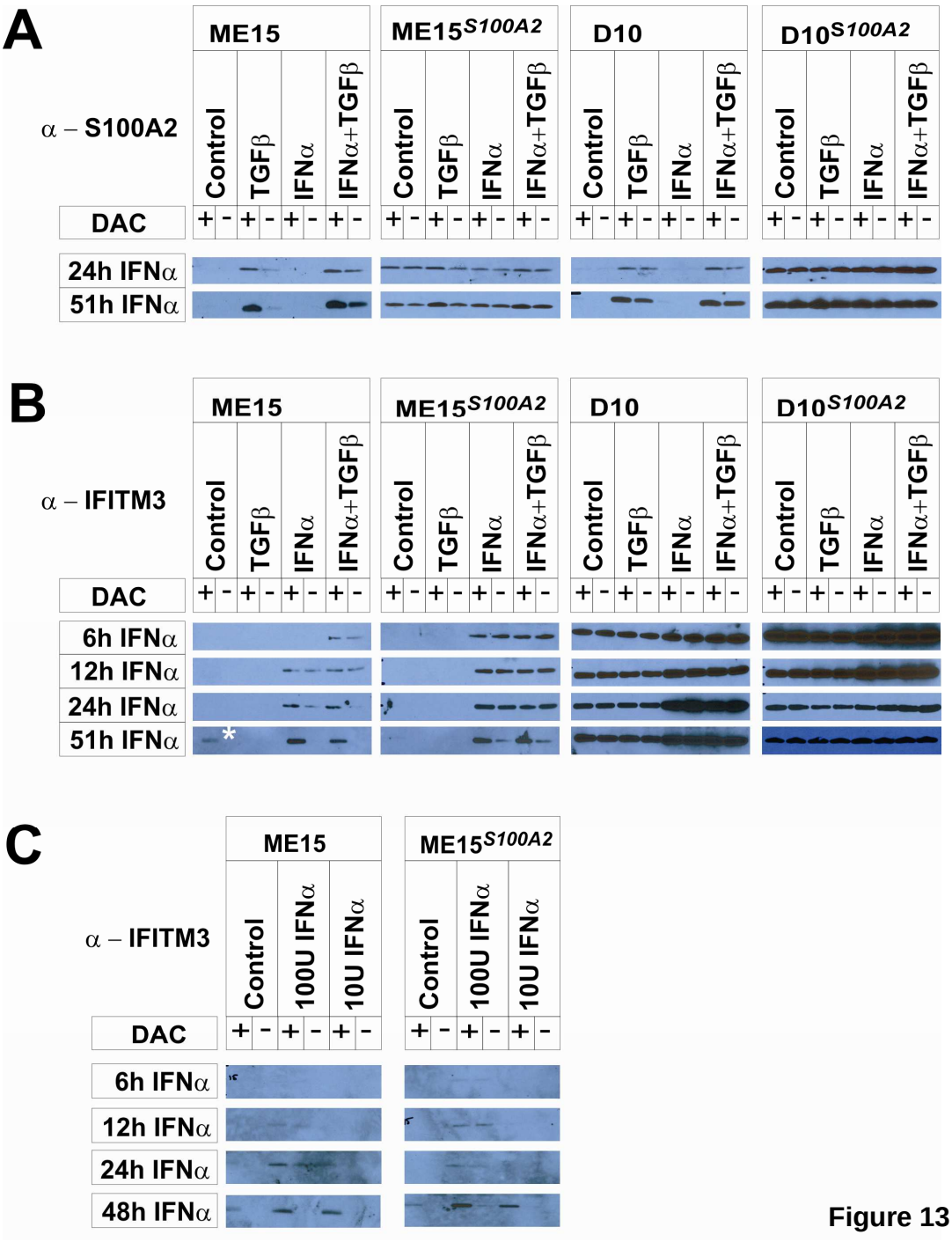

Figure 13

Figure 13. 5-Aza-2'deoxycytidine (DAC) modulates cytokine-induced changes in S100A2 (A) and IFITM3 (B and C) protein levels. IFNα-sensitive ME15 and ME15^{S100A2} (stably over-expressing S100A2) cells, and IFNα-resistant D10 and D10^{S100A2} cells were stimulated with TGFβ (2 ng/ml), IFNα (1000 U/ml) or a combination of both cytokines, in addition to DAC (2 µg/ml). Immunoblot detection of either S100A2 or IFITM3 was performed using total cell extracts from interferon stimulation time points 6h, 12h, 24h or 51h. Note expression of IFITM3 in DAC treated ME15 cells in the absence of administered IFNα (star). Panel C shows IFITM3 expression upon stimulation with different IFNα concentrations plus/ minus DAC treatment.

3.5. No Restoration of Interferon-alpha Sensitivity in D10 Cells upon S-Adenosyl-methionine Supplementation

We have shown that the IFNα-inducible IFITM3 protein exhibits DAC sensitivity in the IFNα-sensitive cell line ME15. However, when the IFNα-resistant cell line D10 is treated with DAC no changes in IFITM3 expression or S100A2 expression are detectable (figure 13). Since IFNα resistance is known to involve DNA methylation we suggested a possible malfunction in the DNA methylation mechanism (Kulaeva, Draghici et al. 2003; Naka, Abe et al. 2006; Reu, Bae et al. 2006). This might include the de novo methylase DNA methyltransferase 3 (DNMT3) or the maintenance methylase DNA methyl transferase 1 (DNMT1) (Ehrlich 2003). It is known that DNMT1 activity decreases in senescent cells leading to hypomethylation (Lopatina, Haskell et al. 2002) and methyltransferases are proposed to be involved in proliferation control (Young and Smith 2001). It was found that a decrease in DNMT1 leads to growth arrest and even to apoptosis and knock down of DNMT1 promotes upregulation of growth control genes such as p21 and RASSF1A (Beaulieu, Morin et al. 2002; Kassis, Zhao et al. 2006). DNMTs exert their methyltransferase activity by using S-adenosyl-methionine (SAM) as methylgroup substrate and one possibility of impairement is the lack of methylgroups for appropriate DNA methylation. Critical levels of S-adenosyl-methionine (SAM) are crucial for functional DNA methylation and we decided to investigate IFITM3 as well as S100A2 expression upon SAM supplementation especially since SAM is furthermore known to restore sensitivity to IFNα in resistant HCV patients (Duong, Christen et al. 2006).

We incubated ME15 and D10 cells with TGFβ, IFNα and a combination of both in the presence or absence of SAM. S100A2 and IFITM3 protein levels were analysed 6, 25 and 50 hours later.

Figure 14. S-adenosyl-methionine (SAM) is not sufficient to restore IFITM3 gene expression control in D10. ME15 and D10 cells were supplemented with SAM (160 mM) and treated with IFNα (1000 U/ml), TGFβ (2 ng/ml) or a combination of both cytokines. Immunoblot detection of either S100A2 (A) or IFITM3 (B) was performed using total cell extracts from interferon stimulation time points 6, 24 or 50h.

ME15 and D10 cells did not exhibit significant differences in S100A2 expression in the absence or presence of SAM at all three time points (figure 14A). There was a slight indication that SAM treatment might suppress S100A2 expression at the earliest investigated time point (figure 14A, 6h). IFITM3 is known to reach maximum expression levels 6 hours after IFNα treatment but SAM supplementation did not visibly alter IFITM3 epression in ME15 cells (figure 14B). In D10 cells IFITM3 is deregulated and IFNα boosts expression further. SAM treatment failed to influence IFITM3 expression significantly, though one could suggest some decrease of IFITM3 expression in the presence of SAM in the control and also the TFGβ samples at the 6 and 25 hours time points (Figure 14B). Nevertheless, SAM was not able to silence IFITM3 expression in control D10 cells indicating that the methylation impairement in D10 cells does not result from insufficient SAM levels.

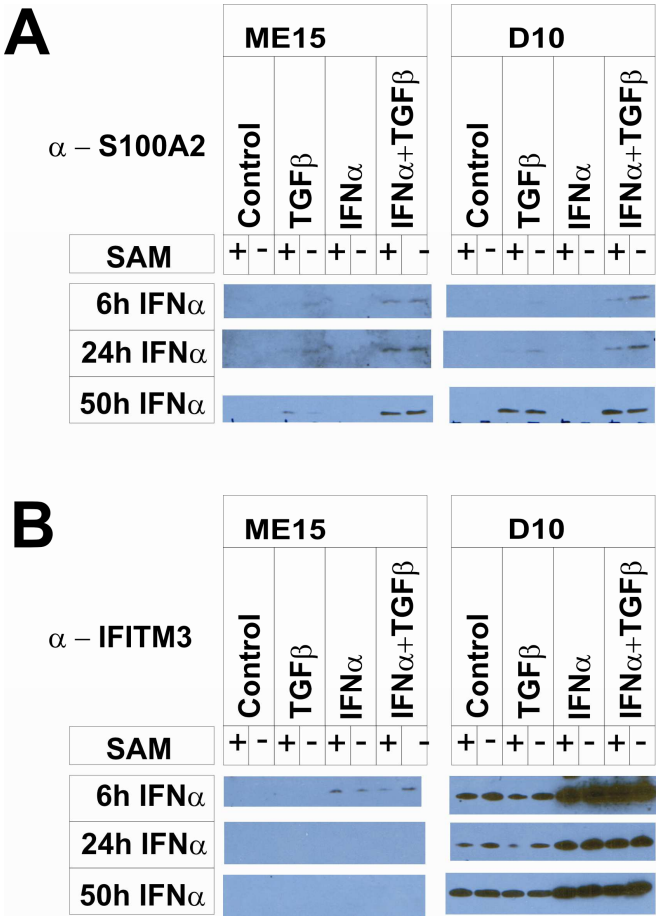

Figure 14

3.6. Lower Response to Interferon-alpha Upon *In Vitro* Methylation

In D10 cells the methylation machinery seems to be impaired (figure 13) and SAM supplementation failed to restore IFITM3 expression control (figure 14B). To investigate the methylation defect observed in figure 13 we decided to introduce *in vitro* methylated plasmids into D10 cells in order to find possible defects in the DNA methyltransferases (DNMTs). For this reason, we transfected both D10 and ME15 cell lines with untreated IFITM3 and IFI6 (interferon inducible protein 6) plasmids described earlier (Brem, Oraszlan-Szovik et al. 2003) as well as SssI methylase-treated plasmids. In order to verify the results from above (figure 14) we included SAM in this experiment. As expected, IFITM3 as well as IFI6 were expressed upon IFNα stimulation in both cell lines. In contrast to previous findings (Brem, Oraszlan-Szovik et al. 2003) D10 cells did not exhibit any differences in expression to ME15 cells and in consistence with the results above SAM supplementation did not alter protein expression. Gene expression of the *in vitro* methylated plasmids was suppressed in both ME15 and D10 cell lines to comparable levels suggesting functional DNMT1 activity in both cell lines. As expected IFNα induced IFITM3 and IFI6 luciferase activity in a proportional manner though without reaching expression levels of methylase-untreated plasmids. These findings rule out a direct malfunction of DNMT1 in D10 cells and the methylation defect found in figure 15 most likely is more complex than we initially thought and might also include other pathways.

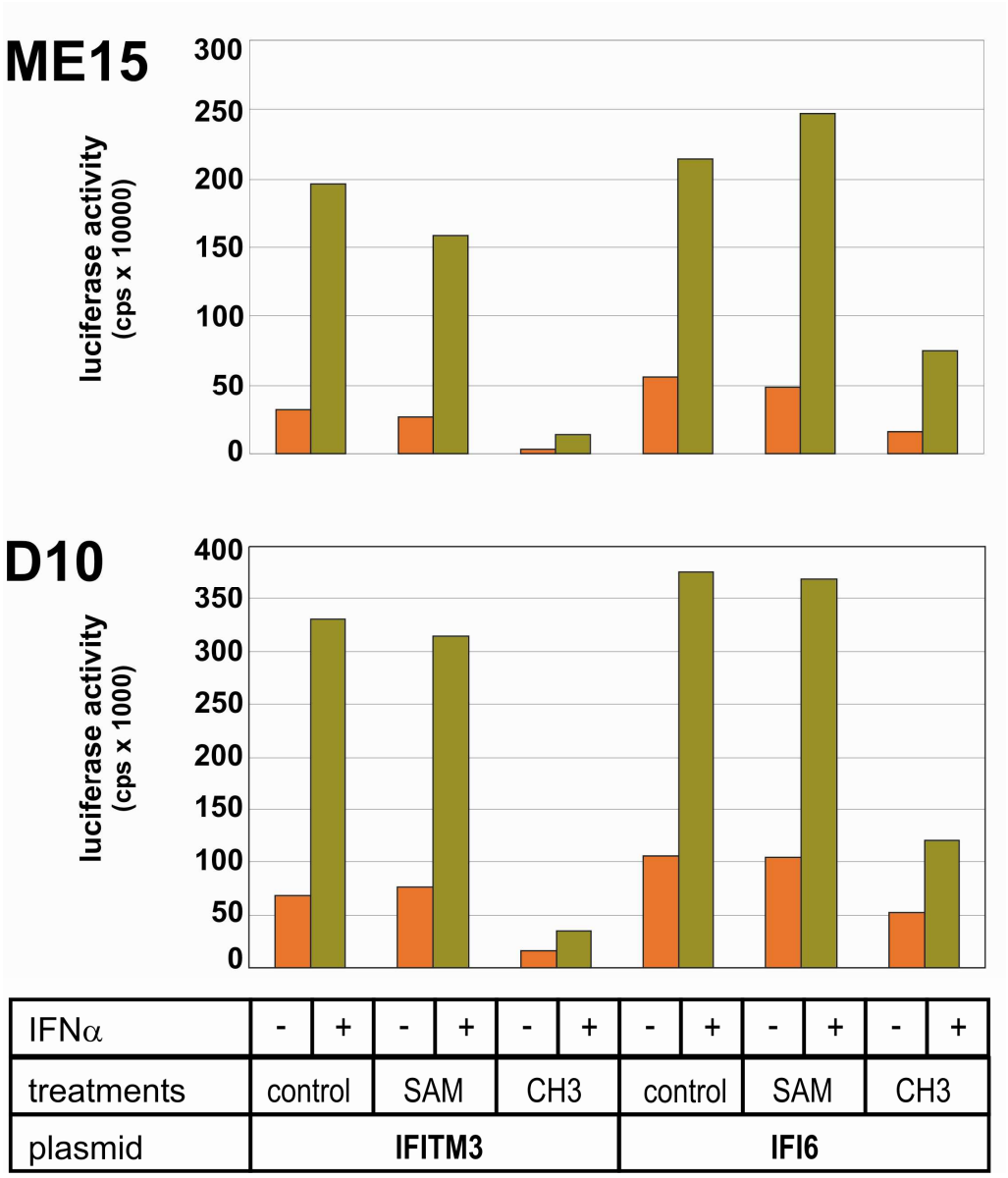

Figure 15

Figure 15. *In vitro* methylated IFITM3 luciferase reporter plasmids do not exhibit any difference in activity in ME15 versus D10 cells. ME15 and D10 cells were transfected with either an IFITM3 luciferase reporter plasmid or an IFI6 luciferase reporter plasmid. Plasmids were *in vitro* methylated before transfection and luciferase activity was compared to non-methylated plasmids with or without SAM supplementation in the media. To induce luciferase activity cells were treated with IFNα for 6 hours.

3.7. ME15 and D10 Cells Exhibit Chromosome Aberrations

To approach the question of a potential methylation machinery defect in D10 cells from another direction we decided to find out whether methylation patterns as well as IFITM3 expression control in D10 cells can be rescued by ME15 cells. For this reason we created tetraploid cells by fusion of ME15 and D10 cells. In order to assure tetraploidity we stably transfected both cell lines with their own antibiotic resistance gene and selected the tetraploid cell line MDbla (for ME15 resistant to puromycin and D10 resistant to blastomycin) under antibiotic pressure.

We first investigated IFITM3 expression both in control as well as IFNα-treated MDbla cells and included the $D10^{S100A2}$ cells as an internal standard. The MDbla cells exhibited deregulated IFITM3 expression indicating that the ME15 cell line was not able to rescue the D10 cell line regarding its IFITM3 gene expression control (figure 16A). Note though that in this newly generated cell line IFITM3 is not visibly inducible by IFNα. In order to verify the tetraploid nature of MDbla we measured the DNA content of all three cell lines, ME15, D10 as well as MDbla by FACS. Unfortunately we realized that MDbla cells did not exhibit the complete tetraploid feature we expected (figure 16B). DNA content is markedly higher but did not double in the course of ME15 and D10 fusion (figure 16B, red lines indicate relative DNA content). In order to verify these findings we decided to investigate the chromosomal content of all three cell lines and performed karyotyping which revealed chromosomal aberrations (figure 16C). Figure 16C shows chromosomes of one individual cell per cell line and it is very clear that chromosomes exhibit massive aberrations. This hold true for all 15 individual cells that were analysed. None of them is comparable to the other with chromosomal distribution being absolutely arbitrary.

In conclusion, ME15 and D10 cells exhibit massive chromosomal aberrations and one could suppose epigenetic malfunctions which are known to be associated with chromosomal instability (Ehrlich 2003). Unfortunately tetraploidity was not achieved in the MDbla cell lines probably due to the original DNA content of ME15 and D10 cells. Nevertheless, DNA content was enhanced in MDbla cells and they furthermore exhibit complete IFNα insensitivity.

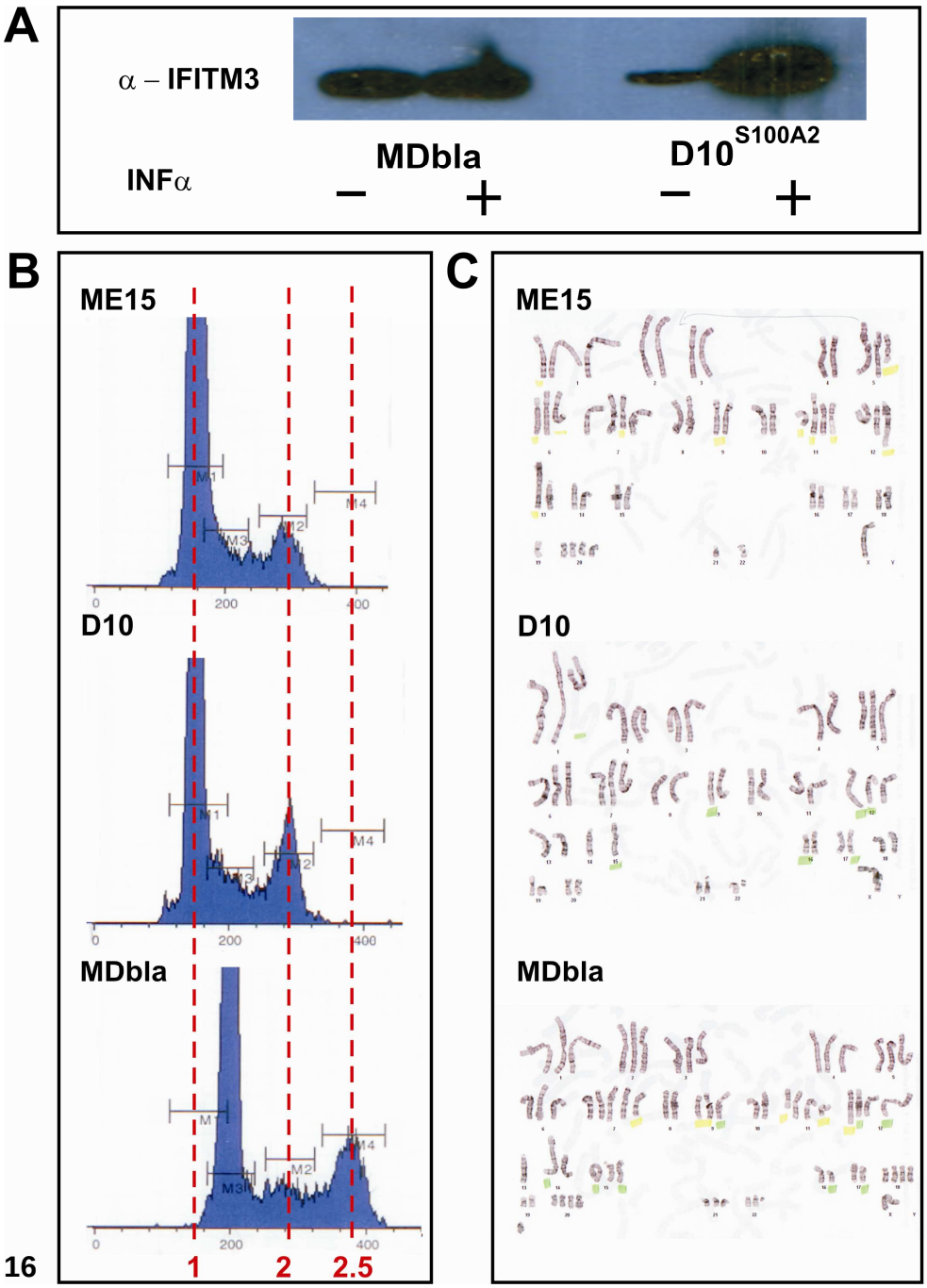

Figure 16

Figure 16. ME15, D10 and the tetraploid cell line MDbla, which is a fusion of ME15 and D10 cells, exhibit massive chromosomal aberrations. MDbla cells were stimulated with IFNα (1000 U/ml) for 8h and immunoblots against IFITM3 were performed from total cell extracts. $D10^{S100A2}$ were included as a positive control (A). ME15, D10 and MDbla cells were labeled with propidium iodide and DNA content was measured using a standard FACS assay (B). Red lines indicate the G1 and S phase in ME15 and D10 cells and also the S phase in MDbla. MDbla cells are clearly not tetraploid. In order to verify the DNA content of MDbla cells, cells underwent karyotyping (C). Here one cell per cell line is depicted demonstrating massive chromosome aberration.

3.8. DNA Wide Methylation State

To this point it is still unclear how the methylation machinery in D10 cells is impaired. The chromosomal aberrations in ME15 and D10 cells may point to impaired methylation in both cell lines (figure 16) as chromosomal aberrations can result from defects in the DNA methylation machinery; a point mutation in DNMT3b has been shown to be involved in ICF disease (Xu, Bestor et al. 1999), RTT syndrome that is known to be caused by dysfunctional MeCP2 protein exhibits deregulation of nuclear architecture (Matarazzo, De Bonis et al. 2009). Additionally genetic instability has been associated with aberrant DNA methylation in liver cirrhosis (Kondo, Kanai et al. 2000). This led us to wonder whether ME15 and D10 cells exhibit genome wide DNA methylation differences. Furthermore, if D10 cells have a defect in the DNA methyltransferase this would also lead to genome-wide demethylation. We therefore investigated CpG methylation genome-wide using Illumina microarrays. In order to monitor a possible demethylating effect of IFNα ME15 cells incubated with IFNα for one hour were included in this study.

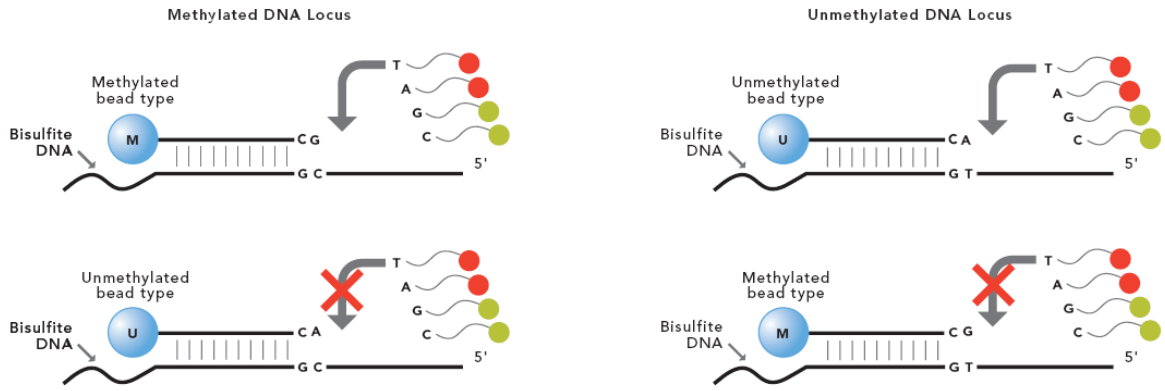

Figure 17

Figure 17. The Infinium assay for methylation. **Weisenberger, D. J., D. V. D. Berg, et al. (2008). "Comprehensive DNA Methylation Analysis on the Illumina® Infinium® Assay Platform." Illumina.** (Weisenberger, Berg et al. 2008)

The Illumina methylation assay includes 14 495 genes with 27 578 CpG sites resulting in an average of two CpG sites per promoter, arrayed on the Infinium HumanMethylation27 BeadChip (Weisenberger, Berg et al. 2008). The technology used to acquire results is illustrated in figure 17. Illumina beads carry either oligos

specific for the methylated or demethylated CpG sites and bisulfite-treated DNA hybridizes. Bisulfite treatment leads to deamination of cytosines given these sites are not protected by a methylgroup. Upon replication of the DNA thymidine is incorporated at the deaminated cytosine sites. The resulting 'point mutation' can then be detected by sequencing. In the Illumina assay the probe is extended with fluorescence-labelled nucleotides according to the methylation of the original sample DNA. Once fluorescence data is collected by the Ilumina scanner a ratio is then calculated between the intensity of the "methylation bead" vs the "un-methylation bead" which is called the beta-value. This beta-value lies between zero and one, and a value below 0.2 indicates a demethylated site whereas values above 0.8 indicate complete methylation for the according CpG site.

In our study beta-values were acquired using Illumina's internal Beadstudio software. Beta-values of ME15 and D10 cells were compared with each other and no major differences in methylation can be observed between the two cell lines, or between the untreated and IFNα-stimulated ME15 cells (figure 18 and 19). This result excludes a direct defect of the methylation machinery such as DNMTs in D10 cells, and ultimately supports the earlier findings in this work. If anything, the distribution of beta-values over all investigated CpG sites demonstrates that ME15 cells exhibit a slightly higher percentage of demethylated CpGs (figure 18). In order to compare single CpG sites with each other the according beta-values established in ME15 and D10 cells were subtracted resulting in a beta-value-difference. Of all the almost 28 000 measured CpG sites only a fraction exhibits a beta-value-difference of at least 0.6). In tables 5 and 6 genes exhibiting the absolute beta-value-difference of more than 0.6 are listed. D10 cells exhibit a generally higher level of methylated CpGs in more genes than ME15 cells (159 in D10 cells and 32 in ME15 cells). Interestingly, D10 cells have 1736 CpG sites that exhibit a higher methylation level (beta-value-difference of at least 0.2) than the corresponding ME15 sites, whereas ME15 cells have only 844 CpG sites that are more highly methylated than the equivalent sites in D10 cells (figure 19). This general impression is consistent with the data shown in figure 18. As ME15 cells treated with IFNα showed no difference in their methylation pattern we conclude that one hour of IFNα stimulation does not alter methylation patterns in ME15 cells (data not shown). It remains unclear why D10 cells exhibit a slightly higher overall CpG methylation than ME15 cells.

For the IFITM3 gene there is one CpG site measured in this assay and the beta-value is at approximately 0.9 in ME15 and 0.6 in D10 cells (figure 21B). Therefore the beta-value-difference in this CpG site is rather minimal and it is difficult to postulate demethylation of the IFITM3 promoter in D10 cells from this one single

CpG site only. Again ME15 cells treated with IFNα contain the same methylation level for the IFITM3 CpG site and IFNα most likely does not modulate methylation levels after one hour of incubation.

In conclusion, the hypothesis of a genome-wide difference in DNA methylation was not supported with this finding. However, there are DNA methylation differences in some CpG sites, one of which is in the IFITM3 promoter. Since only one to two CpG sites were investigated per promoter, e.g. gene, the possibility of major differences in the DNA methylation patterns is not excluded. It is therefore necessary to investigate DNA methylation in more detail.

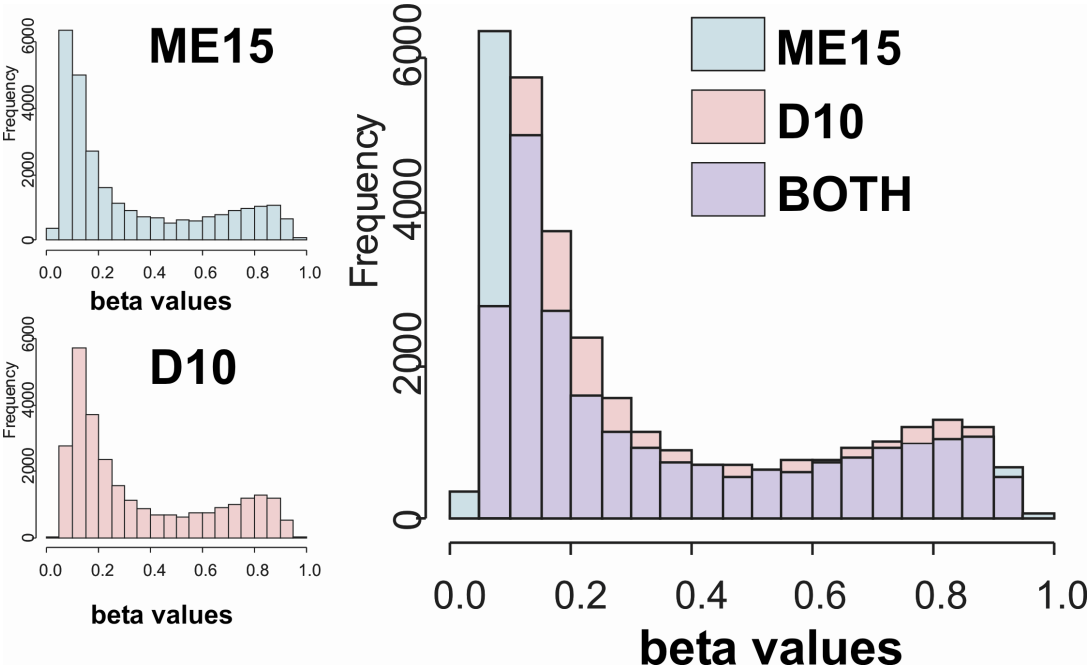

Figure 18

Figure 18. Genome-wide DNA methylation screening reveals only a slight difference in methylation of ME15 and D10 cells. Bisulfite-treated genomic DNA from ME15 and D10 cells was processed and hybridizised to the Illumina Infinium HumanMethylation27 BeadChip. Single methylation sites were analyzed and the internal Illumina software calculated the ratio of methylated versus non-methylated CpG sites to yield beta-values between 0.0 and 1.0. Beta-values between 0.0 and 0.2 are considered demethylated whereas beta-values above 0.8 indicate complete methylation. Frequency of methylation occurrence is shown on the left. Genome-wide beta-values from a total of > 27000 CpGs of ME15 (blue) and D10 (red) are plotted against each other. In general, beta-value distribution is comparable between the two cell lines, with ME15 showing a higher number of unmethylated genes than D10. ME15 vs IFNα treated ME15 are not displayed since there is no difference in methylation.

Table 5. Illumina Chip methylation status with beta-values ME15 > D10

SYMBOL	ME15	D10	ANNOTATION	Difference
PSAT1	0.957	0.045	phosphoserine aminotransferase 1	0.912
CNIH3	0.944	0.136	cornichon homolog 3	0.808
CAV1	0.935	0.145	caveolin 1, caveolae protein, 22kDa	0.790
MKRN3	0.871	0.097	makorin ring finger protein 3	0.774
SERHL	0.959	0.186	serine hydrolase-like	0.773
CHST3	0.926	0.155	carbohydrate (chondroitin 6) sulfotransferase 3	0.770
AQP3	0.864	0.102	aquaporin 3	0.762
CAV1	0.875	0.120	caveolin 1, caveolae protein, 22kDa	0.755
IGFBP7	0.916	0.172	insulin-like growth factor binding protein 7	0.744
HIST1H1B	0.844	0.103	histone cluster 1, H1b	0.741
MLH3	0.872	0.144	mutL homolog 3 (E. coli)	0.729
HMG20B	0.914	0.187	high-mobility group 20B, BRCA2-associated factor 35	0.727
GOLPH2	0.900	0.177	golgi membrane protein 1	0.724
ACSS3	0.851	0.129	acyl-CoA synthetase short-chain family member 3	0.722
RCSD1	0.820	0.098	RCSD domain containing 1	0.722
FAM13C1	0.873	0.153	family with sequence similarity 13, member C	0.720
ID4	0.811	0.095	inhibitor of DNA binding 4, dominant negative helix-loop-helix protein	0.716
TEKT2	0.834	0.121	tektin 2	0.714
CCDC65	0.878	0.167	coiled-coil domain containing 65	0.711
FRZB	0.891	0.181	frizzled-related protein	0.709
PAK3	0.874	0.165	P21 protein (Cdc42/Rac)-activated kinase 3	0.709
CSRP1	0.774	0.069	cysteine and glycine-rich protein 1	0.705
MLH3	0.837	0.146	mismatch repair gene MLH3	0.692
GFOD1	0.850	0.162	glucose-fructose oxidoreductase domain containing 1	0.688
CCR10	0.813	0.132	chemokine (C-C motif) receptor 10	0.681
SULF2	0.880	0.201	sulfatase 2	0.679
ACAA1	0.848	0.170	acetyl-Coenzyme A acyltransferase 1	0.679
C1QTNF6	0.764	0.099	C1q and tumor necrosis factor related protein 6	0.665
FRZB	0.842	0.186	frizzled-related protein	0.656
PAX3	0.887	0.235	paired box 3	0.652
PGK1	0.745	0.095	phosphoglycerate kinase 1	0.650
THBS2	0.814	0.164	thrombospondin 2	0.650
RBBP7	0.808	0.162	retinoblastoma binding protein 7	0.646
C9orf142	0.911	0.266		0.645
FXYD5	0.801	0.157	FXYD domain containing ion transport regulator 5	0.644
CAV1	0.782	0.144	caveolin 1, caveolae protein, 22kDa	0.638
DLG1	0.762	0.135	discs, large homolog 1 (Drosophila)	0.626
PSAT1	0.829	0.205	phosphoserine aminotransferase 1	0.624
DDB2	0.796	0.176	damage-specific DNA binding protein 2, 48kDa	0.619
FAM13C1	0.752	0.133	family with sequence similarity 13, member C	0.619
SYNPO2	0.828	0.209	synaptopodin 2	0.619
CNDP1	0.761	0.144	carnosine dipeptidase 1 (metallopeptidase M20 family)	0.618
ZAR1	0.807	0.194	zygote arrest 1	0.613
CUZD1	0.776	0.164	CUB and zona pellucida-like domains 1	0.612
TINAGL1	0.771	0.166	tubulointerstitial nephritis antigen-like 1	0.605
SULF2	0.923	0.321	sulfatase 2	0.602

Table 6. Illumina Chip methylation status with beta-values D10 > ME15

SYMBOL	ME15	D10	ANNOTATION	Difference
CRABP1	0.231	0.831	cellular retinoic acid binding protein 1	-0.601
SYCE1	0.337	0.938	synaptonemal complex central element protein 1	-0.601
INA	0.275	0.875	internexin neuronal intermediate filament protein, alpha	-0.601
LIN7B	0.164	0.765	lin-7 homolog B (C. elegans)	-0.601
TP53INP1	0.074	0.675	tumor protein p53 inducible nuclear protein 1	-0.601
CTSZ	0.272	0.874	cathepsin Z	-0.602
HIST1H4F	0.171	0.774	histone cluster 1, H4f	-0.602
OXCT1	0.253	0.858	3-oxoacid CoA transferase 1	-0.605
DPM1	0.091	0.697	dolichyl-phosphate mannosyltransferase polypeptide 1, catalytic subunit	-0.606
DPM1	0.170	0.777	dolichyl-phosphate mannosyltransferase polypeptide 1, catalytic subunit	-0.607
LDOC1	0.098	0.705	leucine zipper, down-regulated in cancer 1	-0.607
RBM17	0.148	0.758	RNA binding motif protein 17	-0.610
OXCT1	0.187	0.800	3-oxoacid CoA transferase 1	-0.613
KIT	0.324	0.938	v-kit Hardy-Zuckerman 4 feline sarcoma viral oncogene homolog	-0.614
GRIA1	0.233	0.847	glutamate receptor, ionotropic, AMPA 1	-0.614
TMEM163	0.312	0.927	transmembrane protein 163	-0.614
RCN3	0.141	0.756	reticulocalbin 3, EF-hand calcium binding domain	-0.615
CKAP4	0.083	0.698	cytoskeleton-associated protein 4	-0.616
CYYR1	0.147	0.764	cysteine/tyrosine-rich 1	-0.617
GRM6	0.098	0.716	glutamate receptor, metabotropic 6	-0.617
LTF	0.070	0.689	Lactotransferrin	-0.619
LOXL3	0.131	0.752	lysyl oxidase homolog 3	-0.620
ZNF198	0.189	0.809	zinc finger, MYM-type 2	-0.621
CTSZ	0.170	0.792	cathepsin Z	-0.622
NFATC1	0.135	0.759	nuclear factor of activated T-cells, cytoplasmic, calcineurin-dependent 1	-0.623
VSX2	0.199	0.823	visual system homeobox 2	-0.623
CRABP1	0.220	0.844	cellular retinoic acid-binding protein 1	-0.624
COLEC12	0.221	0.846	collectin sub-family member 12	-0.624
CLDN3	0.221	0.846	claudin 3	-0.624
MEG3	0.284	0.910	maternally expressed 3 (non-protein coding)	-0.626
ELAVL3	0.071	0.699	ELAV (embryonic lethal, abnormal vision, Drosophila)-like 3 (Hu antigen C)	-0.628
LASS6	0.087	0.716	LAG1 homolog, ceramide synthase 6	-0.628
ESX1	0.165	0.793	ESX homeobox 1	-0.629
ESRRB	0.131	0.761	estrogen-related receptor beta	-0.630
KLF11	0.197	0.827	TGFB inducible early growth response 2	-0.631
ASCL2	0.184	0.819	achaete-scute complex homolog 2 (Drosophila)	-0.634
FAM150A	0.224	0.860	family with sequence similarity 150, member A	-0.636
PHOX2A	0.154	0.790	paired-like homeobox 2a	-0.637
WSB2	0.289	0.927	WD repeat and SOCS box-containing 2	-0.637
S100A1	0.109	0.748	calcium-binding protein A1	-0.639
RUSC2	0.194	0.833	RUN and SH3 domain containing 2	-0.639
CD8A	0.252	0.891	CD8a molecule, Leu2	-0.639
SLC35C1	0.213	0.854	GDP-fucose transporter 1	-0.641
PCDHAC2	0.090	0.732	protocadherin alpha subfamily C, 2	-0.642

GPX3	0.130	0.772	glutathione peroxidase 3 (plasma)	-0.643
CKAP4	0.166	0.809	cytoskeleton-associated protein 4	-0.643
CTSZ	0.268	0.912	cathepsin Z	-0.644
ALDH1A3	0.245	0.893	aldehyde dehydrogenase 1 family, member A3	-0.648
KIAA0323	0.135	0.785		-0.651
PSTPIP2	0.283	0.935	proline-serine-threonine phosphatase interacting protein 2	-0.652
HPDL	0.077	0.729	4-hydroxyphenylpyruvate dioxygenase-like	-0.652
PNMA6A	0.200	0.853	paraneoplastic antigen like 6A	-0.653
ABHD8	0.219	0.874	abhydrolase domain containing 8	-0.655
CCDC59	0.073	0.728	coiled-coil domain containing 59	-0.655
SUOX	0.194	0.850	sulfite oxidase	-0.655
DEFA5	0.156	0.812	defensin, alpha 5, Paneth cell-specific	-0.656
IMP4	0.122	0.779	IMP4, U3 small nucleolar ribonucleoprotein, homolog (yeast)	-0.656
SEC31L2	0.224	0.881	SEC31-like 2 (S. cerevisiae)	-0.657
ISG20	0.076	0.734	interferon stimulated gene (20kD)	-0.657
PAQR5	0.102	0.760	progestin and adipoQ receptor family member V	-0.658
HIST1H2BI	0.145	0.805	histone cluster 1, H2bi	-0.660
FAIM	0.092	0.752	Fas apoptotic inhibitory molecule	-0.661
RIBC2	0.193	0.857	43A domain with coiled-coils 2	-0.663
CGREF1	0.167	0.831	cell growth regulator with EF-hand domain 1	-0.664
PHLDA3	0.100	0.764	pleckstrin homology-like domain, family A, member 3	-0.664
LIPG	0.189	0.853	lipase, endothelial	-0.665
GADD45G	0.158	0.824	growth arrest and DNA-damage-inducible, gamma	-0.666
ECE1	0.035	0.704	endothelin converting enzyme 1	-0.669
HIST1H4L	0.173	0.842	histone cluster 1, H4l	-0.669
EFCBP2	0.169	0.839	EF-hand calcium binding protein 2	-0.670
GDF2	0.179	0.849	growth differentiation factor 2	-0.670
C10orf107	0.161	0.831		-0.670
FBXO39	0.135	0.807	F-box protein 39	-0.673
THSD3	0.096	0.771	isthmin 2 homolog (zebrafish)	-0.675
KLF14	0.146	0.822	Kruppel-like factor 14	-0.676
SOX11	0.128	0.805	SRY (sex determining region Y)-box 11	-0.676
PTPN20B	0.124	0.801	protein tyrosine phosphatase, non-receptor type 20B	-0.677
SORBS3	0.108	0.787	sorbin and SH3 domain containing 3	-0.679
SOX8	0.201	0.882	SRY (sex determining region Y)-box 8	-0.680
MAGI2	0.103	0.785	membrane associated guanylate kinase, WW and PDZ domain containing 2	-0.682
HIST1H4F	0.152	0.834	histone cluster 1, H4f	-0.683
SOX11	0.207	0.891	SRY (sex determining region Y)-box 11	-0.684
SLC26A11	0.103	0.787	solute carrier family 26, member 11	-0.684
USP51	0.091	0.777	ubiquitin specific peptidase 51	-0.686
NPR3	0.145	0.832	natriuretic peptide receptor C/guanylate cyclase C	-0.687
LZTS1	0.169	0.857	leucine zipper, putative tumor suppressor 1	-0.688
NTSR1	0.226	0.917	neurotensin receptor 1 (high affinity)	-0.691
PXDN	0.157	0.849	peroxidasin homolog (Drosophila)	-0.691
RAC3	0.244	0.937	rho family; small GTP binding protein Rac3	-0.692
ABTB1	0.168	0.861	ankyrin repeat and BTB (POZ) domain containing 1	-0.693
VILL	0.104	0.797	villin-like	-0.693
GLB1L2	0.191	0.885	galactosidase, beta 1-like 2	-0.693
LSR	0.093	0.787	lipolysis stimulated lipoprotein receptor	-0.695
OTOP3	0.164	0.859	otopetrin 3	-0.695

LZTS1	0.186	0.882	leucine zipper, putative tumor suppressor 1	-0.695
TCF12	0.193	0.890	transcription factor 12	-0.697
STXBP6	0.137	0.834	syntaxin binding protein 6 (amisyn)	-0.697
ADAMTS14	0.152	0.852	ADAM metallopeptidase with thrombospondin type 1 motif, 14	-0.700
MGAT1	0.141	0.844	N-glycosyl-oligosaccharide-glycoprotein N-acetylglucosaminyltransferase	-0.703
HMGA2	0.128	0.831	high mobility group AT-hook 2	-0.703
TLX3	0.177	0.881	T-cell leukemia homeobox 3	-0.704
RAB33A	0.180	0.885	Small GTP-binding protein S10	-0.704
GABRQ	0.159	0.865	GABA-A receptor theta subunit	-0.707
TFAP2E	0.183	0.891	transcription factor AP-2 epsilon	-0.707
TCERG1L	0.089	0.797	transcription elongation regulator 1-like	-0.708
GLRA3	0.097	0.805	Glycine receptor, alpha-3	-0.708
CYB561	0.184	0.893	cytochrome b-561	-0.709
NINL	0.068	0.778	ninein-like	-0.710
H1F0	0.140	0.851	H1 histone family, member 0	-0.711
FOXF1	0.096	0.808	forkhead-related activator 1	-0.711
PROK2	0.127	0.842	prokineticin 2	-0.716
SNX22	0.087	0.803	sorting nexin 22	-0.716
SYN2	0.184	0.901	synapsin II	-0.717
ADCYAP1	0.113	0.833	adenylate cyclase activating polypeptide 1	-0.721
SLC44A3	0.142	0.863	solute carrier family; member 3;	-0.721
PPM1M	0.147	0.869	protein phosphatase 1M (PP2C domain containing)	-0.723
SPPL2B	0.124	0.847	signal peptide peptidase-like 2B	-0.724
CRABP1	0.160	0.885	cellular retinoic acid-binding protein 1	-0.725
ALDH1A3	0.129	0.857	aldehyde dehydrogenase 6	-0.727
SEPT10	0.166	0.894	Septin 10	-0.728
BTBD6	0.102	0.831	lens BTB; glucocorticoid receptor AF-1 coactivator-1	-0.729
CELSR3	0.131	0.864	cadherin, EGF LAG seven-pass G-type receptor 3	-0.734
TRHDE	0.100	0.835	thyrotropin-releasing hormone degrading enzyme	-0.735
HIST1H2AJ	0.097	0.833	histone cluster 1, H2aj	-0.737
GLUL	0.180	0.918	glutamate-ammonia ligase (glutamine synthase)	-0.738
MEG3	0.121	0.859	maternally expressed 3 (non-protein coding)	-0.738
ELF4	0.173	0.912	E74-like factor 4 (ets domain transcription factor)	-0.739
MYOD1	0.160	0.902	myoblast determination protein 1	-0.742
HPDL	0.077	0.820	4-hydroxyphenylpyruvate dioxygenase-like	-0.743
IRXL1	0.100	0.848	mohawk homeobox	-0.749
WNK4	0.132	0.883	protein kinase; lysine deficient 4	-0.751
HIST1H3G	0.112	0.863	histone cluster 1, H3g	-0.751
ZNF342	0.122	0.876	zinc finger protein 296	-0.754
ZC3HAV1L	0.062	0.819	zinc finger CCCH-type, antiviral 1-like	-0.757
ARHGAP4	0.155	0.914	Rho-GAP hematopoietic protein C1	-0.760
ESX1	0.142	0.904	ESX homeobox 1	-0.762
CLDN1	0.133	0.897	senescence-associated epithelial membrane protein 1	-0.764
SOX8	0.148	0.912	SRY (sex determining region Y)-box 8	-0.764
AQP11	0.165	0.930	aquaporin 11	-0.765
GSTP1	0.069	0.838	deafness; X-linked 7; fatty acid ethyl ester synthase III;	-0.769
RHBDD1	0.075	0.844	rhomboid domain containing 1	-0.769
SLC5A7	0.119	0.889	solute carrier family 5 (choline transporter), member 7	-0.770
ADCY8	0.148	0.919	Adenylyl cyclase 8; brain	-0.771

ERBB2IP	0.102	0.873	erbb2 interacting protein	-0.771
PRKCZ	0.130	0.907	protein kinase C, zeta	-0.777
RAB33A	0.128	0.910	RAB33A, member RAS oncogene family	-0.782
NAV1	0.104	0.898	neuron navigator 1	-0.794
SPESP1	0.038	0.833	sperm equatorial segment protein 1	-0.794
RPRM	0.087	0.883	reprimo, TP53 dependent G2 arrest mediator candidate	-0.796
ZNF342	0.075	0.873	zinc finger protein 296	-0.798
ISL2	0.063	0.863	Insulin gene enhancer protein ISL-2	-0.800
DMRT1	0.072	0.880	DM domain expressed in testis 1	-0.808
GABRE	0.094	0.903	GABA(A) receptor	-0.809
TP53INP1	0.102	0.912	p53-inducible p53DINP1	-0.809
CTSZ	0.064	0.875	cathepsin X precursor; preprocathepsin P	-0.811
TLX3	0.120	0.934	homeo box 11-like 2	-0.814
TSC22D1	0.091	0.918	transforming growth factor beta-stimulated protein TSC-22	-0.827
FAS	0.060	0.887	tumor necrosis factor receptor superfamily; member 6	-0.827
ENAH	0.057	0.888	isoform b is encoded by transcript variant 2	-0.831
ALDH1A3	0.066	0.905	aldehyde dehydrogenase 6	-0.839
MAGI2	0.046	0.894	activin receptor interacting protein 1	-0.848
MTMR15	0.035	0.959	myotubularin related protein 15	-0.924

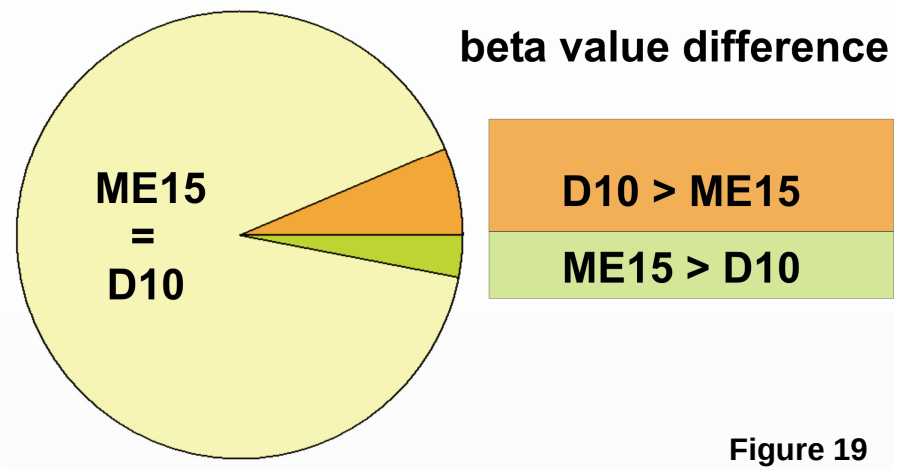

Figure 19. Genome-wide DNA methylation screening reveals only a slight difference in methylation of ME15 and D10 cells. Bisulfite-treated genomic DNA from ME15 and D10 cells was processed and hybridizised to the Illumina Infinium HumanMethylation27 BeadChip. Single methylation sites were analyzed and the internal Illumina software calculated the ratio of methylated versus non-methylated CpG sites to yield beta-values between 0.0 and 1.0. Beta-value-differences were achieved by subtraction of individual beta-values of ME15 and D10 cells. Absolute beta-value-differences [ME15-D10] below 0.2 were plotted against absolute beta-value-differences higher than 0.2. There are 1736 CpG sites with a higher methylation level in D10 cells and 844 CpG sites with a higher methylation level in ME15 cells.

3.9. Methylation State of the IFITM3 Core Promoter in ME15 and D10 Cells.

We have shown above (figure 11, panel B) that recombinant expression of the small calcium binding protein S100A2 enhances IFNα-dependent induction of IFITM3 and S100A2 expression. DNA methylation control of S100A2 core promoter activity has been described (Lee, Tomasetto et al. 1992) and we show in figure 13, panel B, that presence of S100A2 upregulates IFITM3 protein expression to levels comparable to those in DAC-treated ME15 cells. IFITM3 expression levels in D10 cells are neither affected by DAC treatment nor S100A2 over-expression. Nevertheless, the dynamics of IFITM3 expression levels are altered in both ME15 and D10 cells expressing S100A2 compared with the wild type cell lines, independent of DAC treatment. These findings suggest a mechanism in which S100A2-dependent demethylation of the IFITM3 core promoter enhances IFNα responsiveness in ME15 cells and if correct, the model implies that the IFITM3 promoter in D10 is hypomethylated and therefore constitutively active and not responsive to DAC treatment. As genome-wide DNA methylation analysis using the Illumnia Infinium HumanMethylation27 BeadChip only investigates two CpG sites per gene, we decided to study the IFITM3 promoter region in more details, by bisulfite sequencing of a stretch of approximately 500 bp.

We treated ME15 and D10 cells for 1, 6 and 24 hours with 1000 U/ml IFNα before detection of methylated CpG sites by bisulfite sequencing (Frommer, McDonald et al. 1992). To supply S100A2 we either co-stimulated the cells with TGFβ or we used stable S100A2 transfectants of ME15 or D10 cells. Genomic DNA was isolated from cell cultures, treated with sodium bisulfite and the IFITM3 core promoter was amplified by PCR. The amplicons from each of the 32 experimental conditions were subcloned into E. coli, screened by blue/white colony selection and sequenced using an automated capillary sequencer. We then determined the percentage of methylated versus unmethylated C-residues across 19 CpG sites of the IFITM3 core promoter (figure 20). In ME15, ME15^{S100A2} and D10 cells the methylation pattern of control cells (not treated with IFNα) is virtually identical regardless of TGFβ treatment or S100A2 expression (figure 20; '*co'* panels). In D10^{S100A2} CpG sites #492, #434, #425, #366 and #360 are partially demethylated in the presence of TGFβ. This early demethylation pattern is consistent with the dynamics seen in figure 20B, right blot, but is most likely S100A2 independent and caused by other TGFβ inducible pathways (figure 20; lower panel). Consistent with our hypothesis, the overall CpG methylation is notably lower in D10 and D10^{S100A2}

than in ME15 and ME15^{S100A2} and entirely insensitive to IFNα treatment. In particular, the CpG sites directly upstream of the ATG translational start in D10 cells, including sites around the interferon-stimulated regulatory elements (ISRE), are non- or hypomethylated. In summary, the methylation status of the IFITM3 core promoter in D10 cells is largely IFNα treatment independent, although some CpG sites near the 5' end (#512, #492, #434) show IFNα-dependent demethylation.

In ME15 cells dynamic changes in the methylation pattern occur 6 hours after IFNα treatment (figure 20; upper panels). Consistent with our hypothesis, hypo- or demethylation is strictly S100A2 dependent regardless of the supply route. In TGFβ-pretreated ME15 cells demethylation occurs across the entire array of CpG sites 6 hours after IFNα treatment, which coincides with the onset of IFITM3 protein expression. In the ME15^{S100A2} cells a similar CpG demethylation pattern appears 6h after IFNα stimulation in the absence of TGFβ co-stimulation. Thus, supply of transgenic S100A2 protein is sufficient to catalyze hypomethylation and this result further shows that S100A2 is the sole response protein of the TGFβ signaling pathway required for IFNα-inducible IFITM3 core promoter demethylation. 24 hours after IFNα incubation, the methylation pattern in ME15 and ME15^{S100A2} cells reverts to untreated control levels, which coincides with the decay of IFITM3 protein expression (figure 20, panel B). Note that the ME15 promoter CpG sites #427 and #24 are demethylated under all conditions and time points although they are directly adjacent to the methylation modulated CpG sites #225 and #21, respectively. In summary, the data above show for the first time that in the presence of the expressed small calcium protein S100A2, IFNα induces a dynamic and reversible modulation of CpG methylation in the core promoter of its target gene IFITM3.

Figure 20. A. S100A2 modulates promoter methylation of the IFNα-inducible gene IFITM3. A 820bp region of the IFITM3 promoter was amplified from bisulfite-treated genomic DNA. PCR fragments were subcloned and sequenced, and individual sequences were analyzed for CpG vs TgG sites. The number of sequences analyzed for each condition is indicated on the right hand side of the figure. Black boxes indicate 90 - 100% methylation and white boxes indicate 0 - 10% methylation at the specific CpG site across all sequences analyzed. CpG locations are illustrated at the top of the figure; numbers indicate the distance from the translation initiation site. One ISRE element stretches over the CpG site #77 and a sp1 site is located at CpG site #107. ME15, ME15 ^{S100A2} (stably over-expressing S100A2), D10 and D10^{S100A2} cells were treated with IFNα (1000 U/ml) for 1, 6 and 24 hours, as well as TGFβ (2 ng/ml) for 48h, or with a combination of both cytokines. Note the demethylation over the whole sequence at the 6h IFNα treatment in ME15 ^{S100A2} as well as in TGFβ stimulated ME15, indicated by two stars. (B) Methylation pattern in two samples from colon cancer patients (48 being classified as CIMP positive, and 68 as CIMP negative) versus healthy mucosa (‘control 48’ and ‘control 68’).

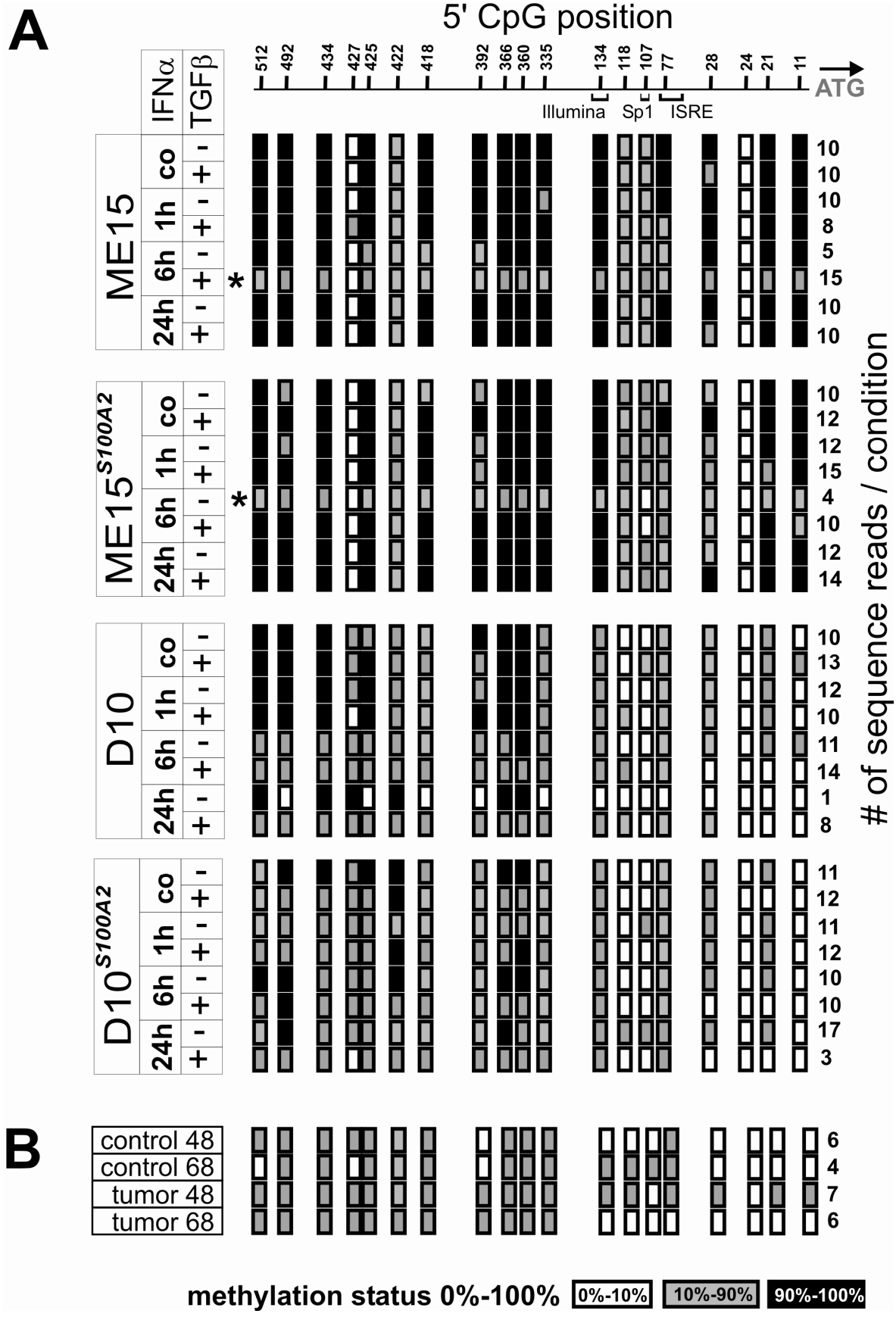
A
5' CpG position
512
492
434
427
425
422
418
392
366
360
335
134
118
107
77
28
24
21
11
ATG
Illumina
Sp1
ISRE
IFNα
TGFβ
ME15
ME15S100A2
D10
D10S100A2
co
1h
6h
24h
*
# of sequence reads / condition
B
control 48
control 68
tumor 48
tumor 68
methylation status 0%-100%
0%-10%
10%-90%
90%-100%

Figure 20

3.10. Methylation State of the IFITM3 Core Promoter in Human Colon Tumor Tissue

We have seen that the IFITM3 core promoter exhibits differences in methylation in ME15 and D10 cells. To investigate clinical relevance of this observance we included colon tumor samples classified as either 'CpG island methylator phenotype' (CIMP) positive or CIMP negative (figure 21B; #68 = CIMP positive, #48 = CIMP negative). Cancerous cells are known to be hypermethylated and this property was assayed as a possible marker for tumors. Interestingly, colon cancer tissues exhibit two different phenotypes: a hyper- and a hypomethylation of target CpG islands which led to the CIMP description in 1999 (reviewed in (Teodoridis, Hardie et al. 2008)). The CIMP classification today is a helpful tool in defining cancer therapies for patients and a CIMP positive diagnosis counts for a worse prognosis.

Overall, the IFITM3 promoter is not methylated in the CIMP positive samples and 50% methylated in the CIMP negative samples (figure 21B). This is seen both in the Illumina Infinium HumanMethylation27 BeadChip array as well as in the bisulfite sequencing analysis (figure 21A and B). The IFITM3 CpG site in the CIMP positive patient samples is completely demethylated in contrast to its control. The CIMP negative samples show no difference for this CpG site in the control or the tumor samples.

We state that our assays both the Illumina Infinium HumanMethylation27 BeadChip array and the bisulfite sequencing are consistent with each other. The Illumnia Infinium HumanMethylation27 BeadChip assay elucidates a general genome-wide DNA methylation overview and bisulfite sequencing yields a higher resolution. Therefore, when a specific promoter region is of interest, bisulfite sequencing produces insight into the DNA methylation pattern providing thorough and significant results.

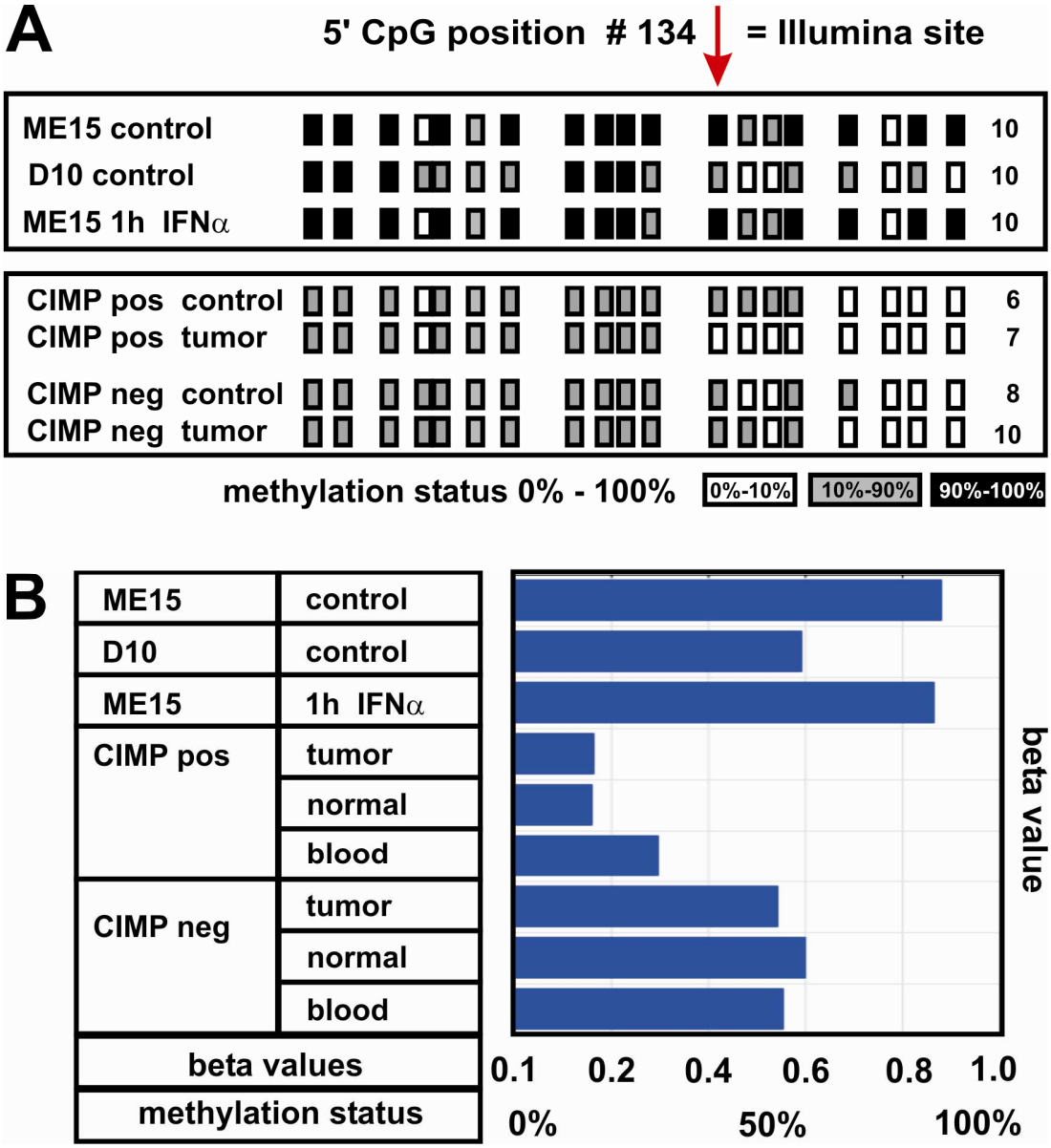

Figure 21

Figure 21. Illumina and bisulfite asssays are consistent. Illumina's beta-values of the IFITM3 were closely investigated in ME15 and D10 cells. Colon cancer CIMP positive and CIMP negative tumor samples were included in this comparison. CpG position #134 corresponds to the CpG site investigated in the Illumina chip array. ME15 control cells as well as IFNα stimulated ME15 cells display total methylation for the site #134 in the Illumina chip array as well as in the bisulfite sequencing assay. This holds true for the partly methylated position #134 in D10 and the CIMP negative tumor samples also. The CIMP positive tumor sample exhibits complete demethylation and again this is seen in both technical arrays.

3.11. P53 Is Non- Responsive In D10 Cells

We have demonstrated that S100A2 indirectly (figure 12) modulates transcriptional response to IFNα in ME15 cells (figure 11). Even though restoration of IFNα sensitivity is independent of gene expression in D10 cells (figure 11B bottom panel) this effect still relies on S100A2 expression. We suspected an epigenetic mechanism being involved in IFNα signaling and thus decided to investigate the methylation patterns of both cell lines which lead to the finding that D10 cells exhibit insensitivity to the demethylating chemical DAC (figure 13), and bisulfite sequencing showed that the IFITM3 promoter is demethylated in D10 cells (figure 20). Investigations as to the degree of a possible DNMT1 failure in D10 cells revealed no obvious defect in its activity thus proposing an alternative pathway aberration (figures 14 and 15). Interestingly, DNMT1 is known be under p53 control in that inactivated p53 binds to the DNMT1 promoter resulting in DNMT1 gene repression (Peterson, Bogler et al. 2003). Activated p53 binds to the S100A2 promoter provided the promoter is not hypermethylated to induce transcription (Tan, Heizmann et al. 1999) and the S100A2 protein binds p53 in a calcium dependant manner therefore enhancing p53 transcriptional activity (Mueller, Schafer et al. 2005). Since p53 is a known protein in cancer development and it is subject to methylation, we decided to investigate p53 signaling in ME15 and D10 cells using a p53 reporter luciferase assay (figure 22).

We found that ME15 cells respond to known inducers of p53 (figure 22). Interestingly both IFNα and TGFβ induce p53 activity in ME15 cells, but co-treatment is not able to activate p53 (Fredy Siegrist; personel communication). In contrast in D10 cells p53 is not responsive independantly of the compound introduced. This result strongly suggests a defect in the p53 signaling pathway in the IFNα resistant D10 cells.

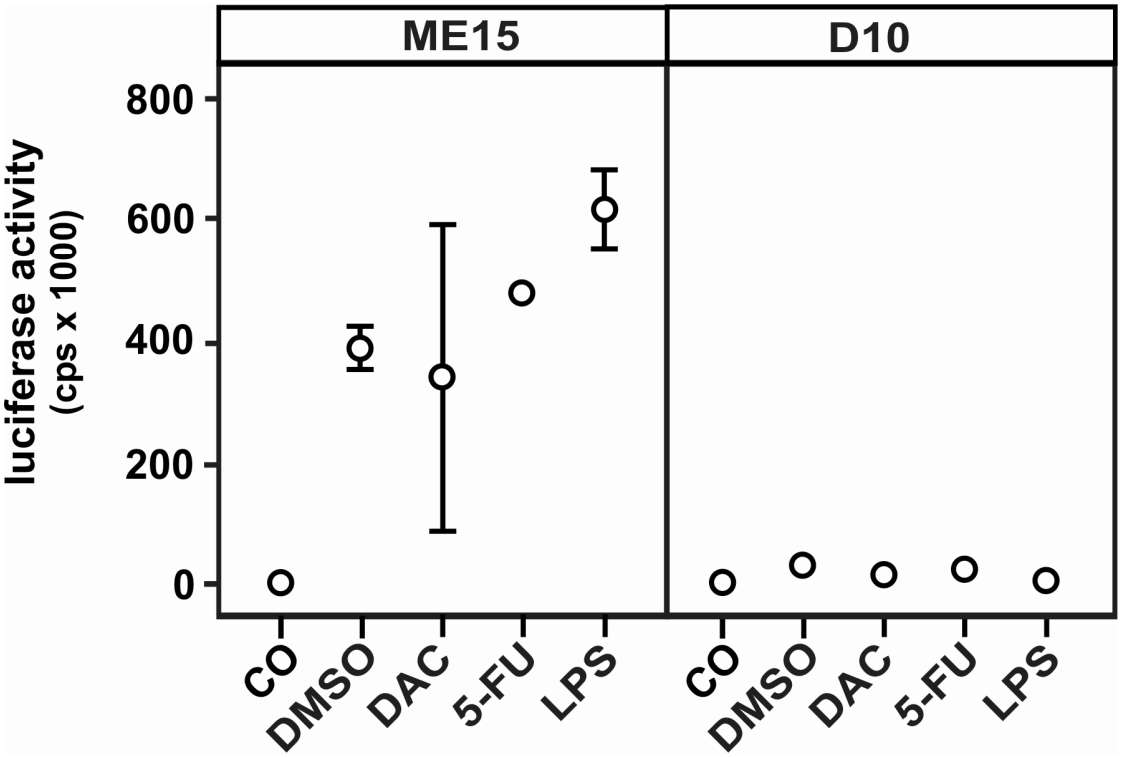

Figure 22

Figure 22. P53 is not functional in the IFNα resistant cell line D10. Cells transfected with a p53 luciferase reporter plasmid were treated with DMSO, DAC, 5-FU and LPS as positive control. Untreated cells were included as reference. In ME15 cells all p53 activators induce significant upregulation of luciferase activity. D10 cells do not respond to stimulation suggesting a p53 signaling defect. Mean values were calculated from quadruplicates and standard deviations are indicated with error bars.

3.12. P21 Is Induced in D10 Cells upon TGF-beta Stimulation

We showed that p53 signaling is defective in D10 cells and we decided to investigate p21 (CDKN1A). Etoposide-induced p53 is known to induce S100A2 as well as p21 (Wang, Rea et al. 1999). P21 is induced upon DNA damage, and translocates to DNA damage breaks where it is involved in DNA repair (Cazzalini, Scovassi et al. 2010). It is proposed that p21 protein levels are degraded when DNA damage is massive (Cazzalini, Scovassi et al. 2010). Foser et al showed that S100A2 is upregulated in ME15 and D10 cells by TGFβ treatment (Foser, Redwanz et al. 2006) and co-stimulation of cells with IFNα and TGFβ may impose apoptotic settings.

We stimulated ME15 and D10 cells with IFNα, TGFβ and a combination of both for 24h in the presence or absence of DAC. In ME15 cells p21, which is under epigenetic control, is constitutively expressed. IFNα or TGFβ stimulation does not further upregulate p21 protein expression (figure 23) but DAC treatment seems to enhance p21 expression in the presence of IFNα. Co-stimulation with IFNα and TGFβ represses p21 completely in ME15 cells which is consistent with the p53 inactivation observed upon co-stimulation in figure 22 (Fredy Siegrist; personel communication). In D10 cells p21 is not visibly expressed but interestingly enough, TGFβ induces p21. Consistent with previous data gene expression is DAC insensitive in these cells (figure 23).

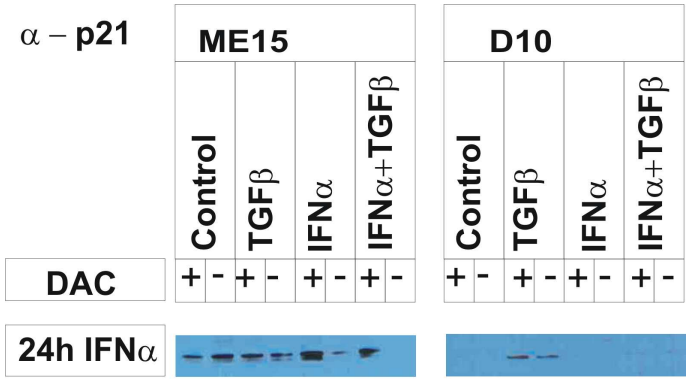

Figure 23

Figure 23. P21 protein expression in ME15 and D10 cells. Cells were treated with IFNα, TGFβ and a combination of both for 24h in the presence or absence of DAC. P21 is not expressed in the IFNα resistant cell line D10 but induced upon TGFβ stimulation in a DAC insensitive manner. In ME15 cells p21 is expressed in control cells and p21 protein levels are not visibly altered by TGFβ stimulation. P21 is slightly downregulated in IFNα stimulated cells and markedly enhanced by DAC treatment in the presence of IFNα or IFNα and TGFβ co-stimulation. Co-treatment in the absence of DAC downregulates p21 protein expression completely.

4. DISCUSSION

We have shown above that cytoplasmic expression of S100A2 enhances the expression of a subset of genes in ME15 cells upon IFNα stimulation. Using the IFNα-inducible gene IFITM3 as a model we demonstrate by bilsufite sequencing dynamic changes in the CpG methylation status of the IFITM3 core promoter in ME15 cells, whilst key residues of this promoter in the IFNα resistant cell line D10 were hypomethylated regardless of IFNα treatment and S100A2 expression.

The catalytic function of S100A2 and the majority of calcium binding protein family members is unknown (Eckert et al., 2004) and to our knowledge this is the first report that links S100A2 and cytokine-inducible epigenetic modulation of CpG sites in the core promoter of an IFNα target gene. In figure 11B we show that only a subset of IFNα-inducible genes is affected by S100A2 over-expression (figure 11B). Known IFNα response genes like IFI44L, IFITM3, IFITM5 or OAS are further upregulated in $ME15^{S100A2}$ cells compared to their upregulation in ME15 cells (figure 11B, cluster 3 and table 2). Such a response could be required to control acute viral infections *in vivo*. On the contrary expression of other classical IFNα response genes such as STATs (signal transducers and activators of transcription) or the major histocompatibilty complex I are not affected in $ME15^{S100A2}$ by IFNα treatment (figure 11B, cluster 2 and table 2) showing specificity of the mechanism mediated by S100A2 in ME15 cells.

We have identified five genes that are unexpectedly rendered IFNα inducible in $ME15^{S100A2}$ cells (figure 11B, cluster 1). Apart from S100A2 itself, the four genes apolipoprotein E, β-actin, the reductase/ dehydrogenase DHR2 and the mitogen activated kinase kinase 5 (MAP2K5) are clustered together (figure 11B, cluster 1) showing that this activating mechanism is not restricted to S100A2. Expression data from untreated $ME15^{S100A2}$ cells were used to calculate the change factors of IFNα-treated cells, and upregulation relates therefore to activation of the genomic copy (chromosome 1q21) of S100A2. It is known that the S100A2 promoter is methylated in many cell types (Lee, Tomasetto et al. 1992; Wicki, Franz et al. 1997; Feng, Xu et al. 2001; Lindsey, Lusher et al. 2007) and this includes ME15 cells, since we show that DAC treatment elevates the TGFβ-inducible expression of S100A2 (figure 13A). Upregulation of S100A2 transcription by IFNα requires only intracellular S100A2 protein and an indirect mechanism is potentially responsible for mediating IFNα responsiveness. It has been described that Ca^{2+} is required for phosphorylation and activation of the methyl binding protein MeCP2, which in turn dissociates from the methylated BDNF promoter, whereupon transcription is induced (Chen, Chang et al.

2003). Also, in neuronal cells, GADD45β-promoted demethylation of specific genes such as BDNF and FGF is calcium sensitive (Ma, Jang et al. 2009). These findings strongly link calcium signaling with epigenetic regulation. We have applied three independent protein localization techniques for subcellular detection of S100A2. Based on its modulation activity we expected nuclear localization, however, all methods clearly suggested a cytoplasmic localization which rules out a direct nuclear function as a DNA methylation modifying enzyme (figure 12, panel A and B). It has been shown that S100 type calcium binding proteins are able to shuttle between the cytoplasm and the nucleus following cell stimulation (Schafer and Heizmann 1996; Mandinova, Atar et al. 1998). Upon calcium stimulation in human keratinocytes the S100C/A11 protein is phosphorylated, binds to nucleolin, transfers to the nucleus and liberates the Sp1 transcription factor which then transcriptionally activates p21 to inhibit DNA synthesis (Miyazaki, Sakaguchi et al. 2004). To rule out such a transient translocation we analyzed cells transfected with a tagged S100A2 expression construct at 6h and 20h post transfection using cell fractionation by differential centrifugation, and found consistent cytoplasmic localization with traces present in the membrane fraction (figure 12B). So far, the results obtained indicate that a direct participation of S100A2 in the transcription or DNA methylation is unlikely. Thus, the modulatory effect of S100A2 on gene expression and DNA methylation in ME15 cells is indirect.

DAC treatment revealed that S100A2 expression is sensitive to methylation in ME15 cells, confirming previous findings (Lee, Tomasetto et al. 1992; Wicki, Franz et al. 1997; Feng, Xu et al. 2001). Interestingly, over-expressing S100A2 in cells showed a reduced impact of DAC on protein expression, suggesting that S100A2 regulates its own expression in a similar manner to DAC. Furthermore, S100A2 protein levels remained unchanged after TGFβ induction regardless of DAC treatment in $ME15^{S100A2}$ and $D10^{S100A2}$ cells. A feasible explanation is the antiproliferative activity of S100A2, which upon further increase by TGFβ treatment possibly results in a growth arrest (figure 13A; panel second from the left). This conclusion is supported by the fact that the apparent levels of S100A2 do not increase any more at the 51h time point in the recombinant cell line.

On the other hand, S100A2 protein levels are not altered in the IFNα-resistant D10 cells (figure 10) upon DAC treatment (figure 13A, panel second from the right). This also holds true for the IFITM3 protein (figure 13B) which leads to the notion that the IFITM3 promoter is hypo- or demethylated in D10 cells. We confirmed this hypothesis by bisulfite sequencing (figure 20). The IFITM3 gene is constitutively expressed in D10 cells and stimulation with IFNα further up-regulates the protein and

mRNA levels (Figure 13; (Brem, Oraszlan-Szovik et al. 2003). Functional response to IFNα treatment regarding its gene expression was postulated previously, as the D10 cell line was shown to exhibit a delayed rather than defective signaling (Certa, Wilhelm-Seiler et al. 2003). These results were confirmed because D10 cells expressed IFNα-inducible genes upon IFNα stimulus; but in contrast to the ME15 cells, IFNα-responsive gene expression in D10 cells is not modulated by S100A2 (figure 11B, bottom panel). Since spontaneous IFNα production or mutations in the core promoter of the IFITM3 allele have been ruled out as possible causes of deregulation of IFITM3 expression in D10 cells (Certa, Seiler et al. 2001), it was postulated previously that epigenetic aberrations might be involved in the IFNα-resistance of the D10 cell line (Brem, Oraszlan-Szovik et al. 2003), and our results strongly support the concept of a defect in the methylation machinery.

It has been shown that the chromatin-remodeling activity of the ubiquitous BAF complex in human HeLa cells enables binding of the Sp1 transcription factor to its cognate site, resulting in gene expression. Liu et al. found that the IFITM3 promoter region contains an Sp1 binding site (figure 20, 5' CpG position #107) which upon removal by mutagenesis led to diminished IFITM3 expression, by up to approximately 50% (Liu, Kang et al. 2002). The hypomethylation of the entire region in D10 cells probably enhances the accessibility for transcription factors, which results in constitutive production of IFITM3. Following IFNα stimulation, the transcriptional activator complex IFR9 is formed and transcription of the IFITM3 gene is then driven by these two transcription factors, generating maximal levels of IFITM3 in D10 cells (Brem et al., 2003). Included in cluster three of figure 11B is the small proline rich protein SPRR2D. Like S100A2, the SPRRs are located on chromosome 1 constituting the epidermal differentiation complex (Tan, Sun et al. 2006). The calcium inducible SPRR2D has been shown to have a POU domain of the OCT11 binding element as well as a Sp1 transcription factor binding site and an ISRE binding element (Tesfaigzi and Carlson, 1999) therefore supporting the concept of a combinatory Sp1 and interferon signaling.

In contrast to ME15 cells the IFITM3 promoter is hypomethylated in D10 cells. This leads to the question which epigenetic aberrations might be involved in the low promoter methylation in these cells. Additionally the low promoter methylation might deliver an explanation why D10 cells exhibit IFNα resistance. Defects in DNA methyltransferase are associated with growth arrest (Kassis, Zhao et al. 2006) and the methyltransferase substrate SAM leads to restored sensitivity to IFNα in HCV patients (Duong, Christen et al. 2006). SAM supplementation was not able to restore IFITM3 expression to basal levels in D10 cells (figure 14) and the transient IFITM3

promoter does not exhibit significant differences in IFNα-induced activity (figure 15) demonstrating functionality of the maintenance DNA methyltransferase (DNMT1) in both ME15 as well as D10 cells. This excludes a direct defect in DNMT1 because the *in vitro* methylated IFITM3 promoters were equally well suppressed in the transfected ME15 and D10 cells (figure 15). Methylation defects often occur after DNA replication where only one DNA strand is methylated therefore discriminating mother from daughter strands and serving as a template for DNMT1 (Holliday and Pugh 1975). Since in our experimental set-up the cells completed only one round of DNA replication it is possible that the methylation defect remains undetected and therefore it would be necessary to investigate the IFITM3 promoter sensitivity to IFNα over a longer timecourse. Genome-wide DNA methylation is slightly higher in D10 cells (figure 19) and there are an overall higher number of CpG sites with low methylation in ME15 than in D10 cells (figure 18), again arguing against dysfunctional DNMT1 in D10 cells. Interestingly, it was found that over-expression of the DNMT1 protein leads to tumor-specific hypermethylation, which has been associated with the positive CpG island methylator phenotype (CIMP) (Ting, Jair et al. 2004; Teodoridis, Hardie et al. 2008). According to our investigations, the specific hypomethylation observed in the IFITM3 promoter does not involve a defect in the DNMT1 protein expression and the DNA methylation abberration is likely to be related to an alternate malfunction of the methylation machinery.

Microarrays have shown that DNMT1 mRNA is expressed at the same level both in ME15 and D10 cells (Siegrist et al., unpublished data) but protein levels and activities have not been investigated. Interestingly, inactivated p53 represses the DNMT1 promoter and DNMT1 transcription levels increase upon stress-induced p53 activation, to meet immediate DNA repair requirements (Peterson, Bogler et al. 2003). Additionally, the p53-inducible p21 protein inhibits DNMT1 expression in MCF7 cells, closely relating DNMT1 repression to cell cycle arrest (Tan and Porter 2009). DNMT1 expression is upregulated significantly during G1 phase (Robertson, Keyomarsi et al. 2000) and it is possible that this upregulation is not detected in standard microarray studies since cells are not synchronized. It has been suggested that aberrations in cell-cycle regulated expression of DNMT1 lead to subsequent demethylation of DNA after several cell cycles (Robertson, Keyomarsi et al. 2000). P53 is not functional in D10 cells (figure 22) and might therefore constitutively bind to the DNMT1 promoter, hence inhibiting cell-cycle dependant upregulation of DNMT1. This could explain the hypomethylation of the IFITM3 promoter in D10 cells. Fusion of ME15 and D10 cells revealed clearly that the ME15 cell line was not able to rescue the D10 cell line in terms of silencing the otherwise constitutively expressed IFITM3 (figure 16A).

Interestingly, in these MDbla cells IFITM3 expression is not inducible by IFNα and showed maximal levels. It is therefore possible that the MDbla cells are under constant stress due to their chromosome content, which results in the activation of functional p53 provided by the ME15 cell line to reach maximal levels of IFITM3 in the absence of IFNα treatment. It is important to realize that functional DNMT1 would not actually be able to "re"-methylate the IFITM3 promoter of the D10 cell line because DNMT1 requires hemimethylated DNA strands (Holliday and Pugh 1975; Ting, Jair et al. 2004). Whichever methylation machinery defect is involved in the aberrant DNA methylation of the IFITM3 promoter is not related to a direct defect in the DNA maintenance methyltransferase DNMT1.

FACS showed that the MDbla cell line does not contain four sets of chromosomes, as also seen by karyotyping (figure 16B and C). Karyotyping additionally revealed that the chromosomes both in ME15 and D10 cells exhibited massive aberrations. These findings support the notion that there is a DNA methylation defect in D10 cells since chromosome aberrations are known to result from the loss of functional MeCP2 as observed in the RTT syndrome (Matarazzo, De Bonis et al. 2009) or malfunctions of DNMT3b as seen in ICF (Xu, Bestor et al. 1999). Interestingly, ME15 cells are equally affected by this phenotype and it is likely that the chromosomal aberrations are due to the fact that both cells are cancer cell lines. In cancer the absence of telomerase during continuous proliferation leads to the shortening of the telomers which can result in subsequent chromosomal aberrations (Raynaud, Sabatier et al. 2008). Also, in some cancers the integration of viruses such as HBV into the genome promotes chromosomal instability (Neuveut, Wei et al.). The mechanisms involved in chromosomal aberrations of ME15 and D10 cells remain elusive.

The enhanced IFNα-induced IFITM3 and TGFβ-induced S100A2 expression in ME15 cells following DAC treatment indicate an involvement of DNA methylation in the gene expression control. However, In D10 cells IFITM3 and S100A2 expression exhibit insensitivity to DAC treatment. These findings prompted us to analyze whether any dynamic changes in the DNA methylation of the IFITM3 core promoter are responsible for upregulation in ME15 cells. Furthermore, we wondered whether there are differences in DNA methylation of the IFITM3 core promoter in D10 cells compared to ME15 cells.

Genome-wide DNA methylation analysis did not reveal major differences in the methylation pattern of known CpG islands which is consistent with the observation of chromosomal aberrations in both cell lines (figures 16, 18 and 19);

plus the methylation of the IFITM3 promoter region investigated by the Illumina Infinium HumanMethylation27 BeadChip array was restricted to one CpG site only. The IFITM3 promoter lacks classical CpG islands but we found 19 potential CpG methylation target sites in a 500 base stretch upstream of the transcription initiation site, which resembles the organization of the S100A2 promoter that is known to be regulated by DNA methylation (Wicki, Franz et al. 1997; Rehman, Cross et al. 2005). In figure 13A, we show the basic methylation pattern of the IFITM3 core promoter in ME15 cells, which is not altered upon induction of gene expression with IFNα. In the presence of S100A2, supplied either by TGFβ treatment or recombinant expression, partial hypomethylation of selected sites occurs 6 hours after IFNα stimulation, leading to elevated IFITM3 gene expression as shown in figure 11B. A complete and precise reset of promoter methylation to the naive status occurs 24 hours after stimulation.

In D10 cells, IFITM3 is constitutively expressed and we showed that the IFITM3 promoter is hypomethylated in the absence of any treatment or stimulus (figure 20). It is known that the transcription factor Sp1 binds to promoter regions, given that their binding sites are demethylated, and as described above IFITM3 has also been shown to bind Sp1 (Liu, Kang et al. 2002). The insulin growth factor binding protein 3 (IGFBP3), which exhibits antiproliferative activity, binds MeCP2 in its methylated promoter region, therefore interfering with the Sp1 transcription binding site and leading to silencing of gene expression (Kudo 1998; Chang, Wang et al. 2004). Additionally, Sp1 is deacetylated in a hepatic cell line by the hepatitis B virus X protein through the recruitment of histone deacetylaese (HDACs) in a p53-independent manner (Shon, Shon et al. 2009). In normal cells Sp1 acetylation is increased in response to stress, therefore DNA-binding of Sp1 is enhanced and transcription of stress response genes is amplified (Shon, Shon et al. 2009). IGFBP3 is known to be an upstream effector of p21 and induction of IGFBP3 through DNA demethylation along with stress-induced activated Sp1 binding might lead to p21 activation and inhibit proliferation (Peng, Wang et al. 2008). IGFBP3 restores IFNα sensitivity in D10 cells in the presence of TGFβ (Foser, Redwanz et al. 2006) and a p53-independent action mediated by IGFBP3 through p21 is conceivable (figure 23). Taken together, the results show that the Sp1 transcription factor is involved in the mediation of antiproliferation by epigenetic means and that binding to the demethylated IFITM3 promoter region provides a plausible explanation for the constitutive IFITM3 protein expression in the D10 cell line.

We have previously shown that TGFβ treatment is able to restore the antiproliferative response to IFNα in the resistant melanoma cell line D10, which

indicates a functional link of these signaling cascades (Foser, Redwanz et al. 2006). Transfection experiments have corroborated that S100A2 expression is necessary and sufficient for this response. Here we demonstrate that S100A2 is mandatory for dynamic IFNα-mediated hypomethylation of the IFITM3 core promoter in ME15 cells, leading to increased protein expression.

S100A2 is proposed to modulate cellular response to oxidative stress and one way in which this might occur is by stabilizing p53 and protecting it from degradation or de-activation (Li, Gudjonsson et al. 2009). It is known that suppressors of cytokine signaling 1 (SOCS1) bound to DNA damage proteins bind and activate p53 to induce senescence (Calabrese, Mallette et al. 2009). We propose that the combined antiproliferative activities of IFNα and S100A2 induce stress conditions, which can lead to activation of the tumor suppressor gene p53 (Vousden and Prives 2009). Takaoka et al. have shown that IFNα/β induces expression of p53 under adverse growth conditions and cell cycle arrest (Takaoka, Hayakawa et al. 2003), which occur in ME15 cells when co-treated with TGFβ and IFNα (Foser, Redwanz et al. 2006). S100A2 is a well documented target gene of p53 (Tan, Heizmann et al. 1999; Mueller, Schafer et al. 2005; Lapi, Iovino et al. 2006) and is known to bind p53 in a calcium dependant manner, thereby enhancing transcriptional p53-activity (Mueller, Schafer et al. 2005). This indirect mechanism could explain the acquired inducibility of S100A2 by IFNα (figure 11B, cluster 1).

Interestingly, Foser et al. (Foser, Redwanz et al. 2006) have identified two additional p53 target genes with growth inhibitory activity in ME15 and D10 cells stimulated with IFNα and TGFβ: insulin growth factor binding protein 3 (IGFBP3) and GADD45. GADD45 is a DNA repair protein which was recently identified as a marker for genotoxicity and apoptosis (Olaharski, Albertini et al. 2009). The same genes were also identified in previous studies (Foser, Redwanz et al. 2006), supporting the view that p53 signaling is activated in response to the antiproliferative state of the cells. In figure 22, we showed that the established inducers of p53 signaling like DAC or 5-fluorouracil are able to activate a transfected p53 reporter construct in ME15 cells whilst D10 cells do not respond, suggesting a defect in the p53 signaling cascade. Additionally, p21, which is induced by p53, is not expressed in D10 cells (figure 23) supporting the finding of a defect in the p53 pathway. Indeed, loss of p21 expression in cancer cells is associated with late stage tumors (Seoane 2004). Interestingly, TGFβ is able to induce p21 expression in D10 cells, suggesting p53-independent induction of p21. This has been described by Sonegawa et al. who show calcium-activated nuclear translocation of S100C/A11 upon TGFβ stimulation to induce p21 expression, and that loss of this pathway leads to TGFβ resistance

(Sonegawa, Nukui et al. 2007; Sakaguchi, Sonegawa et al. 2008). P21 has two Sp1 binding sites and promoter hypermethylation leads to transcriptional repression even upon stimulation (Zhu, Srinivasan et al. 2003). Such a hypermethylation of the Sp1 transcription factor binding site in the p21 promoter could be associated with IFNα resistance in D10 cells.

A mechanism of dynamic, inducible CpG methylation has been shown for the inflammatory cytokine IL2, a key regulator of T-cell responses (Murayama, Sakura et al. 2006). Stimulation of lymphocytes with PMA (phorbol 12-myristate 13-acetate) leads to an intracellular calcium release, which results in translocation of the T-cell transcription factor NFAT from the cytoplasm to the nucleus and binding to the IL2 core promoter. Next, a single CpG site of the promoter is demethylated in an unknown way, which leads to transition of the “naive state” to the “active state” and facilitates transcription by OCT1 one hour after PMA stimulation. The equivalent “naive state” of the IFITM3 core promoter is shown in figure 20, where IFNα alone does not alter the methylation pattern in a 24h time course experiment. In contrast to IL2, the IFITM3 promoter in this methylation state is fully responsive to IFNα signaling in ME15 cells. However, expression of S100A2 triggers dynamic hypomethylation of the IFITM3 promoter at key residues, which enhances the IFNα response 6 hours after IFNα stimulation and sets the promoter in a “hyperactive” state with enhanced response and expression of IFITM3. After 24 hours the promoter methylation state is reset to the naive state. To our knowledge reversible and cytokine-inducible promoter activation through a DNA methylation based mechanism has not been shown before.

The observation of S100A2-mediated, IFNα-inducible hypomethylation of the IFITM3 core promoter raises the question of whether this occurs through passive of active demethylation. Passive demethylation occurs during DNA replication, when daughter strand methylation is inhibited. The methylation patterns shown in figure 20 were compiled from individual Sanger-sequencing reads of subcloned core promoter amplicons; complete demethylation of all CpG target sites is rare, consistent with a passive mechanism (figure 24, bottom left). Active demethylation has been shown in plants and insects and involves recruitment of glycosylases to specific chromosomal locations and genes followed by demethylation and transcriptional activation (Ooi and Bestor 2008; Gehring, Reik et al. 2009). So far, there is only circumstantial evidence for active demethylation in mammals (Morgan, Santos et al. 2005) and the current result favors a passive mechanism. It is interesting to note that evidence is emerging that DNA repair enzymes and glycosylases might function as active demethylating agents in mammals, as suggested for the GADD45 protein, which is induced in our

experimental system following IFNα and TGFβ stimulation (Foser, Redwanz et al. 2006; Rai, Huggins et al. 2008; Ma, Guo et al. 2009; Schmitz, Schmitt et al. 2009). Regardless of the mechanism that leads to the changes in the methylation status of the IFITM3 promoter after stimulation, it remains entirely unclear how the activated status of the promoter is reset to the naive state after 24 hours.

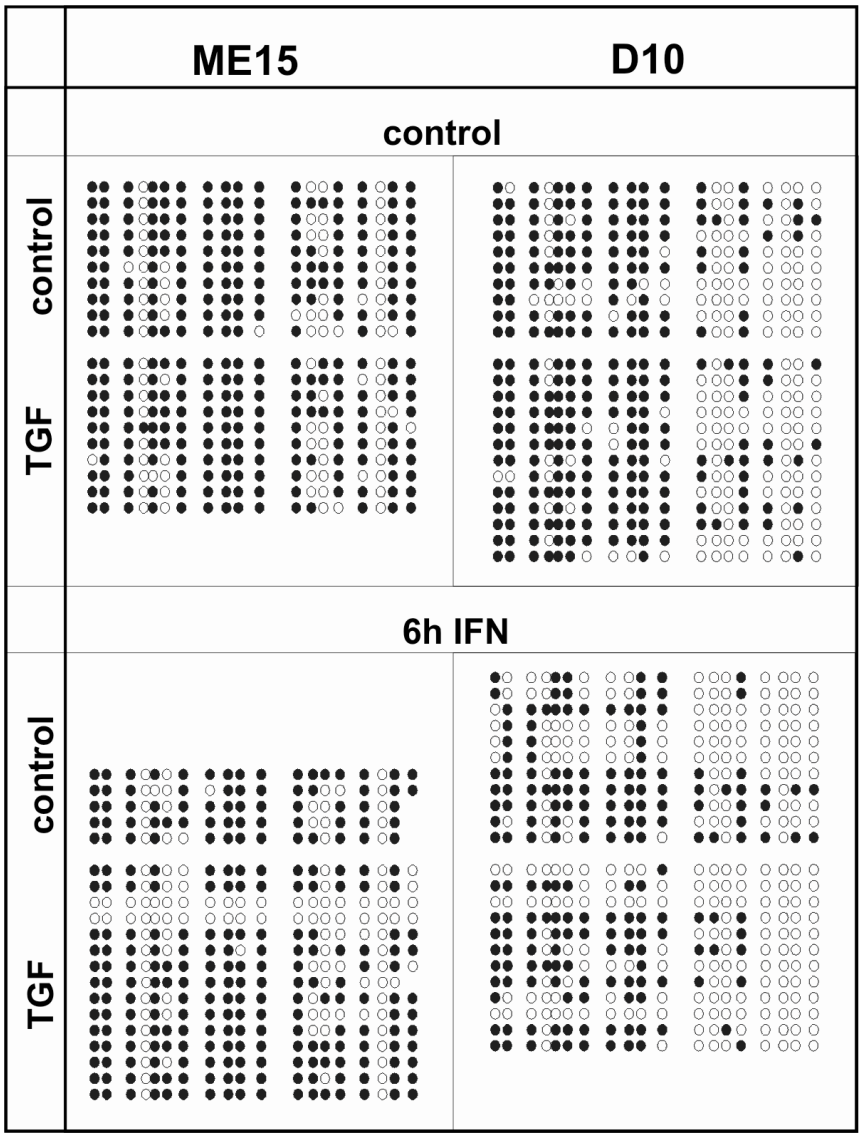

Figure 24

Figure 24. Individual Sanger-sequence reads of bisulfite-treated genomic DNA. ME15 and D10 cells were stimulated with TGFβ and IFNα**,** genomic DNA was bisulfite-treated and sequenced and individual sequences are displayed. Black circles indicate a methylated site and white circles a demethylated site. Note the two completely demethylated sequences in the ME15 cells treated with both TGFβ and IFNα.

Our laboratory has reported previously that IFNα treatment leads to a significant intracellular calcium release which is required for the antiproliferative activity of S100A2 (Foser, Redwanz et al. 2006). In neuronal cells it has been shown that GADD45β promotes calcium sensitive demethylation of specific genes like BDNF or FGF (Ma, Jang et al. 2009). GADD45β is a p53 target gene (Kastan, Zhan et al. 1992) which is expressed upon growth arrest through promoter hypomethylation (Qiu, Zhou et al. 2004). Additionally, p21 activates GADD45 genes which themselves act on a signaling pathway to induce TGFβ in the stress response to DNA damage (Passos, Nelson et al.). Thus, it is reasonable to propose that IFNα-induced calcium release is required to activate GADD45β in our experimental system after cytokine stimulation. The cytoplasmic localization of S100A2 eliminates a direct function of S100A2 in the nucleus and we propose that the antiproliferative state of the cells induced by activated S100A2 and IFNα treatment triggers demethylation of selected target genes, which would augment the response to IFNα. The IFITM3 core promoter in D10 cells showed a significantly higher degree of demethylation compared to the ME15 cells in the naive and active state, which presumably leads to the constitutive expression. Interestingly, we demonstrated a lack of p53 activity in D10 cells (figure 22) and this result points to a role of p53 signaling in dynamic, cytokine induced promoter methylation.

In our cell-based model, expression of the IFNα-inducible antiproliferative IFITM3 protein is enhanced in the presence of S100A2 and the concomitant hypomethylation of the IFITM3 core promoter exhibits reversibility to the naive methylation state 24 hours after IFNα stimulus. Resistance to IFNα in renal carcinoma as well as melanoma cells can be overcome either by DAC treatment or DNA methyltransferase (DNMT1) depletion by transfection of antisense oligonucleotides (Reu, Bae et al. 2006). Additionally, IFNα resistant HCV replicon harboring cells become sensitive to IFNα upon treatment with DAC (Naka, Abe et al. 2006). Thus, modification of IFNα target gene expression through promoter methylation might be a natural mechanism to adapt the responses to pathogen challenge.

5. CONCLUSION

Using a wide range of different technologies I was able to investigate S100A2 as well as DAC modulated IFNα signaling in the two human melanoma cell lines ME15 and D10. I demonstrate for the first time dynamic demethylation upon IFNα and TGFβ co-treatment in the IFITM3 core promoter of the IFNα sensitive cell line ME15. The TGFβ inducible small calcium binding protein S100A2 is sufficient to promote this demethylation in ME15 cells. It was shown that S100A2 induces sensitivity to IFNα in D10 cells in that its proliferation rate is decreased. Interestingly, in the IFNα resistant D10 cells the core promoter of IFITM3 is hypomethylated and cytokine treatmens do not influence the methylation status. Hypomethylation is known to be a reliable marker for a progressed tumor cell line and the p53 signaling defect in the D10 cells is also pointing in the direction of a more progressed tumor stage. The expression pattern measured by microarray are consistent with a possible lower methylation status in the D10 cell line versus the ME15 cell line, but investigation of the genome wide methylation status revealed that ME15 cells exhibit lower general methylation of investigated CpG sites than D10 cells. Thus per definition ME15 cells are in a more progressed tumor state than D10 cells concerning the methylation state. This means that the methylation status itself does not alone explain the IFNα resistance of D10 cells, especially since D10 cells exhibit sensitivity both to TGFβ as well as S100A2 in that their proliferation rate does decrease. The IFNα resistance observed in the D10 cell line apparently is specific for the IFNα signaling and might involve promoter demethylation of genes under explicit IFNα expression control. Interestingly D10 cells are defective in their p53 pathway and this might play a role in resistance of D10 cells to IFNα.

In ME15 cells the partially methylated IFITM3 core promoter is inducible under normal growth conditions by IFNα. Stress, growth conditions or stimuli like TGFβ induce S100A2 expression which following IFNα treatment leads to enhancement of IFITM3 expression though demethylation of the IFITM3 core promoter. Such an additional boost of IFITM3 expression could for instance control proliferation of metastasizing tumor cells where normal levels are insufficient. At least in ME15 cells we can reproduce this model in cell culture and it is plausible to propose that constitutive expression of IFITM3 in D10 cells is partially due to the extensive hypomethylation of the core promoter.

Anyhow, having two levels of IFNα response intensities is an economic way for cells in their viral and tumor defense. The basic expression level of IFNα-inducible genes is operating in all cells and tissues with normal responses to IFNα and is

based on our current understanding of FNα signaling. The enhanced intensity of the IFNα response is probably used under acute circumstances where improved defenses are required to combat for example high loads of viral invaders. This second level of IFNα response is entirely dependent on S100A2 and IFNα stimulation. We have shown that IFNα stimulation leads to a significant intracellular calcium release within seconds (Foser et al., 2006). It is plausible to propose that this transient Ca^{2+} release leads to reversible activation of S100A2, which is consistent with the dynamic changes of IFITM3 core promoter methylation occurring in ME15 cells.

In conclusion, dynamic promoter methylation adds an additional layer of complexity to the IFNα signaling pathways and tight control of IFNα key response genes like IFITM3 might be required for comprehensive control of the IFNα response.

Figure 25. Overview of protein interactions. S100A2 expression is induced by TGFβ and activated by IFNα-induced elevated calcium levels. This leads to enhanced stress levels which modulate other gene expressions. S100A2 works as a modulator of p53 protein activation. IFNα leads to induction of p53 under stress conditions which then might act to further upregulate TGFβ-induced S100A2 and other proteins such as IGFBP3 and PTGFβ. Stress conditions and p53 as well as p21 are known modulators of DNA damage proteins, DNA methyltransferases and glycosylases.

Dotted arrows indicated methylation dependant activities, the other arrows indicate gene regulation. Black boxes indicate genes, grey circles indicate proteins. ‘CpGmethyl’ stands for methylated promoter region.

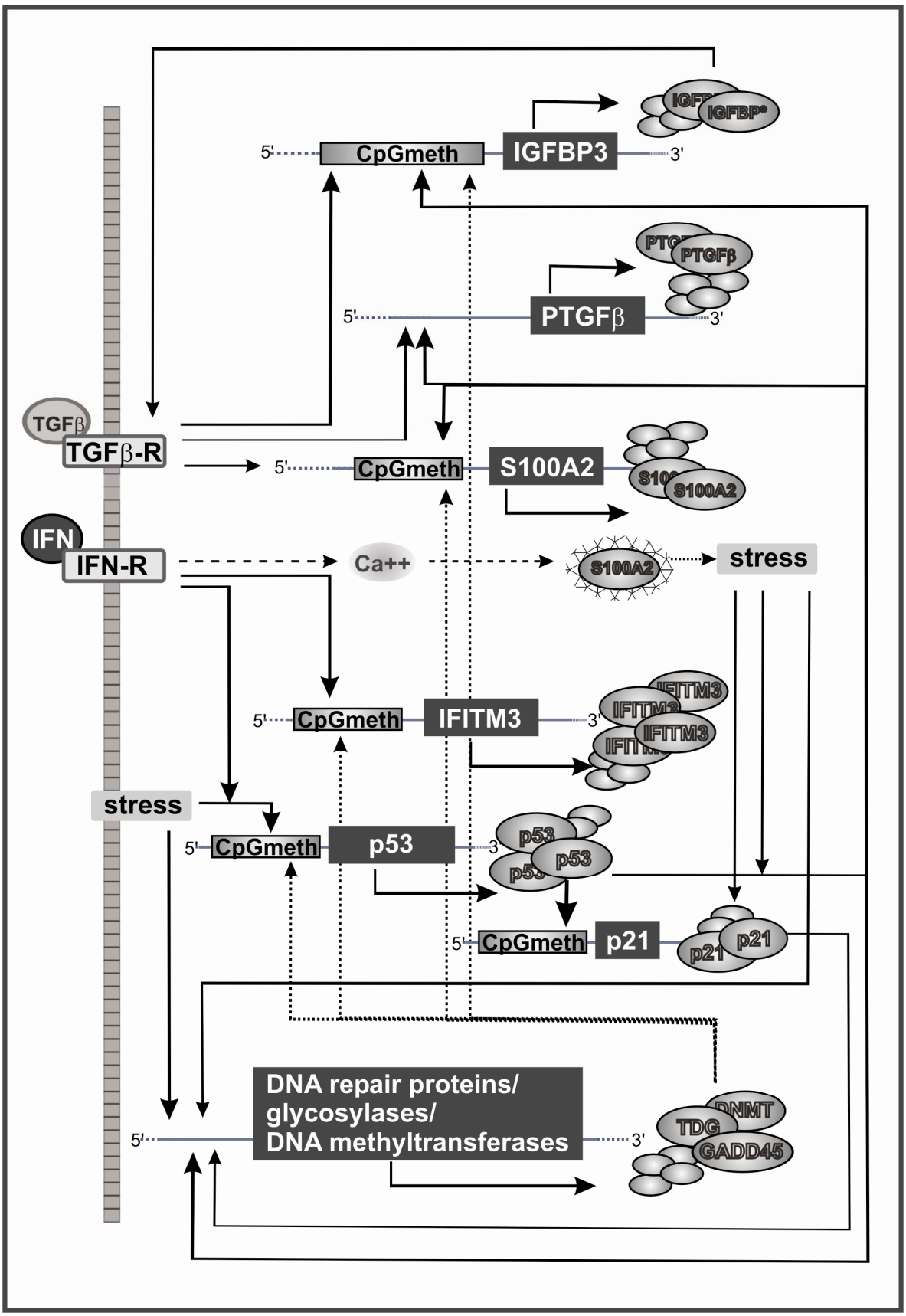
IGFBP*
5'
CpGmeth
IGFBP3
3'
PTGFβ
5'
PTGFβ
3'
TGFβ
TGFβ-R
5'
CpGmeth
S100A2
S100A2
IFN
IFN-R
Ca++
S100A2
stress
5'
CpGmeth
IFITM3
3'
IFITM3
IFITM3
stress
5'
CpGmeth
p53
3'
p53
p53
5'
CpGmeth
p21
p21
p21
DNA repair proteins/
glycosylases/
DNA methyltransferases
5'
3'
DNMT
TDG
GADD45

Figure 25

6. OUTLOOK

My work demonstrates dynamic demethylation of the IFITM3 promoter upon cytokine treatment in ME15 cells. Therefore I was able to shed light on the question of how S100A2 modulates gene expression in these cells. Furthermore I observed that the IFITM3 promoter is hypomethylated in D10 cells. Since these cells are IFNα resistant I propose a possible defect in the methylation machinery of D10 cells. However, I was not able to show a direct involvement of the methylation machinery in IFNα resistance in D10 cells. So the following question remains elusive: why does S100A2 restore IFNα sensitivity in D10 cells?

S100A2 does not function as a transcription factor, a methylation binding protein or a methyltransferase since it was not found to translocate to the nucleus. However, Miyakazy et al. observed translocation of another S100 protein (S100C/A11) one hour after stimulation with TGFβ (Miyazaki, Sakaguchi et al. 2004). I measured S100A2 translocation at 24h or 48h time points of INFα stimulus and it would be interesting to investigate potential S100A2 translocation after one hour. Nevertheless, it is likely that traces of S100A2 protein in the nucleus would have still been detectable after 24 hours if the protein had translocated to the nucleus. As explained in the discussion S100A2 might well act as a stress factor and therefore induce DNA repair proteins which then affect DNA methylation. The indirect mechanism of S100A2 does not exclude a potential involvement in dynamic promoter demethylation.

It remains unclear if S100A2 and IFNα act on the methylation status of ME15 cells in a genome wide manner, or if this action is specific. The microarray data indicate that S100A2 exhibits a very distinct action on the transcription levels of a subset of IFNα-inducible genes and therefore implies specificity. Genome wide CpG methylation arrays provide a useful overview of DNA demethylation even though only a limited number of CpGs are investigated per promoter region or CpG island. As a next step we would like to investigate genome-wide demethylation 6 hours post-stimulation, to allow comparison with bisulfite sequencing experiments. In order to confirm that the observed demethylation is specific, it would be necessary to investigate a control such as OCT4, which is a developmental gene that is completely methylated in mature cells, by bisulfite sequencing (Athanasiadou, de Sousa et al.). Investigation of promoter methylation of genes in cluster 3 (figure 13B) will additionally shed light on the possible action of DNA methylation. Furthermore, others have shown that DNA methylation is strand specific and it will be interesting to

investigate the upper strand of the IFITM3 promoter (Kangaspeska, Stride et al. 2008; Metivier, Gallais et al. 2008).

Bisufite sequencing revealed that the whole DNA fragment investigated was subject to demethylation and this observation suggests passive demethylation. To confirm whether this demethylation is passive we will measure DNA synthesis by BrdU incorporation upon IFNα stimulation. Another way would be to synchronize cells before DNA methylation investigation, a technique used by others where cells are starved for three days with serum-free medium (Metivier, Gallais et al. 2008).

In contrast to Sanger sequencing, pyrosequencing provides information on the methylation ratio at individual CpG sites across a cell population, however this does not reveal CpG methylation patterns along individual DNA strands. Therefore we decided to investigate CpG methylation using Sanger sequencing. Once we have determined whether DNA demethylation is active or passive in our system we will investigate the CpGs of interest using pyrosequencing, a method that allows a higher throughput.

The p53 signaling defect in D10 cells points towards a more progressed tumor stage in these cells. P53 knock-downs in ME15 cells might illuminate possible effects of p53 signaling in these human melanoma cells. It is possible that ME15 p53 knock-down cells could exhibit IFNα resistance but this must be investigated experimentally. It will be interesting to explore the correlation of IFNα, TGFβ and p53 signaling with epigenetics in my cellular model (figure 25).

7. LITERATURE

Akira, S., S. Uematsu, et al. (2006). "Pathogen recognition and innate immunity." Cell **124**(4): 783-801.

Allfrey, V. G., R. Faulkner, et al. (1964). "Acetylation and Methylation of Histones and Their Possible Role in the Regulation of Rna Synthesis." Proc Natl Acad Sci U S A **51**: 786-94.

Amir, R. E., I. B. Van den Veyver, et al. (1999). "Rett syndrome is caused by mutations in X-linked MECP2, encoding methyl-CpG-binding protein 2." Nat Genet **23**(2): 185-8.

Athanasiadou, R., D. de Sousa, et al. "Targeting of de novo DNA methylation throughout the Oct-4 gene regulatory region in differentiating embryonic stem cells." PLoS One **5**(4): e9937.

Bannister, A. J., P. Zegerman, et al. (2001). "Selective recognition of methylated lysine 9 on histone H3 by the HP1 chromo domain." Nature **410**(6824): 120-4.

Beaulieu, N., S. Morin, et al. (2002). "An essential role for DNA methyltransferase DNMT3B in cancer cell survival." J Biol Chem **277**(31): 28176-81.

Berridge, M. J., P. Lipp, et al. (2000). "The versatility and universality of calcium signalling." Nat Rev Mol Cell Biol **1**(1): 11-21.

Bird, A. (2009). "On the track of DNA methylation: an interview with Adrian Bird by Jane Gitschier." PLoS Genet **5**(10): e1000667.

Bird, A., M. Taggart, et al. (1985). "A fraction of the mouse genome that is derived from islands of nonmethylated, CpG-rich DNA." Cell **40**(1): 91-9.

Bird, A. P. (1993). "Functions for DNA methylation in vertebrates." Cold Spring Harb Symp Quant Biol **58**: 281-5.

Bird, A. P. and E. M. Southern (1978). "Use of restriction enzymes to study eukaryotic DNA methylation: I. The methylation pattern in ribosomal DNA from Xenopus laevis." J Mol Biol **118**(1): 27-47.

Bogdanovic, O. and G. J. Veenstra (2009). "DNA methylation and methyl-CpG binding proteins: developmental requirements and function." Chromosoma **118**(5): 549-65.

Borden, E. C., G. C. Sen, et al. (2007). "Interferons at age 50: past, current and future impact on biomedicine." Nat Rev Drug Discov **6**(12): 975-90.

Brannan, C. I., E. C. Dees, et al. (1990). "The product of the H19 gene may function as an RNA." Mol Cell Biol **10**(1): 28-36.

Brem, R., K. Oraszlan-Szovik, et al. (2003). "Inhibition of proliferation by 1-8U in interferon-alpha-responsive and non-responsive cell lines." Cell Mol Life Sci **60**(6): 1235-48.

Calabrese, V., F. A. Mallette, et al. (2009). "SOCS1 links cytokine signaling to p53 and senescence." Mol Cell **36**(5): 754-67.

Campbell, A. (1981). "Some general questions about movable elements and their implications." Cold Spring Harb Symp Quant Biol **45 Pt 1**: 1-9.

Cazzalini, O., A. I. Scovassi, et al. (2010). "Multiple roles of the cell cycle inhibitor p21(CDKN1A) in the DNA damage response." Mutat Res.

Certa, U., M. Seiler, et al. (2001). "High density oligonucleotide array analysis of interferon- alpha2a sensitivity and transcriptional response in melanoma cells." Br J Cancer **85**(1): 107-14.

Certa, U., M. Wilhelm-Seiler, et al. (2003). "Expression modes of interferon-alpha inducible genes in sensitive and resistant human melanoma cells stimulated with regular and pegylated interferon-alpha." Gene **315**: 79-86.

Chadha, K. C., J. L. Ambrus, Jr., et al. (2004). "Interferons and interferon inhibitory activity in disease and therapy." Exp Biol Med (Maywood) **229**(4): 285-90.

Chang, Y. S., L. Wang, et al. (2004). "Mechanisms underlying lack of insulin-like growth factor-binding protein-3 expression in non-small-cell lung cancer." Oncogene **23**(39): 6569-80.

Chen, W. G., Q. Chang, et al. (2003). "Derepression of BDNF transcription involves calcium-dependent phosphorylation of MeCP2." Science **302**(5646): 885-9.

Cunningham, B. A. (2001). "A Growing Issue: Cell Proliferation Assays." The Scientist **15**(13): 26.

Deblandre, G. A., O. P. Marinx, et al. (1995). "Expression cloning of an interferon-inducible 17-kDa membrane protein implicated in the control of cell growth." J Biol Chem **270**(40): 23860-6.

Decker, T., M. Muller, et al. (2005). "The yin and yang of type I interferon activity in bacterial infection." Nat Rev Immunol **5**(9): 675-87.

Deshpande, R., T. L. Woods, et al. (2000). "Biochemical characterization of S100A2 in human keratinocytes: subcellular localization, dimerization, and oxidative cross-linking." J Invest Dermatol **115**(3): 477-85.

Donato, R. (2001). "S100: a multigenic family of calcium-modulated proteins of the EF-hand type with intracellular and extracellular functional roles." Int J Biochem Cell Biol **33**(7): 637-68.

Duong, F. H., V. Christen, et al. (2006). "S-Adenosylmethionine and betaine correct hepatitis C virus induced inhibition of interferon signaling in vitro." Hepatology **43**(4): 796-806.

Eckert, R. L., A. M. Broome, et al. (2004). "S100 proteins in the epidermis." J Invest Dermatol **123**(1): 23-33.

Ehrlich, M. (2003). "The ICF syndrome, a DNA methyltransferase 3B deficiency and immunodeficiency disease." Clin Immunol **109**(1): 17-28.

Ehrlich, M., M. A. Gama-Sosa, et al. (1982). "Amount and distribution of 5-methylcytosine in human DNA from different types of tissues of cells." Nucleic Acids Res **10**(8): 2709-21.

Epstein, C. J., S. Smith, et al. (1978). "Both X chromosomes function before visible X-chromosome inactivation in female mouse embryos." Nature **274**(5670): 500-3.

Esteller, M. (2005). "Aberrant DNA methylation as a cancer-inducing mechanism." Annu Rev Pharmacol Toxicol **45**: 629-56.

Esteller, M., P. G. Corn, et al. (2001). "A gene hypermethylation profile of human cancer." Cancer Res **61**(8): 3225-9.

Fan, J., Z. Peng, et al. (2008). "Gene-expression profiling in Chinese patients with colon cancer by coupling experimental and bioinformatic genomewide gene-expression analyses: identification and validation of IFITM3 as a biomarker of early colon carcinogenesis." Cancer **113**(2): 266-75.

Feinberg, A. P. and B. Tycko (2004). "The history of cancer epigenetics." Nat Rev Cancer **4**(2): 143-53.

Feng, G., X. Xu, et al. (2001). "Diminished expression of S100A2, a putative tumor suppressor, at early stage of human lung carcinogenesis." Cancer Res **61**(21): 7999-8004.

Feng, Q. and Y. Zhang (2001). "The MeCP1 complex represses transcription through preferential binding, remodeling, and deacetylating methylated nucleosomes." Genes Dev **15**(7): 827-32.
Foser, S., I. Redwanz, et al. (2006). "Interferon-alpha and transforming growth factor-beta co-induce growth inhibition of human tumor cells." Cell Mol Life Sci **63**(19-20): 2387-96.
Foser, S., A. Schacher, et al. (2003). "Isolation, structural characterization, and antiviral activity of positional isomers of monopegylated interferon alpha-2a (PEGASYS)." Protein Expr Purif **30**(1): 78-87.
Foser, S., K. Weyer, et al. (2003). "Improved biological and transcriptional activity of monopegylated interferon-alpha-2a isomers." Pharmacogenomics J **3**(6): 312-9.
Fraga, M. F., M. Herranz, et al. (2004). "A mouse skin multistage carcinogenesis model reflects the aberrant DNA methylation patterns of human tumors." Cancer Res **64**(16): 5527-34.
Fridman, A. L., R. Rosati, et al. (2007). "Epigenetic and functional analysis of IGFBP3 and IGFBPrP1 in cellular immortalization." Biochem Biophys Res Commun **357**(3): 785-91.
Frommer, M., L. E. McDonald, et al. (1992). "A genomic sequencing protocol that yields a positive display of 5-methylcytosine residues in individual DNA strands." Proc Natl Acad Sci U S A **89**(5): 1827-31.
Gardiner-Garden, M. and M. Frommer (1987). "CpG islands in vertebrate genomes." J Mol Biol **196**(2): 261-82.
Gehring, M., W. Reik, et al. (2009). "DNA demethylation by DNA repair." Trends Genet **25**(2): 82-90.
Gimona, M., Z. Lando, et al. (1997). "Ca2+-dependent interaction of S100A2 with muscle and nonmuscle tropomyosins." J Cell Sci **110 (Pt 5)**: 611-21.
Gottschling, D. E. (2007). Epigenetics: From Phenomenon to Field. Epigenetics. Cold SPrin Harbor, NY, Cold SPrin Harbor Laboratory Press**:** 1-13.
Greenhalgh, C. J. and D. J. Hilton (2001). "Negative regulation of cytokine signaling." J Leukoc Biol **70**(3): 348-56.
Gurdon, J. B. and R. A. Laskey (1970). "The transplantation of nuclei from single cultured cells into enucleate frogs' eggs." J Embryol Exp Morphol **24**(2): 227-48.
Gutterman, J. U. (1994). "Cytokine therapeutics: lessons from interferon alpha." Proc Natl Acad Sci U S A **91**(4): 1198-205.
Henco, K., J. Brosius, et al. (1985). "Structural relationship of human interferon alpha genes and pseudogenes." J Mol Biol **185**(2): 227-60.
Holliday, R. and J. E. Pugh (1975). "DNA modification mechanisms and gene activity during development." Science **187**(4173): 226-32.
Hurlock, E. C. t. (2001). "Interferons: potential roles in affect." Med Hypotheses **56**(5): 558-66.
Isaacs, A. and J. Lindenmann (1957). "Virus interference. I. The interferon." Proc R Soc Lond B Biol Sci **147**(927): 258-67.
Jones, P. A. and P. W. Laird (1999). "Cancer epigenetics comes of age." Nat Genet **21**(2): 163-7.
Jones, P. A. and S. M. Taylor (1980). "Cellular differentiation, cytidine analogs and DNA methylation." Cell **20**(1): 85-93.
Kangaspeska, S., B. Stride, et al. (2008). "Transient cyclical methylation of promoter DNA." Nature **452**(7183): 112-5.

Kassis, E. S., M. Zhao, et al. (2006). "Depletion of DNA methyltransferase 1 and/or DNA methyltransferase 3b mediates growth arrest and apoptosis in lung and esophageal cancer and malignant pleural mesothelioma cells." J Thorac Cardiovasc Surg **131**(2): 298-306.

Kastan, M. B., Q. Zhan, et al. (1992). "A mammalian cell cycle checkpoint pathway utilizing p53 and GADD45 is defective in ataxia-telangiectasia." Cell **71**(4): 587-97.

Keppler, A., S. Gendreizig, et al. (2003). "A general method for the covalent labeling of fusion proteins with small molecules in vivo." Nat Biotechnol **21**(1): 86-9.

Kirkwood, J. M. (1998). "Systemic adjuvant treatment of high-risk melanoma: the role of interferon alfa-2b and other immunotherapies." Eur J Cancer **34 Suppl 3**: S12-7.

Kondo, Y., Y. Kanai, et al. (2000). "Genetic instability and aberrant DNA methylation in chronic hepatitis and cirrhosis--A comprehensive study of loss of heterozygosity and microsatellite instability at 39 loci and DNA hypermethylation on 8 CpG islands in microdissected specimens from patients with hepatocellular carcinoma." Hepatology **32**(5): 970-9.

Kudo, S. (1998). "Methyl-CpG-binding protein MeCP2 represses Sp1-activated transcription of the human leukosialin gene when the promoter is methylated." Mol Cell Biol **18**(9): 5492-9.

Kulaeva, O. I., S. Draghici, et al. (2003). "Epigenetic silencing of multiple interferon pathway genes after cellular immortalization." Oncogene **22**(26): 4118-27.

Lapi, E., A. Iovino, et al. (2006). "S100A2 gene is a direct transcriptional target of p53 homologues during keratinocyte differentiation." Oncogene **25**(26): 3628-37.

Laskey, R. A. and J. B. Gurdon (1970). "Genetic content of adult somatic cells tested by nuclear transplantation from cultured cells." Nature **228**(5278): 1332-4.

Lee, S. W., C. Tomasetto, et al. (1992). "Down-regulation of a member of the S100 gene family in mammary carcinoma cells and reexpression by azadeoxycytidine treatment." Proc Natl Acad Sci U S A **89**(6): 2504-8.

Lewin, A. R., L. E. Reid, et al. (1991). "Molecular analysis of a human interferon-inducible gene family." Eur J Biochem **199**(2): 417-23.

Li, J., F. Chen, et al. (2010). "Inhibition of STAT1 methylation is involved in the resistance of hepatitis B virus to Interferon alpha." Antiviral Res **85**(3): 463-469.

Li, J., C. Zou, et al. (2006). "DSS1 is required for the stability of BRCA2." Oncogene **25**(8): 1186-94.

Li, Y., J. E. Gudjonsson, et al. (2009). "Transgenic expression of S100A2 in hairless mouse skin enhances Cxcl13 mRNA in response to solar-simulated radiation." Arch Dermatol Res **301**(3): 205-17.

Lindsey, J. C., M. E. Lusher, et al. (2007). "Epigenetic deregulation of multiple S100 gene family members by differential hypomethylation and hypermethylation events in medulloblastoma." Br J Cancer **97**(2): 267-74.

Liu, H., H. Kang, et al. (2002). "Maximal induction of a subset of interferon target genes requires the chromatin-remodeling activity of the BAF complex." Mol Cell Biol **22**(18): 6471-9.

Lopatina, N., J. F. Haskell, et al. (2002). "Differential maintenance and de novo methylating activity by three DNA methyltransferases in aging and immortalized fibroblasts." J Cell Biochem **84**(2): 324-34.

Losick, R. (1998). "Summary: three decades after sigma." Cold Spring Harb Symp Quant Biol **63**: 653-66.

Luscher, U., L. Filgueira, et al. (1994). "The pattern of cytokine gene expression in freshly excised human metastatic melanoma suggests a state of reversible anergy of tumor-infiltrating lymphocytes." Int J Cancer **57**(4): 612-9.
Ma, D. K., J. U. Guo, et al. (2009). "DNA excision repair proteins and Gadd45 as molecular players for active DNA demethylation." Cell Cycle **8**(10): 1526-31.
Ma, D. K., M. H. Jang, et al. (2009). "Neuronal activity-induced Gadd45b promotes epigenetic DNA demethylation and adult neurogenesis." Science **323**(5917): 1074-7.
Maeda, S., R. McCandliss, et al. (1980). "Construction and identification of bacterial plasmids containing nucleotide sequence for human leukocyte interferon." Proc Natl Acad Sci U S A **77**(12): 7010-3.
Maelandsmo, G. M., V. A. Florenes, et al. (1997). "Differential expression patterns of S100A2, S100A4 and S100A6 during progression of human malignant melanoma." Int J Cancer **74**(4): 464-9.
Mandinova, A., D. Atar, et al. (1998). "Distinct subcellular localization of calcium binding S100 proteins in human smooth muscle cells and their relocation in response to rises in intracellular calcium." J Cell Sci **111 (Pt 14)**: 2043-54.
Matarazzo, M. R., M. L. De Bonis, et al. (2009). "Lessons from two human chromatin diseases, ICF syndrome and Rett syndrome." Int J Biochem Cell Biol **41**(1): 117-26.
Mathieu, O. and J. Bender (2004). "RNA-directed DNA methylation." J Cell Sci **117**(Pt 21): 4881-8.
Mc Clintock, B. (1951). "Chromosome organization and genic expression." Cold Spring Harb Symp Quant Biol **16**: 13-47.
McKeon, C., H. Ohkubo, et al. (1982). "Unusual methylation pattern of the alpha 2 (I) collagen gene." Cell **29**(1): 203-10.
Metivier, R., R. Gallais, et al. (2008). "Cyclical DNA methylation of a transcriptionally active promoter." Nature **452**(7183): 45-50.
Miller, C. H., S. G. Maher, et al. (2009). "Clinical Use of Interferon-gamma." Ann N Y Acad Sci **1182**: 69-79.
Missiaglia, E., M. Donadelli, et al. (2005). "Growth delay of human pancreatic cancer cells by methylase inhibitor 5-aza-2'-deoxycytidine treatment is associated with activation of the interferon signalling pathway." Oncogene **24**(1): 199-211.
Miyazaki, M., M. Sakaguchi, et al. (2004). "Involvement of interferon regulatory factor 1 and S100C/A11 in growth inhibition by transforming growth factor beta 1 in human hepatocellular carcinoma cells." Cancer Res **64**(12): 4155-61.
Morgan, H. D., F. Santos, et al. (2005). "Epigenetic reprogramming in mammals." Hum Mol Genet **14 Spec No 1**: R47-58.
Mueller, A., T. Bachi, et al. (1999). "Subcellular distribution of S100 proteins in tumor cells and their relocation in response to calcium activation." Histochem Cell Biol **111**(6): 453-9.
Mueller, A., B. W. Schafer, et al. (2005). "The calcium-binding protein S100A2 interacts with p53 and modulates its transcriptional activity." J Biol Chem **280**(32): 29186-93.
Muller, H. R. and J. R. Tyler (1930). "The Effect of the X-Ray on the Nodules of Verruga Peruana." J Exp Med **51**(1): 23-26.
Murayama, A., K. Sakura, et al. (2006). "A specific CpG site demethylation in the human interleukin 2 gene promoter is an epigenetic memory." Embo J **25**(5): 1081-92.

Naeim, F., D. S. Hoon, et al. (1987). "Reactivity of neoplastic cells of hairy cell leukemia with antisera to S-100 protein." Am J Clin Pathol **88**(1): 86-91.
Naka, K., K. Abe, et al. (2006). "Epigenetic silencing of interferon-inducible genes is implicated in interferon resistance of hepatitis C virus replicon-harboring cells." J Hepatol **44**(5): 869-78.
Naka, T., M. Fujimoto, et al. (2005). "Negative regulation of cytokine and TLR signalings by SOCS and others." Adv Immunol **87**: 61-122.
Neuveut, C., Y. Wei, et al. "Mechanisms of HBV-related hepatocarcinogenesis." J Hepatol.
Nielsen, K., S. Heegaard, et al. (2005). "Altered expression of CLC, DSG3, EMP3, S100A2, and SLPI in corneal epithelium from keratoconus patients." Cornea **24**(6): 661-8.
Ohno, S., W. D. Kaplan, et al. (1959). "Formation of the sex chromatin by a single X-chromosome in liver cells of Rattus norvegicus." Exp Cell Res **18**: 415-8.
Olaharski, A., S. Albertini, et al. (2009). "Evaluation of the GreenScreen GADD45alpha-GFP indicator assay with non-proprietary and proprietary compounds." Mutat Res **672**(1): 10-6.
Ooi, S. K. and T. H. Bestor (2008). "The colorful history of active DNA demethylation." Cell **133**(7): 1145-8.
Pansky, A., P. Hildebrand, et al. (2000). "Defective Jak-STAT signal transduction pathway in melanoma cells resistant to growth inhibition by interferon-alpha." Int J Cancer **85**(5): 720-5.
Passos, J. F., G. Nelson, et al. "Feedback between p21 and reactive oxygen production is necessary for cell senescence." Mol Syst Biol **6**: 347.
Pedrocchi, M., B. W. Schafer, et al. (1994). "Expression of Ca(2+)-binding proteins of the S100 family in malignant human breast-cancer cell lines and biopsy samples." Int J Cancer **57**(5): 684-90.
Peng, L., J. Wang, et al. (2008). "The role of insulin-like growth factor binding protein-3 in the growth inhibitory actions of androgens in LNCaP human prostate cancer cells." Int J Cancer **122**(3): 558-66.
Pennisi, E. (2009). "History of science. The case of the midwife toad: fraud or epigenetics?" Science **325**(5945): 1194-5.
Pestka, S. (2003). "A dance between interferon-alpha/beta and p53 demonstrates collaborations in tumor suppression and antiviral activities." Cancer Cell **4**(2): 85-7.
Peterson, E. J., O. Bogler, et al. (2003). "p53-mediated repression of DNA methyltransferase 1 expression by specific DNA binding." Cancer Res **63**(20): 6579-82.
Qiu, W., B. Zhou, et al. (2004). "Hypermethylation of growth arrest DNA damage-inducible gene 45 beta promoter in human hepatocellular carcinoma." Am J Pathol **165**(5): 1689-99.
Rai, K., I. J. Huggins, et al. (2008). "DNA demethylation in zebrafish involves the coupling of a deaminase, a glycosylase, and gadd45." Cell **135**(7): 1201-12.
Raynaud, C. M., L. Sabatier, et al. (2008). "Telomere length, telomeric proteins and genomic instability during the multistep carcinogenic process." Crit Rev Oncol Hematol **66**(2): 99-117.
Rehman, I., S. S. Cross, et al. (2005). "Promoter hyper-methylation of calcium binding proteins S100A6 and S100A2 in human prostate cancer." Prostate **65**(4): 322-30.

Reid, L. M., N. Minato, et al. (1981). "Influence of anti-mouse interferon serum on the growth and metastasis of tumor cells persistently infected with virus and of human prostatic tumors in athymic nude mice." Proc Natl Acad Sci U S A **78**(2): 1171-5.

Reu, F. J., S. I. Bae, et al. (2006). "Overcoming resistance to interferon-induced apoptosis of renal carcinoma and melanoma cells by DNA demethylation." J Clin Oncol **24**(23): 3771-9.

Robertson, K. D., K. Keyomarsi, et al. (2000). "Differential mRNA expression of the human DNA methyltransferases (DNMTs) 1, 3a and 3b during the G(0)/G(1) to S phase transition in normal and tumor cells." Nucleic Acids Res **28**(10): 2108-13.

Rougier, N., D. Bourc'his, et al. (1998). "Chromosome methylation patterns during mammalian preimplantation development." Genes Dev **12**(14): 2108-13.

Rubinstein, M., S. Rubinstein, et al. (1978). "Human leukocyte interferon purified to homogeneity." Science **202**(4374): 1289-90.

Sakaguchi, M., H. Sonegawa, et al. (2008). "S100A11, an dual mediator for growth regulation of human keratinocytes." Mol Biol Cell **19**(1): 78-85.

Salama, I., P. S. Malone, et al. (2008). "A review of the S100 proteins in cancer." Eur J Surg Oncol **34**(4): 357-64.

Sansom, O. J., K. Maddison, et al. (2007). "Mechanisms of disease: methyl-binding domain proteins as potential therapeutic targets in cancer." Nat Clin Pract Oncol **4**(5): 305-15.

Schafer, B. W. and C. W. Heizmann (1996). "The S100 family of EF-hand calcium-binding proteins: functions and pathology." Trends Biochem Sci **21**(4): 134-40.

Schmitz, K. M., N. Schmitt, et al. (2009). "TAF12 recruits Gadd45a and the nucleotide excision repair complex to the promoter of rRNA genes leading to active DNA demethylation." Mol Cell **33**(3): 344-53.

Sciences, R. A. (2010). Cell Index.

Seoane, J. (2004). "p21(WAF1/CIP1) at the switch between the anti-oncogenic and oncogenic faces of TGFbeta." Cancer Biol Ther **3**(2): 226-7.

Shon, J. K., B. H. Shon, et al. (2009). "Hepatitis B virus-X protein recruits histone deacetylase 1 to repress insulin-like growth factor binding protein 3 transcription." Virus Res **139**(1): 14-21.

Sonegawa, H., T. Nukui, et al. (2007). "Involvement of deterioration in S100C/A11-mediated pathway in resistance of human squamous cancer cell lines to TGFbeta-induced growth suppression." J Mol Med **85**(7): 753-62.

Spiegel, R. J. (1987). "Clinical overview of alpha interferon. Studies and future directions." Cancer **59**(3 Suppl): 626-31.

Stark, G. R., I. M. Kerr, et al. (1998). "How cells respond to interferons." Annu Rev Biochem **67**: 227-64.

Stedman, E. (1950). "Cell specificity of histones." Nature **166**(4227): 780-1.

Takaoka, A., S. Hayakawa, et al. (2003). "Integration of interferon-alpha/beta signalling to p53 responses in tumour suppression and antiviral defence." Nature **424**(6948): 516-23.

Tan, H. H. and A. G. Porter (2009). "p21(WAF1) negatively regulates DNMT1 expression in mammalian cells." Biochem Biophys Res Commun **382**(1): 171-6.

Tan, M., C. W. Heizmann, et al. (1999). "Transcriptional activation of the human S100A2 promoter by wild-type p53." FEBS Lett **445**(2-3): 265-8.

Tan, Y. F., X. Y. Sun, et al. (2006). "Gene expression pattern and hormonal regulation of small proline-rich protein 2 family members in the female mouse reproductive system during the estrous cycle and pregnancy." Reprod Nutr Dev **46**(6): 641-55.

Taniguchi, T. and A. Takaoka (2001). "A weak signal for strong responses: interferon-alpha/beta revisited." Nat Rev Mol Cell Biol **2**(5): 378-86.

Teodoridis, J. M., C. Hardie, et al. (2008). "CpG island methylator phenotype (CIMP) in cancer: causes and implications." Cancer Lett **268**(2): 177-86.

Ting, A. H., K. W. Jair, et al. (2004). "Mammalian DNA methyltransferase 1: inspiration for new directions." Cell Cycle **3**(8): 1024-6.

Uze, G. and D. Monneron (2007). "IL-28 and IL-29: newcomers to the interferon family." Biochimie **89**(6-7): 729-34.

Vidigal, P. G., J. J. Germer, et al. (2002). "Polymorphisms in the interleukin-10, tumor necrosis factor-alpha, and transforming growth factor-beta1 genes in chronic hepatitis C patients treated with interferon and ribavirin." J Hepatol **36**(2): 271-7.

Vousden, K. H. and C. Prives (2009). "Blinded by the Light: The Growing Complexity of p53." Cell **137**(3): 413-31.

Wade, P. A., A. Gegonne, et al. (1999). "Mi-2 complex couples DNA methylation to chromatin remodelling and histone deacetylation." Nat Genet **23**(1): 62-6.

Wade, P. A., P. L. Jones, et al. (1998). "Histone deacetylase directs the dominant silencing of transcription in chromatin: association with MeCP2 and the Mi-2 chromodomain SWI/SNF ATPase." Cold Spring Harb Symp Quant Biol **63**: 435-45.

Wang, Y., T. Rea, et al. (1999). "Identification of the genes responsive to etoposide-induced apoptosis: application of DNA chip technology." FEBS Lett **445**(2-3): 269-73.

Weisenberger, D. J., D. V. D. Berg, et al. (2008). "Comprehensive DNA Methylation Analysis on the Illumina® Infinium® Assay Platform." Illumina.

Wicki, R., C. Franz, et al. (1997). "Repression of the candidate tumor suppressor gene S100A2 in breast cancer is mediated by site-specific hypermethylation." Cell Calcium **22**(4): 243-54.

Xu, G. L., T. H. Bestor, et al. (1999). "Chromosome instability and immunodeficiency syndrome caused by mutations in a DNA methyltransferase gene." Nature **402**(6758): 187-91.

Yarmolinsky, M. B. (1981). "Summary." Cold Spring Harb Symp Quant Biol **45 Pt 2**: 1009-15.

Young, J. I. and J. R. Smith (2001). "DNA methyltransferase inhibition in normal human fibroblasts induces a p21-dependent cell cycle withdrawal." J Biol Chem **276**(22): 19610-6.

Zhu, W. G., K. Srinivasan, et al. (2003). "Methylation of adjacent CpG sites affects Sp1/Sp3 binding and activity in the p21(Cip1) promoter." Mol Cell Biol **23**(12): 4056-65.

Zimmer, D. B., P. Wright Sadosky, et al. (2003). "Molecular mechanisms of S100-target protein interactions." Microsc Res Tech **60**(6): 552-9.

8. ABBREVIATIONS

5-FU	5-fluoruracil
AAF	alpha-interferon activation factor
BDNF	brain-derived neurotrophic factor
Ca^{2+}	calcium
CHF	changefactor
CIMP	CpG Island Methylator Phenotype
cpm	counts per minute
D10	human melanoma cell line D10
DAC	5-aza-2'deoxycytidine
DMSO	dimethyl sulfoxide
DNMT1	maintenance DNA methyl transferase
DNMT3	*de novo* DNA methyl transferase
DSS1	split hand/ foot malformation (ectrodactyly) type 1
FGF	fibroblast growth factor
Gadd45	growth arrest and DNA-damage-inducible
GAS	interferon-gamma activated site
h	hours
H19	imprinted maternally expressed transcript (non-protein coding)
HBV	Hepatitis B virus
HCV	hepatitis C virus
HDAC	histone deacetylase
IFI6	interferon inducible protein 6
IFITM1 (9-27)	interferon inducible transmembrane protein 1
IFITM2 (1-8D)	interferon inducible transmembrane protein 2
IFITM3 (1-8U)	interferon inducible transmembrane protein 3
IFNAR1	interferon alpha receptor 1
IFNAR2	interferon alpha receptor 2
IFNα	interferon-alpha
$IFN\alpha^{K134}$	pegylated form of IFNα-2A
IFNβ	interferon-beta
IFNγ	interferon-gamma
IGFBP3	insulin growth factor binding protein 3
IL2	Interleukin 2
IRF1	interferon regulatory factor 1
IRF2	interferon regulatory factor 2
IRF9	interferon regulatory factor 9
ISGF3	interferon stimulated gene factor 3
ISRE	interferon-stimulated response elements
JAK	janus kinase
LPS	lipopolysaccharide

MAP2K5	mitogen-activated protein kinase kinase 5
MBD	methyl binding domain protein
MDbla	fused cell line from ME15 and D10
ME15	human melanoma cell line ME15
MeCP2	methyl CpG binding protein 2 (Rett syndrome)
NFAT	Transcription factor
OCT1	POU class 2 homeobox 1
OCT11	POU class 2 homeobox 11
P	primary cell line
p21	Cdkn1a, cyclin-dependent kinase inhibitor 1A
p48	interferon regulatory factor 9
PIAS	protein inhibitor of activated STAT
PMA	phorbol 12-myristate 13-acetate
PTGF-β	growth differentiation factor 15
S100A2	small calcium binding protein 2
SAM	S-adenosyl-methionine
SOCS	suppressor of cytokine signaling
Sp1	Sp1 transcription factor
STAT1	signal transducer and activator of transcription 1
STAT2	signal transducer and activator of transcription 2
TG	transgenic cell line
TGFβ	transforming growth factor beta
TP53	Tumor protein 53
TYK	tyrosine kinase
U	unit

9. MANUSCRIPT

Interferon-alpha promotes S100A2 dependant dynamic demethylation of the IFITM3 core promoter

Rachel Scott[a], Fredy Siegrist[a], Stefan Foser[b] and Ulrich Certa[a]*

[a]*Department non-clinical Safety, F. Hoffmann-La Roche AG, 4070 Basel (Switzerland)*

[b]*Clinical Biomarkers, F. Hoffmann-La Roche AG, 4070 Basel (Switzerland)*

Abbrevations: IFNα, interferon-alpha; IFITM3, interferon inducible transmembrane protein 3; S100A2, small calcium binding protein 2; DAC, 5'-aza-2'deoxycytidine; ISRE, interferon stimulated regulatory element; TGFβ, transforming growth factor beta; U, unit; HCV, hepatitis C virus

Running Head: Cytokine dependant dynamic promoter methylation

* corresponding author: Prof. Dr. Ulrich Certa, F. Hoffmann-La Roche Ltd., Postfach, CH-4070 Basel, Switzerland. Tel.: +41 61 687 53 40; fax +41 61 688 1448.

E-mail address: ulrich.certa@roche.com

Abstract

In human melanoma cell lines, the calcium binding protein S100A2 augments the antiproliferative activity of interferon-alpha (IFNα) by an unknown mechanism. We show by microarray profiling that recombinant overexpression of S100A2 upregulates the expression of a subset of IFNα response genes beyond the maximal cytokine inducible level including the tumor suppressor gene IFITM3. Treatment of ME15 melanoma cells with the demethylating agent 5'-aza-2'deoxycytidine (DAC) results in a significant increase of IFITM3 expression following IFNα stimulation suggesting a DNA methylation mediated mechanism. We demonstrate by bisulfite sequencing of the IFITM3 core promoter that IFNα triggers reversible hypomethylation of specific CpG sites in the presence of S100A2.

Key words. Interferon signaling, calcium binding proteins, transcriptional enhancement, DNA methylation, S100A2 protein

1. Introduction

Interferon was discovered 50 years ago as a host derived interference activity induced by heat inactivated viral particles (Isaacs and Lindenmann 1957). The advent of a novel technique termed “high performance liquid chromatography” enabled purification of interferon from virus infected leukocytes 20 years after its discovery (Rubinstein and others 1978). Cloning and recombinant expression of IFNα paved the way for the first protein based medicine (Maeda and others 1980). Since then, several additional interferons were discovered that are involved either in antiviral responses (type I) or play a role in immune defense (type II) (Stark and others 1998).

A hallmark of interferon type I cytokines is the induction of antiproliferative activity coupled to transcriptional induction of target genes. IFNα inducible genes are divided into primary and secondary response genes (PRG’s and SRG’s) according to their activation mode. PRG’s are induced early after cytokine stimulation and contain single or tandem interferon stimulated regulatory elements (ISRE’s) in the core promoter region whilst SRG’s lack such motifs and show delayed induction by an unknown mechanism. Microarray experiments have revealed, that IFNα resistance is associated with reduced but not defective transcriptional activity in human melanoma cell lines (Certa and others 2003). The exact mechanism of resistance in clinical settings like hepatitis C virus infections is still unclear and dependent on host and pathogen factors (Gale and Foy 2005; Mbow and Sarisky 2004).

Recently, we have addressed the molecular mechanism of IFNα resistance in melanoma cell lines as a model. Co-stimulation of the resistant line D10 with IFNα

and transforming growth factor beta (TGFβ) for instance restores antiproliferative activity and leads to cooperative upregulation of 28 genes including the small calcium binding protein S100A2 (Foser and others 2006). Stable overexpression of S100A2 together with IFNα stimulation enhances inhibition of cell proliferation in the responder line ME15 by an unknown mechanism.

The S100 type calcium binding proteins belong to a class of genes with pleiotropic functions and properties (Eckert and others 2004). Shared feature of all S100 proteins is the so called EF-hand motif which binds calcium ions resulting in dimerization and catalytic activation (Donato 2001). Calcium signaling is involved in a wide range of cellular functions (Berridge and others 2000) and tissue and cell type specific expression of calcium binding proteins is an important mechanism to provide cell type specific Ca^{2+} signal transduction leading to stress response, epidermal wound repair, cell differentiation or tumorigenic disorders (Zimmer and others 2003). S100 proteins are distinguished by their different subcellular distribution patterns and can undergo translocation between cellular compartments in response to a stimulus (Mandinova and others 1998). In addition, certain family members interact directly with the transcription machinery and sense Ca^{2+} levels triggering intracellular release when necessary (Mandinova and others 1998; Schafer and Heizmann 1996).

In melanoma and breast tumors S100A2 expression is often suppressed which points to a role in growth control under normal circumstances (Maelandsmo and others 1997; Pedrocchi and others 1994). DNA methylation studies of the S100A2 core promoter in mammary and prostate cancer have shown significant hypermethylation, which apparently suppresses S100A2 expression. (Lee and others 1992; Rehman and others 2005; Wicki and others 1997). We have shown previously (Foser and others 2006) that recombinant overexpression of S100A2 in the human

melanoma cell line ME15 leads to significant enhancement of antiproliferative activity induced by IFNα.

Several studies link DNA methylation and IFNα signaling, e.g. senescence can be induced in the immortalized Li-Fraumeni syndrome cells by treatment with the DNA demethylating and DNA methyltransferase (DNMT) inhibitory agent 5'-aza-2'deoxycytidine (DAC) and interestingly IFNα treatment induces a similar effect in these cells (Fridman and others 2007). In mice, suppression of endogenous IFNs enhances development of metastases (Reid and others 1981) and microarray studies with DAC treated immortalized human cells revealed deregulation of a significant number of IFN pathway genes (Kulaeva and others 2003).

Here we approach the molecular mechanism of how S100A2 enhances the antiproliferative activity of IFNα. Using microarray based mRNA profiling we found that S100A2 upregulates the expression of a small number IFNα response genes including IFITM3, a gene with antiproliferative activity. We investigated core promoter DNA methylation of IFITM3 as a possible mechanism for enhancement of expression and show that DAC treatment enhances the response to IFNα in ME15 cells. We show by bisulfite sequencing of the IFITM3 core promoter in a time course experiment, that IFNα induces reversible hypomethylation of specific CpG residues 6 hours after incubation only when S100A2 is expressed. Finally, we show virtually complete hypomethylation of the IFITM3 core promoter in the melanoma line D10, where IFITM3 is constitutively expressed without IFNα stimulation.

2. Material and Methods

2.1. Cell lines

The primary human melanoma cell lines ME15 and D10 were kindly supplied by Prof. Giulio Spagnioli (University of Basel) and have been described elsewhere (Luscher and others 1994; Pansky and others 2000). The ME15^{S100A2} cell line has been described by Foser et. al. (Brem and others 2003; Foser and others 2006; Luscher and others 1994; Pansky and others 2000).

2.2. Antibodies, cytokines and reagents

Antibody against IFITM3 (1-8U) has been described previously (Brem and others 2003). Rabbit-anti-S100A2 serum was kindly provided by Prof. C.W. Heizmann (University of Zürich). Goat anti-rabbit IgG (H+L) horseradish peroxidase (HRP) conjugate was obtained from BioRad (Basel, Switzerland). Alexa Fluor 555 goat anti-rabbit IgG (H+L) was purchased from Invitrogen (Basel, Switzerland). IFNα (IFNα2a, Roferon®-A) and its monopegylated isomer K134 (IFNα^{K134} (Foser and others 2006)) were provided by F. Hoffmann-La Roche Ltd. (Basel, Switzerland). TGFβ was purchased from Calobiochem (Germany) and 5- aza-2'-deoxycytidine (DAC) from Sigma (Basel, Switzerland). Lipopolysaccharide (LPS) was purchased from Sigma (Basel, Switzerland) and 5-fluoruracil (5-FU) at Fluka (Buchs, Switzerland).

2.3. Cell culture

All cell lines were cultured at 37℃ in a 5% CO_2 atmosphere in RPMI 1640 medium (GIBCO Life Sciences, Paisley, U.K.) supplemented with 10% fetal bovine serum (FBS), L-glutamine (2 mM), sodium pyruvate (1 mM), nonessential amino acids, antibiotics, and 10 mM HEPES buffer (Certa and others 2003).

2.4. Cell treatments

For oligonucleotide array analysis ME15 and ME15^{S100A2} melanoma cell lines were grown in triplicate cultures for 2 days with either IFNα^{K134} (1000 U/ml) , TGFβ (2 ng/ml) or a combination of both cytokines (Fig. 1A). ME15 and ME15^{S100A2} cells were treated with IFNα (1000 U/ml) for 2 days in order to verify IFITM3 mRNA expression by quantitative real-time PCR (Fig. 1B). To investigate IFITM3 protein levels in the presence and absence of S100A2, ME15 and ME15^{S100A2} melanoma cell lines were stimulated with IFNα (1000 U/ml) for 8 hours (Fig. 1C). For cell fractionation ME15 as well as ME15^{S100A2} cells were treated with IFNα (1000 U/ml), TGFβ (2 ng/ml) or a combination of both cytokines for 2 days or ME15 cells were transfected with SNAP-S100A2-Bam and SNAP-S100A2-Eco vectors for 6 and 20 hours (data not shown). In the S100A2 immunofluorescence localization assay cells were incubated with both IFNα (1000 U/ml) and TGFβ (2 ng/ml) or either the SNAP-S100A2-Bam or the SNAP-S100A2-Eco recombinant vector for two days (data not shown). To promote genome wide demethylation the cell lines were treated with 5- aza-2'-deoxycytidine (DAC) (2 μg/ml) or a control along with IFNα (1000 U/ml, 100 U/ml or 10 U/ml), TGFβ (1 μg/ml) or a combination of both cytokines with incubation times depicted in figure 2. For the IFITM3 promoter methylation analysis ME15, ME15^{S100A2} and D10 cells were stimulated with IFNα (1000 U/ml) according to figure 3. In order to induce S100A2

expression ME15 cells were incubated with TGFβ (2 ng/ml) for 2 days. For the reporter assays ME15 and D10 cells were transfected with the according luciferase plasmids and incubated with 5-fluoruracil (5-FU, 10 μg/ml, in DMSO dilution), lipopolysaccharide (LPS, 100 μg/ml, in DMSO dilution), 0.1% DMSO alone or DAC (2 μg/ml) (Fig. 4).

2.5. Oligonucleotide array analysis

Total RNA was isolated, processed and hybridized to Affymetrix U95Av2 human microarrays according to the manufacturer's instructions (for details see (Foser and others 2006)). After intensities were recorded by laser scanning, normalized data was analyzed for differential expression using RACE-A software as described (Certa and others 2003). Genes with a standard deviation smaller than the absolute change in signal intensity, a signal intensity of a minimum of 50 RFUs, and an absolute change factor (CHF) of at least 2 (Certa and others 2003) were considered. Expression data from untreated cells (ME15 and ME15^{S100A2}) were used as baseline to calculate the change factor values. The raw data are available on request.

2.6. Quantitative Real-time PCR

Upon reverse transcription of total RNA, IFITM3 and GAPDH derived cDNA were detected by real-time PCR using primers and dual-labeled fluorogenic probes (Applied Biosystems assay reagents Hs03057129_s1 and Hs99999905_m1, respectively). Amplification reactions were performed using 2x TaqMan® Fast Universal Mastermix (Applied Biosystems) and realtime change of fluorescence

intensity was monitored using an ABI 7500 detection system (Applied Biosystems). Data was analyzed with the comparative cycle threshold method.

2.7. Immunoblotting

Cell fractions or total calibrated protein extracts, were separated by SDS PAGE and electroblotted onto nitrocellulose membranes, which were blocked in commercial blocking buffer (SuperBlock® Blocking Buffer; Pierce Chemical Co., Thermo Fisher Scientific Inc., Rockford, IL, USA). Proteins were detected using primary antibodies against IFITM3 at a dilution of 1:2000 or S100A2 at a dilution of 1:1000 and a horse-radish-peroxidase (HRP)-conjugated secondary antibody diluted 1:5000 for detection with a chemiluminescent substrate (SuperSignal West Pico Chemiluminescent; Pierce Chemical Co., Thermo Fisher Scientific Inc., Rockford, IL, USA).

2.8. Transfections and Plasmids

All transfections were performed using either FuGENE® from F. Hoffmann-La Roche Ltd. (Basel, Switzerland), Optifect or LipofectAMINE 2000 reagents from Invitrogen (Basel, Switzerland) according to the manufacturer's protocol. PcDNA3 -S100A2 was kindly provided by Prof. C.W. Heizmann (University of Zürich). The firefly, pGL3-tk-luc, and the renilla, phRL tkluc, luciferase plasmids were purchased from Promega (Dübendorf, Switzerland). The p53 reporter plasmid was constructed by an insertion of two p53 target sequences of the GADD45 promoter region into the pGL3-tk-luc plasmid and was a kind gift of K. Schad (F. Hoffmann-La Roche Ltd., Basel, Switzerland).

2.9. Cell fractionation

ME15, ME15^{S100A2} and D10 cells were harvested and fractionated using a commercial kit according to the instructions supplied (Qiagen Qproteome Cell Compartment Kit, Qiagen, Hombrechtikon, Switzerland).

2.10. Cloning of SNAP-tagged S100A2

The 970bp fragment containing the entire S100A2 coding region was amplified from pcDNA3 -S100A2 (Foser and others 2006) by PCR using primers with internal EcoR1 and BamH1 sites (underlined in the following primer sequences) for subcloning into pSEMS-26m (Covalys Witterswil, Switzerland) to generate N- or C-terminal fusion proteins with SNAP-Tag. Following primers were used for the C-terminal construct, pSEMS-S100A2-Eco: forward (nucleotide at position 317, RSN;NM_005978) 5'- CCT GGT CTG CCA CGA ATT CAT G**AT G**TG CAG TTCT and backward (nucleotide at position 611, RSN;NM_005978) 5'- CCC GAC GGG TCT GGC TGG G**CT T**AA GTC TTG. For the N-terminal construct, pSEMS-S100A2-Bam, primers were as follows: forward (nucleotide at position 317, RSN;NM_005978) 5'- CCT GGT CTG CCA CGG ATC CAT G**AT G**TG CAG TTCT and backward (nucleotide at position 612, RSN;NM_005978) 5'- CCGA CGG GTC TGG CTG GG**A CT**C CTA GGT GAA. All sequences were verified and screened for correct orientation by standard automated DNA sequencing using standard sequencing primers.

2.11. Immunofluorescence

Approximately 2000 ME15 cells and 4000 cells of each ME15^{S100A2} and D10 were seeded in 4-well Lab-Tek® II Chamber Slides™ (LabTek, Nunc Inc., Langenselbold, Germany). The following day, cells were treated with a combination of IFNα (1000 U/ml) and TGFβ (2 ng/ml) or a control, followed by an incubation time of 2 days. All subsequent cell manipulations were performed on ice. Cells were washed twice with ice-cold OptiMEM from Invitrogen (Basel, Switzerland) and fixed for 2 minutes using 70% acetone kept at -20ºC. After two additional washes with ice-cold PBS the samples were treated with Image-iT® FX signal enhancer from Invitrogen (Basel, Switzerland) for 30 minutes and blocked for 1.5 hours in PBS containing 1% Bovine Serum Albumin (BSA) (Sigma, Basel, Switzerland), 1% Normal Goat Serum (NSG) (Sigma, Basel, Switzerland) and 1‰ Ova Albumin (OVA) (Fluka, Basel, Switzerland). Cells were incubated for 1 hour with anti-S100A2 serum at a dilution of 1:500 in blocking solution. After washing twice with PBS containing 1% BSA for 5 minutes, cells were stained with Alexa Fluor 555 diluted 1:100 in PBS containing 1% BSA for 1 hour. Cells were washed twice for 5 minutes with PBS. Images were recorded with a Zeiss Axiovert 135 microscope using Axiocam software (Zeiss, Feldbach, Switzerland).

2.12. DNA wide demethylation by 5- aza-2'-deoxycytidine (DAC) treatment

Approximately 10'000 ME15 cells and 20'000 ME15^{S100A2} cells were seeded in 6-well plates. Cells were grown for three days following stimulation with TGFβ (1 μg/ml), IFNα (1000 U/ml) or a combination of both cytokines, in the presence or absence of

DAC (2 μg/ml). After 6,12, 24 and 51 hours cells were washed twice with PBS, resuspended in standard lysis buffer and the whole protein extract was thereafter used for immunoblot analysis (Fig. 3A and B). The same procedure was applied for the IFNα sensitivity experiment with 100 U/ml or 10 U/ml IFNα treatment in the presence or absence of DAC (2 μg/ml) (Fig. 3C).

2.13. Promoter methylation analysis

ME15, ME15^{S100A2} and D10 melanoma cell lines were treated with IFNα (1000 U/ml) for 1, 6 and 24 hours. In order to promote S100A2 expression in ME15 cells they were pretreated with TGFβ (2 ng/ml) for 2 days. Isolated genomic DNA was bisulfite treated using the Zymo EZ DNA Methylation™ Kit (Orange, CA, USA) according to the manufactures protocol with 2μg of DNA input. The bottom strand of the IFITM3 promoter was amplified to yield an 820 bp fragment using bisulfite adjusted primers designed to cover 19 CpG sites adjacent to the translation initiation site (ATG) (forward primer (Chromosome 11: 311612) 5'-ATA ATC CAA CTA CCT AAA CAC CATA and backward primer (Chromosome 11: 310793) 5'- GGT TTG GAT AGT GTG ATT TAT GGT GTT TA) with the PCR program consisting of following parameters: initial incubation time of 10 minutes at 95℃, 40 c ycles with 1 minute at 94℃, 1 minute at 58℃ and 1 minute at 72℃ and an addition al 10 minutes at 72℃ for final elongation. Amplified fragments were cloned into the pCR®2.1-TOPO® vector (Invitrogen, Basel, Switzerland) and transformed into XL1-blue (Stratagene, La Jolla, CA, USA) or TOP10 (Invitrogen, Basel, Switzerland) competent cells and plated on IPTG/ X-gal containing agar plates. Plasmids from white colonies were isolated and sequenced using an ABI 3730xl DNA analyzer instrument and generic vector based

primers using standard procedures. Following computer assisted alignment with the clustalw GCG-program the methylation state of CpG sites was determined and a Wilson's test showed significances of methylation changes for each treatment condition (Wilson 1927).

2.14. P53 luciferase reporter assay

ME15 and D10 cells were transfected with a combination of the p53 negative firefly and the control renilla luciferase plasmid or with the p53 reporter plasmid firefly along with the renilla luciferase control plasmid ('2 x p53 in pGl3-tk-luc' and phRL tkluc') in quadruplicates at a confluency of approximately 50% in 24 wells. To ensure efficient transfection reaction cells were incubated for 6 hours whereupon medium was replaced with culture medium containing either 5-fluoruracil (5-FU), lipopolysaccharide (LPS, 100 ug/mL, in DMSO dilution), 0.1% DMSO alone or DAC at the standard concentration. Cells were further incubated for 48 hours before luciferase activity was measured by Dual Luciferase Reporter Assay System (Promega, Dübendorf, Switzerland).

3. Results

3.1. Transcriptional responses to IFNα in the presence of S100A2

We have shown previously that the TGFβ-inducible calcium binding protein S100A2 inhibits growth of stably transfected human melanoma cell lines (Foser and others 2006). The antiproliferative activity however, requires co-stimulation with IFNα, which induces calcium release required for the activation of all calcium binding proteins. In order to test whether constitutive expression of S100A2 modulates the induction of IFNα-inducible genes, we first performed an mRNA expression microarray analysis of S100A2-transfected human ME15 melanoma cells with untransfected cells as control (Fig. 1A). In addition to IFNα, we treated cell cultures with TGFβ and the combination of both cytokines in order to detect possible interactions of S100A2 with the TGFβ signaling pathway. In $ME15^{S100A2}$ cells, one cluster of genes is significantly upregulated by overexpression of S100A2 as compared with the parent line ME15 (Fig. 1A, cluster 2, Table 1). For clarity, the calculated change factors for all genes in clusters 1 and 2 are shown in table 1.

Gene cluster two in figure 1A contains IFITM3 and other known IFNα-inducible genes like p27, 9-27 or 2-5 oligoadenylate cyclase and this gene cluster is upregulated in the presence of S100A2 beyond maximal IFNα inducible levels. Another regulated gene in cluster two is the small proline-rich protein 2d (SPRR2D) which along with the S100 proteins is located on chromosome 1q21, forming the proposed epidermal differentiation complex (Mischke and others 1996). Other regulated genes like ISG15, STAT1 or MHC class 1 are part of cluster one and are insensitive to S100A2

overexpression (Fig. 1A, cluster 1, Table 1). In contrast to the genes in cluster two (Fig. 1A, cluster 2, Table 1), none of these genes has documented antiproliferative activity. TGFβ or combined IFNα/ TGFβ responses are in general not affected by S100A2 expression in ME15 or ME15^{S100A2} cells, although certain genes appear moderately downregulated (Fig. 1A).

Within the group of IFNα inducible genes that is further upregulated by S100A2, IFITM3 is the only gene with documented antiproliferative activity (Brem and others 2003) and elevated levels would explain augmented inhibition of cell growth and proliferation. IFITM3 expression enhancement in the presence of S100A2 was verified using real time PCR (Fig. 1B) To support this finding, we determined the protein levels in ME15^{S100A2} cells treated with IFNα. After treatment of ME15 and ME15^{S100A2} cells with 1000 U/ml of IFNα for 8 hours, protein extracts were analyzed by immunoblotting using rabbit serum against IFITM3 (Brem and others 2003). Consistent with mRNA expression, we found elevated levels of IFITM3 in ME15^{S100A2} relative to untransfected ME15 cells (Fig. 1C). Thus, S100A2-mediated upregulation of IFITM3 provides a plausible explanation for increased antiproliferative activity of IFNα in this cell line.

3.2. Core promoter methylation modulates expression levels of S100A2 and IFITM3

Treatment of ME15 cells with 1000 U/ml IFNα induces maximal antiproliferation and expression of IFITM3 approximately 6 hours after stimulation (data not shown). Therefore, an IFNα independent mechanism must account for elevated expression. By immunofluorescence, protein tagging and cell fractionation, we have shown cytoplasmic localization of S100A2 which rules out the obvious possibility that

S100A2 operates in the nucleus as transcriptional enhancer or co-factor (data not shown). Microarray studies with 5-aza-2'-deoxycytidine (DAC) treated cells show enhanced expression of several IFNα target genes suggesting that promoter methylation modulates the activity and response to IFNα (Kulaeva and others 2003) .

To assess this possibility, we stimulated ME15 cells with cytokines and compared the expression levels of S100A2 and IFITM3 in the presence or absence of the cytosine analog DAC as a general methylation inhibitor. S100A2 was included as positive control, because this promoter is known to be methylated (Lee and others 1992; Wicki and others 1997) and expression in ME15 cells is TGFβ inducible. As expected, DAC treatment results in significant upregulation of S100A2 expression in TGFβ treated cells suggesting S100A2 promoter methylation in ME15 cells (Fig. 2A, left panel). Co-stimulation with TGFβ and IFNα leads to elevated S100A2 expression even without DAC treatment which suggests the possibility that IFNα modulates the methylation status of the S100A2 core promoter (Fig. 2A, left panel). Interestingly, the levels of S100A2 in stably transfected cells were not modified by either treatment, including TGFβ, suggesting that a certain expression threshold that cannot be exceeded through activation of the chromosomal copy of S100A2 probably due cell damage or proliferation arrest. The results above confirm the literature for ME15 cells and validate the conditions for DAC treatment.

We next analyzed expression of the IFNα inducible gene IFITM3 in the same samples by immunoblotting (Fig. 2B). As expected, IFITM3 is inducible by IFNα but not by TGFβ and co-incubation with both cytokines has no obvious impact on expression. However, when cells are treated with DAC the duration of IFITM3 expression is extended to 51 hours after treatment compared to untreated cells (Fig.

2B, left panel) suggesting a methylation dependent modification of the core promoter. We noted, that DAC treatment alone is sufficient to turn on expression of IFITM3 in the absence of IFNα treatment (Fig. 1B, left panel; 51 h time point) suggesting activation by generic transcription factors.

The experiments so far suggest that S100A2 is necessary and sufficient to induce IFNα dependent changes in core promoter methylation. When S100A2 is supplied by transgenic expression (ME15^{S100A2}), the apparent levels of IFITM3 proteins are insensitive to DAC treatment (Fig. 2B, right panel) although expression of IFITM3 seems to decline more rapidly without DAC treatment perhaps due to re-methylation (Fig. 2B, right panel; 51 h time point).

To test whether DAC increases IFITM3 promoter sensitivity in ME15 and ME15^{S100A2} cells we used 10U or 100U IFNα for induction. In untreated cells low levels of IFITM3 are detectable 12 hours after induction followed by rapid decline (Fig. 2C). In contrast, in DAC treated cells IFITM3 is detectable 48 hours after induction at both IFNα doses (10U or 100U). As shown in figure 2B, detectable IFNα independent expression occurs in DAC treated cells after 51 hours.

In summary, DAC treatment enhances the sensitivity and response of the S100A2 and IFITM3 core promoters after stimulation with TGFβ. and IFNα, respectively.

3.3. Methylation state of the IFITM3 core promoter in ME15 cells

In order to demonstrate IFITM3 core promoter methylation in ME15 cells *in vivo* we used conventional bisulfite sequencing to examine the methylation status of individual CpG sites in the IFITM3 promoter (Frommer and others 1992). Since

IFITM3 induction is time dependent we included a time course and DNA was extracted 1, 6 and 24 hours after IFNα (1000 U/ml) stimulation followed by bisulfite treatment, PCR amplification of the IFITM3 core promoter fragment and sequencing. We then determined the percentage of methylated versus unmethylated C-residues across 19 CpG sites of the IFITM3 core promoter (Fig. 3). Note that the CpG site at 422 is a known SNP which is altered in our cell line (C→ T), therefore eliminating one methylation site from our investigation to give 18 CpG sites. Under these experimental conditions, we did not observe any significant changes of the baseline CpG methylation pattern over all time points indicating that regular induction of IFITM3 expression does not require any modifications of the methylation status of CpG sites in the core promoter (Fig. 3A).

Next we repeated the experiment in the presence of S100A2 supplied either by TGFβ treatment of ME15 cells or by transgenic expression ($ME15^{S100A2}$). Under both conditions, we observed significant hypomethylation across the entire panel of CpG sites 6 hours after IFNα treatment (Fig. 3 panel B and C). 24 hours after IFNα treatment the methylation status reverts to the pattern of untreated control cells which coincides with the decay of IFITM3 protein expression (Fig. 2, panel B). Note also, that CpG sites 427 and 24 remain demethylated under all conditions although they are directly adjacent to sites that are targets of dynamic modification.

IFITM3 expression in the human melanoma cell line D10 is constitutive and does not require IFNα stimulation (Brem and others 2003). Based on the studies above, we expected significant, S100A2 independent hypomethylation of the core promoter resulting in IFNα independent expression. We thus treated D10 cells with IFNα as above and determined the methylation status of the core promoter by

bisulfite sequencing (Fig. 3, panel D). In contrast to ME15, the CpG sites around the ISRE site show almost complete demethylation independent of IFNα treatment.

In summary, demethylation of CpG sites of the IFITM3 core promoter is associated with improved expression and response. IFNα dependent changes in methylation status require expression of the small calcium protein S100A2.

4. Discussion

We have shown that expression of the calcium binding protein S100A2 modifies the transcription efficiency of a small number of IFNα target genes. Maximal IFNα-inducible IFITM3 levels are associated with dynamic and reversible changes of the methylation state of the core promoter; these methylations are INFα dependent and require the presence of S100A2. Elevated expression of IFITM3 provides a plausible explanation for the strong antiproliferative activity induced by co-stimulation of ME15 cells with IFNα and TGFβ.

To our knowledge this is the first report that links S100A2 and cytokine-inducible epigenetic modulation of CpG sites in the core promoter of an IFNα target gene. The catalytic function of S100A2 and of the majority of calcium binding protein family members is unknown (Eckert and others 2004). In the microarray experiment shown in figure 1, *bona fide* IFNα response genes like IFI44L, IFITM3, IFITM5 or OAS are further upregulated in ME15^{S100A2}, cells and bisulfite sequencing of these promoters is the subject of current studies in our laboratory. Expression of other classical IFNα response genes such as STATs (signal transducers and activators of transcription) (Fig. 1A, cluster 2) is not affected in ME15^{S100A2} which shows specificity of the mechanism supported by S100A2.

It is known that the promoter methylation status regulates expression of S100A2 in many cell types and tumor cell lines (Lee and others 1992) and this is also the case for ME15 as DAC treatment elevates the TGFβ-inducible expression level of S100A2 (Fig. 2A). It has been described that Ca^{2+} is required for phosphorylation and activation of the methyl binding protein MeCP2 which then releases the methylated

BDNF promoter, whereupon transcription is induced (Chen and others 2003). Also, in neuronal cells, GADD45β-promoted demethylation of specific genes such as BDNF or FGF is calcium sensitive (Ma and others 2009b). These findings strongly link calcium signaling with epigenetic regulation.

The enhanced expression of IFITM3 in response to IFNα following DAC treatment prompted us to analyze whether alterations in DNA methylation of the core promoter are responsible for upregulation. The IFITM3 promoter lacks classical CpG islands but we found 19 potential CpG methylation target sites 500 bases upstream of the transcription initiation site, 18 of which are present in ME15 cells. In figure 3A, we show the basic methylation pattern of the IFITM3 core promoter in ME15 cells, which is not altered upon induction of gene expression with IFNα. In the presence of S100A2 supplied either by TGFβ treatment or recombinant expression, partial hypomethylation of selected sites occurs 6 hours after IFNα stimulation, leading to elevated IFITM3 gene expression, as shown in figure 1B. A complete and precise reset of promoter methylation to the naive status occurs 24 hours after stimulation.

In D10 cells, IFITM3 is constitutively expressed and we show that the IFITM3 promoter is hypomethylated in the absence of any treatment or stimulus (Fig. 3D). Liu et al. showed that the IFITM3 promoter region contains an Sp1 binding site (Fig. 3, 5' CpG position # 107) that upon removal by mutagenesis leads to a reduction of IFITM3 expression to about 50% (Liu and others 2002), providing a plausible explanation for the constitutive IFITM3 protein expression in the D10 cell line.

We have previously shown that TGFβ treatment is able to restore the antiproliferative response to IFNα in resistant melanoma D10, which indicates a functional link of these signaling cascades (Foser and others 2006). Transfection experiments have confirmed that S100A2 expression is necessary and sufficient for

this response(Foser and others 2006). Here we demonstrate that S100A2 is mandatory for cyclical IFNα-mediated hypomethylation of the IFITM3 core promoter in ME15 cells, leading to increased protein expression. The cytosolic localization of S100A2 rules out a direct function of this protein in the nucleus (data not shown). We propose that the antiproliferative activity of IFNα and the growth inhibitory activity of S100A2 induce apoptotic conditions, which can lead to activation of the tumor suppressor gene p53. Takaoka et al. have shown that IFNα/β induces expression of p53 under adverse growth conditions and cell cycle arrest (Takaoka and others 2003), which occurs in ME15 cells after treatment with TGFβ and IFNα (Foser and others 2006). S100A2 is a well documented target gene of p53 (Lapi and others 2006; Mueller and others 2005; Tan and others 1999).

In figure 4 we show that established inducers of p53 signaling like DAC or 5-fluorouracil are able to activate a transfected p53 reporter construct in ME15 cells, whilst D10 cells do not respond, suggesting a defect in the p53 signaling cascade. Thus, the enhanced antiproliferative activity induced by co-stimulation with IFNα and TGFβ may trigger further upregulation of growth control genes, perhaps by modifying the methylation status of key residues in the target gene promoters as shown here for IFITM3.

Mechanisms of dynamic, inducible CpG methylation have been shown previously. The trefoil factor 1 (TFF1) is a protein that is known to be under estrogen control and its promoter undergoes cyclical demethylation upon estrogen stimulation by recruitment of the *de novo* DNA methyltransferase 3a and 3b (DNMT3a and DNMT3b), thymine DNA glycosylase (TDG) and base excision repair (BER) proteins in a cell cycle independant manner (Metivier and others 2008) (Kangaspeska and others 2008). The promoter of the inflammatory cytokine IL2 undergoes

demethylation upon stimulation with PMA (phorbol 12-myristate 13-acetate) (Murayama and others 2006). The mechanism in this case involves intracellular calcium release, which results in translocation of the T-cell transcription factor NFAT from the cytoplasm to the nucleus and binding to the IL2 core promoter where a single CpG site of the promoter is hypomethylated. This leads to transition of the "naive state" to the "active state" and facilitates transcription by OCT1 1 hour after PMA stimulation. The similar "naive state" of the IFITM3 core promoter is shown in figure 3A. In contrast to IL2, the IFITM3 promoter in this methylation state is fully responsive to IFNα signaling in ME15 cells but IFNα alone does not alter the methylation pattern in a 24 h time course experiment. However, expression of S100A2 triggers time-dependant hypomethylation of the IFITM3 promoter at key residues, which enhances the IFNα response 6 hours after IFNα stimulation and sets the promoter in a "hyperactive" state with enhanced response and expression of IFITM3. After 24 hours the promoter methylation is reset to the naive state. To our knowledge reversible and cytokine inducible promoter activation through a DNA methylation based mechanism has not been shown before.

The observation of S100A2-mediated, IFNα-inducible hypomethylation of the IFITM3 core promoter raises the question of the mechanism by which this occurs. Passive hypomethylation occurs during DNA replication where daughter strand methylation is inhibited and therefore absent or partial. The methylation patterns shown in figure 3 were compiled from individual Sanger-sequencing reads of subcloned core promoter amplicons and complete demethylation of all CpG target sites is rare, which is in agreement with a passive mechanism (data not shown). So far, only a few reports provide evidence for active demethylation in mammals and the results presented favour a passive mechanism (Metivier and others 2008; Morgan

and others 2005). It is interesting to note that evidence is arising that DNA repair enzymes as well as glycosylases might function as active demethylating agents in mammals, as suggested for the GADD45 protein, which is induced in our experimental system following IFNα and TGFβ stimulation (Foser and others 2006; Ma and others 2009a; Rai and others 2008; Schmitz and others 2009). Regardless of the mechanism that leads to changes in the methylation status of the IFITM3 promoter after stimulation, it remains entirely unclear how the activated status of the promoter is reset to the naive state after 24 hours and how this might be related to a decay of IFNα signaling.

Our laboratory has previously shown that IFNα treatment leads to a significant intracellular calcium release which is required for the antiproliferative activity of S100A2 (Foser and others 2006). In neuronal cells it has been shown that GADD45β promotes calcium sensitive demethylation of specific genes like BDNF or FGF (Ma and others 2009b). GADD45β is a p53 target gene (Kastan and others 1992) which is expressed upon growth arrest through promoter hypomethylation (Qiu and others 2004). Thus, it is reasonable to propose that IFNα-induced calcium release is required to activate GADD45β in our experimental system after cytokine stimulation. The cytoplasmic localization of S100A2 eliminates a direct function of S100A2 in the nucleus and we propose that the antiproliferative state of the cells induced by activated S100A2 and IFNα treatment triggers demethylation of selected target genes, which would augment the response to IFNα. The IFITM3 core promoter of D10 cells shows a significantly higher degree of demethylation compared to ME15 cells in the naive and active states, which leads to constitutive expression.

Interestingly, we failed to demonstrate p53 activity in D10 cells (Fig. 4) and this result points to a role of p53 signaling in dynamic, cytokine-induced promoter methylation.

In our cell-based model, expression of the IFNα-inducible antiproliferative IFITM3 protein is enhanced in the presence of S100A2 and the concomitant hypomethylation of the IFITM3 core promoter exhibits reversibility to the naive methylation state 24 hours after IFNα stimulus. Resistance to IFNα in renal carcinoma as well as melanoma cells can be overcome either by DAC treatment or DNA methyltransferase (DNMT1) depletion by transfection of antisense oligonucleotides (Reu and others 2006) and IFNα-resistant HCV replicant-harboring cells become sensitive to IFNα upon treatment with DAC (Naka and others 2006). Thus, modification of IFNα target gene expression through promoter methylation might be a natural mechanism to adapt the responses to pathogen challenge.

In conclusion, dynamic promoter methylation adds an additional layer of complexity to the IFNα signaling pathways and tight control of IFNα key response genes like IFITM3 might be required for comprehensive control of the IFNα response.

Acknowledgements

We are especially grateful to Dr. M. Browner and Dr. L. Burleigh for critical reading and editing of the manuscript prior to submission. Thanks go to all members of the Certa laboratory for support and stimulating discussions.

Author Disclosure Statement

No competing financial interests exist.

Literature

Berridge MJ, Lipp P, Bootman MD. 2000. The versatility and universality of calcium signalling. Nat Rev Mol Cell Biol 1(1):11-21.

Brem R, Oraszlan-Szovik K, Foser S, Bohrmann B, Certa U. 2003. Inhibition of proliferation by 1-8U in interferon-alpha-responsive and non-responsive cell lines. Cell Mol Life Sci 60(6):1235-48.

Certa U, Wilhelm-Seiler M, Foser S, Broger C, Neeb M. 2003. Expression modes of interferon-alpha inducible genes in sensitive and resistant human melanoma cells stimulated with regular and pegylated interferon-alpha. Gene 315:79-86.

Chen WG, Chang Q, Lin Y, Meissner A, West AE, Griffith EC, Jaenisch R, Greenberg ME. 2003. Derepression of BDNF transcription involves calcium-dependent phosphorylation of MeCP2. Science 302(5646):885-9.

Donato R. 2001. S100: a multigenic family of calcium-modulated proteins of the EF-hand type with intracellular and extracellular functional roles. Int J Biochem Cell Biol 33(7):637-68.

Eckert RL, Broome AM, Ruse M, Robinson N, Ryan D, Lee K. 2004. S100 proteins in the epidermis. J Invest Dermatol 123(1):23-33.

Foser S, Redwanz I, Ebeling M, Heizmann CW, Certa U. 2006. Interferon-alpha and transforming growth factor-beta co-induce growth inhibition of human tumor cells. Cell Mol Life Sci 63(19-20):2387-96.

Fridman AL, Rosati R, Li Q, Tainsky MA. 2007. Epigenetic and functional analysis of IGFBP3 and IGFBPrP1 in cellular immortalization. Biochem Biophys Res Commun 357(3):785-91.

Frommer M, McDonald LE, Millar DS, Collis CM, Watt F, Grigg GW, Molloy PL, Paul CL. 1992. A genomic sequencing protocol that yields a positive display of 5-methylcytosine residues in individual DNA strands. Proc Natl Acad Sci U S A 89(5):1827-31.

Gale M, Jr., Foy EM. 2005. Evasion of intracellular host defence by hepatitis C virus. Nature 436(7053):939-45.

Isaacs A, Lindenmann J. 1957. Virus interference. I. The interferon. Proc R Soc Lond B Biol Sci 147(927):258-67.

Kangaspeska S, Stride B, Metivier R, Polycarpou-Schwarz M, Ibberson D, Carmouche RP, Benes V, Gannon F, Reid G. 2008. Transient cyclical methylation of promoter DNA. Nature 452(7183):112-5.

Kastan MB, Zhan Q, el-Deiry WS, Carrier F, Jacks T, Walsh WV, Plunkett BS, Vogelstein B, Fornace AJ, Jr. 1992. A mammalian cell cycle checkpoint pathway utilizing p53 and GADD45 is defective in ataxia-telangiectasia. Cell 71(4):587-97.

Kulaeva OI, Draghici S, Tang L, Kraniak JM, Land SJ, Tainsky MA. 2003. Epigenetic silencing of multiple interferon pathway genes after cellular immortalization. Oncogene 22(26):4118-27.

Lapi E, Iovino A, Fontemaggi G, Soliera AR, Iacovelli S, Sacchi A, Rechavi G, Givol D, Blandino G, Strano S. 2006. S100A2 gene is a direct transcriptional target of p53 homologues during keratinocyte differentiation. Oncogene 25(26):3628-37.

Lee SW, Tomasetto C, Swisshelm K, Keyomarsi K, Sager R. 1992. Down-regulation of a member of the S100 gene family in mammary carcinoma cells and

reexpression by azadeoxycytidine treatment. Proc Natl Acad Sci U S A 89(6):2504-8.

Liu H, Kang H, Liu R, Chen X, Zhao K. 2002. Maximal induction of a subset of interferon target genes requires the chromatin-remodeling activity of the BAF complex. Mol Cell Biol 22(18):6471-9.

Luscher U, Filgueira L, Juretic A, Zuber M, Luscher NJ, Heberer M, Spagnoli GC. 1994. The pattern of cytokine gene expression in freshly excised human metastatic melanoma suggests a state of reversible anergy of tumor-infiltrating lymphocytes. Int J Cancer 57(4):612-9.

Ma DK, Guo JU, Ming GL, Song H. 2009a. DNA excision repair proteins and Gadd45 as molecular players for active DNA demethylation. Cell Cycle 8(10):1526-31.

Ma DK, Jang MH, Guo JU, Kitabatake Y, Chang ML, Pow-Anpongkul N, Flavell RA, Lu B, Ming GL, Song H. 2009b. Neuronal activity-induced Gadd45b promotes epigenetic DNA demethylation and adult neurogenesis. Science 323(5917):1074-7.

Maeda S, McCandliss R, Gross M, Sloma A, Familletti PC, Tabor JM, Evinger M, Levy WP, Pestka S. 1980. Construction and identification of bacterial plasmids containing nucleotide sequence for human leukocyte interferon. Proc Natl Acad Sci U S A 77(12):7010-3.

Maelandsmo GM, Florenes VA, Mellingsaeter T, Hovig E, Kerbel RS, Fodstad O. 1997. Differential expression patterns of S100A2, S100A4 and S100A6 during progression of human malignant melanoma. Int J Cancer 74(4):464-9.

Mandinova A, Atar D, Schafer BW, Spiess M, Aebi U, Heizmann CW. 1998. Distinct subcellular localization of calcium binding S100 proteins in human smooth

muscle cells and their relocation in response to rises in intracellular calcium. J Cell Sci 111 (Pt 14):2043-54.

Mbow ML, Sarisky RT. 2004. What is disrupting IFN-alpha's antiviral activity? Trends Biotechnol 22(8):395-9.

Metivier R, Gallais R, Tiffoche C, Le Peron C, Jurkowska RZ, Carmouche RP, Ibberson D, Barath P, Demay F, Reid G and others. 2008. Cyclical DNA methylation of a transcriptionally active promoter. Nature 452(7183):45-50.

Mischke D, Korge BP, Marenholz I, Volz A, Ziegler A. 1996. Genes encoding structural proteins of epidermal cornification and S100 calcium-binding proteins form a gene complex ("epidermal differentiation complex") on human chromosome 1q21. J Invest Dermatol 106(5):989-92.

Morgan HD, Santos F, Green K, Dean W, Reik W. 2005. Epigenetic reprogramming in mammals. Hum Mol Genet 14 Spec No 1:R47-58.

Mueller A, Schafer BW, Ferrari S, Weibel M, Makek M, Hochli M, Heizmann CW. 2005. The calcium-binding protein S100A2 interacts with p53 and modulates its transcriptional activity. J Biol Chem 280(32):29186-93.

Murayama A, Sakura K, Nakama M, Yasuzawa-Tanaka K, Fujita E, Tateishi Y, Wang Y, Ushijima T, Baba T, Shibuya K and others. 2006. A specific CpG site demethylation in the human interleukin 2 gene promoter is an epigenetic memory. Embo J 25(5):1081-92.

Naka K, Abe K, Takemoto K, Dansako H, Ikeda M, Shimotohno K, Kato N. 2006. Epigenetic silencing of interferon-inducible genes is implicated in interferon resistance of hepatitis C virus replicon-harboring cells. J Hepatol 44(5):869-78.

Pansky A, Hildebrand P, Fasler-Kan E, Baselgia L, Ketterer S, Beglinger C, Heim MH. 2000. Defective Jak-STAT signal transduction pathway in melanoma cells resistant to growth inhibition by interferon-alpha. Int J Cancer 85(5):720-5.

Pedrocchi M, Schafer BW, Mueller H, Eppenberger U, Heizmann CW. 1994. Expression of Ca(2+)-binding proteins of the S100 family in malignant human breast-cancer cell lines and biopsy samples. Int J Cancer 57(5):684-90.

Qiu W, Zhou B, Zou H, Liu X, Chu PG, Lopez R, Shih J, Chung C, Yen Y. 2004. Hypermethylation of growth arrest DNA damage-inducible gene 45 beta promoter in human hepatocellular carcinoma. Am J Pathol 165(5):1689-99.

Rai K, Huggins IJ, James SR, Karpf AR, Jones DA, Cairns BR. 2008. DNA demethylation in zebrafish involves the coupling of a deaminase, a glycosylase, and gadd45. Cell 135(7):1201-12.

Rehman I, Cross SS, Catto JW, Leiblich A, Mukherjee A, Azzouzi AR, Leung HY, Hamdy FC. 2005. Promoter hyper-methylation of calcium binding proteins S100A6 and S100A2 in human prostate cancer. Prostate 65(4):322-30.

Reid LM, Minato N, Gresser I, Holland J, Kadish A, Bloom BR. 1981. Influence of anti-mouse interferon serum on the growth and metastasis of tumor cells persistently infected with virus and of human prostatic tumors in athymic nude mice. Proc Natl Acad Sci U S A 78(2):1171-5.

Reu FJ, Bae SI, Cherkassky L, Leaman DW, Lindner D, Beaulieu N, MacLeod AR, Borden EC. 2006. Overcoming resistance to interferon-induced apoptosis of renal carcinoma and melanoma cells by DNA demethylation. J Clin Oncol 24(23):3771-9.

Rubinstein M, Rubinstein S, Familletti PC, Gross MS, Miller RS, Waldman AA, Pestka S. 1978. Human leukocyte interferon purified to homogeneity. Science 202(4374):1289-90.

Schafer BW, Heizmann CW. 1996. The S100 family of EF-hand calcium-binding proteins: functions and pathology. Trends Biochem Sci 21(4):134-40.

Schmitz KM, Schmitt N, Hoffmann-Rohrer U, Schafer A, Grummt I, Mayer C. 2009. TAF12 recruits Gadd45a and the nucleotide excision repair complex to the promoter of rRNA genes leading to active DNA demethylation. Mol Cell 33(3):344-53.

Stark GR, Kerr IM, Williams BR, Silverman RH, Schreiber RD. 1998. How cells respond to interferons. Annu Rev Biochem 67:227-64.

Takaoka A, Hayakawa S, Yanai H, Stoiber D, Negishi H, Kikuchi H, Sasaki S, Imai K, Shibue T, Honda K and others. 2003. Integration of interferon-alpha/beta signalling to p53 responses in tumour suppression and antiviral defence. Nature 424(6948):516-23.

Tan M, Heizmann CW, Guan K, Schafer BW, Sun Y. 1999. Transcriptional activation of the human S100A2 promoter by wild-type p53. FEBS Lett 445(2-3):265-8.

Wicki R, Franz C, Scholl FA, Heizmann CW, Schafer BW. 1997. Repression of the candidate tumor suppressor gene S100A2 in breast cancer is mediated by site-specific hypermethylation. Cell Calcium 22(4):243-54.

Wilson EB. 1927. Probable inference, the law of succession, and statistical inference. J. Am. Stat. Assoc. 22:209-212.

Zimmer DB, Wright Sadosky P, Weber DJ. 2003. Molecular mechanisms of S100-target protein interactions. Microsc Res Tech 60(6):552-9.

Figure legends

FIG. 1. S100A2 modulates expression efficiency of IFNα-inducible genes.

S100A2 modulates the transcription of selected IFNα target genes (*A*). ME15 and ME15 recombinant S100A2 ($ME15^{S100A2}$) cell cultures were treated with $IFN\alpha^{K134}$, TGFβ or both cytokines for two days followed by RNA extraction and processing of the samples for microarray analysis and data processing. Downregulated genes are shown in blue and induced genes in red and maximum color intensity corresponds to a 2- fold change (CHF). IFNα-inducible genes with a common S100A2-dependent expression mode after IFNα induction in ME15 cells are boxed (cluster 2) and IFNα-inducible genes with no apparent S100A2 dependency appear in cluster 1.

Enhancement of IFITM3 expression in ME15 and $ME15^{S100A2}$ cells in the presence of S100A2 (*B* and *C*). ME15 and ME15 recombinant S100A2 ($ME15^{S100A2}$) cell cultures were treated with IFNα for two days followed by RNA extraction and processing of the samples for real time PCR analysis (*B*). For protein analysis, cell cultures were treated with IFNα for 8 hours and cell lysates were probed by immunoblotting with α–IFITM3 antibodies (*C*).

The apparent IFITM3 mRNA and protein levels are increased in cells expressing recombinant S100A2 relative to the parental cell line.

FIG. 2. DAC (5'-aza-2'-deoxycytidine) treatment enhances the induction efficiency of S100A2 and IFITM3. ME15 and $ME15^{S100A2}$ cell cultures were treated with cytokines for 24 and 51 hours as indicated in the presence (DAC +) or absence (DAC -) of DAC.

Detection of S100A2 protein in DAC treated ME15 and $ME15^{S100A2}$ cells by immunoblotting (*A*). Cell lysates were electroblotted for each condition and probed

with S100A2. Note that DAC enhanced, time dependent S100A2 expression is only evident in parental ME15 cells, whilst no significant changes occur in ME15^{S100A2}.
Impact of DAC treatment on the expression of IFITM3 in ME15 and ME15^{S100A2} cell lines treated for 6, 12, 24 or 51 hours using the cytokine treatment protocol as above (*B).* DAC treatment affects the IFITM3 levels in ME15 and ME15^{S100A2} cells and low-level expression occurs 51 hours after DAC treatment without IFNα stimulation in ME15 (highlighted by a white asterisk in the left data panel).
DAC increases the sensitivity of the IFITM3 promoter to IFNα stimulation (*C*). ME15 and ME15^{S100A2} cells were treated with 10U or 100U of IFNα for the times indicated. In both lines 10U of IFNα are sufficient for induction of IFITM3 in the presence of DAC for an extended period of 48 hours. Consistent with the experiments shown in (*B*), IFNα independent expression occurs 48 hours after DAC incubation in both lines.

FIG. 3. S100A2 expression is sufficient to modulate IFNα induced dynamic and reversible methylation of the IFITM3 core promoter. ME15 cells were cultured in the absence (*A*) or presence (*B*) of TGFβ for S100A2 induction. TGFβ treatment was not necessary for ME15^{S100A2} cells (*C*) and the IFNα resistant cell line D10 was included in this experiment as well (*D*). All cell lines were analyzed 0, 1, 6 and 24 hours after IFNα stimulus.
Total genomic DNA from each culture was isolated, bisulfite treated and the IFITM3 core promoter was amplified using a bisulfite converted DNA adapted PCR protocol (for details see materials and methods). The amplicons were subcloned and sequenced from both ends using vector born primers. The number of clones sequenced per time point and treatment conditions is indicated on the right to the

methylation status of individual CpG sites displayed as boxes. White filling indicates bisulfite conversion of individual CpG sites in at least nine out of ten clones (0-10% methylation). Grey indicates conversion of single CpG sites in two to eight per ten sequence reads(11-89% methylation) and black indicates conversion in one out of ten sequence reads (90-100% methylation). The nucleotide positions of the CpG sites upstream of the ATG start codon are indicated and the position of the ISRE consensus binding site is depicted.

FIG. 4. P53 is not functional in the IFNα resistant cell line D10. Cells transfected with a p53 luciferase reporter plasmid were treated with DMSO, DAC, 5-FU and LPS as positive control. Untreated cells were included as reference. In ME15 cells all p53 activators induce significant upregulation of luciferase activity. D10 cells do not respond to stimulation suggesting a p53 signaling defect.

Table 1. Change factors of genes in clusters 1 and 2 of figure 1A

DESCRIPTION	SYMBOL	CHGF ME15	CHGF ME15^{S100A2}
cluster 1			
beta-2-microglobulin	B2M	3.3	2.94
interferon-induced protein 35	IFI35	1.83	1.98
beta-2-microglobulin	B2M	2.93	2.51
beta-2-microglobulin	B2M	2.38	2.1
signal transducer and activator of transcription 1, 91kda	STAT1	3.72	3.07
signal transducer and activator of transcription 1, 91kda	STAT1	4.28	3.1
interferon-induced protein with tetratricopeptide repeats 1	IFIT1	11.78	6.35
signal transducer and activator of transcription 1, 91kda	STAT1	16.79	11.77
interferon-induced protein with tetratricopeptide repeats 1	IFIT1	8.59	5.27
ubiquitin-conjugating enzyme e2l 6	UBE2L6	7.78	4.42
lectin, galactoside-binding, soluble, 3 binding protein	LGALS3	1.4	1.71
major histocompatibility complex, class i, f	HLA-F	1.55	1.4
major histocompatibility complex, class i, f	HLA-F	2.96	2.57
major histocompatibility complex, class i, b	HLA-B	3.35	4.37
isg15 ubiquitin-like modifier	ISG15	14.84	14.17
interferon, alpha-inducible protein 6	IFI6	9.09	13.12
isg15 ubiquitin-like modifier	ISG15	18.43	22.7
cluster 2			
small proline-rich protein 2d	SPRR2D	0.5	1.37
dehydrogenase/reductase (sdr family) member 2	DHRS2	0.64	6.22
interferon-induced protein 44-like	IFI44L	5.89	8.86
interferon induced transmembrane protein 3 (1-8u)	IFITM3	1.6	6.52
interferon induced transmembrane protein 1 (9-27)	IFITM1	9.73	27.19
proteasome (prosome, macropain) subunit, beta type, 9	PSMB9	1.97	2.46
interferon induced transmembrane protein 1 (9-27)	IFITM1	3.62	19.79
interferon-induced protein 35	IFI35	1.43	2.69
interferon-stimulated transcription factor 3, gamma 48kda	IRF9	1.71	4.07
2`,5`-oligoadenylate synthetase 1, 40/46kda	OAS1	5.75	13.62
2`-5`-oligoadenylate synthetase 2, 69/71kda	OAS2	1.42	2.19
bone marrow stromal cell antigen 2	BST2	41.07	62.6
interferon, alpha-inducible protein 27	IFI27	65.94	111.36

Table 1. The calculated change factors for the interferon-induced genes in clusters 1 and 2 of figure 1A are shown together with the annotation and official gene symbol. Change factors (CHF) were calculated as described in material and methods (section 2.5). ME15 refers to native cells and ME15^{S100A2} are cells stably transfected with S100A2 cDNA.

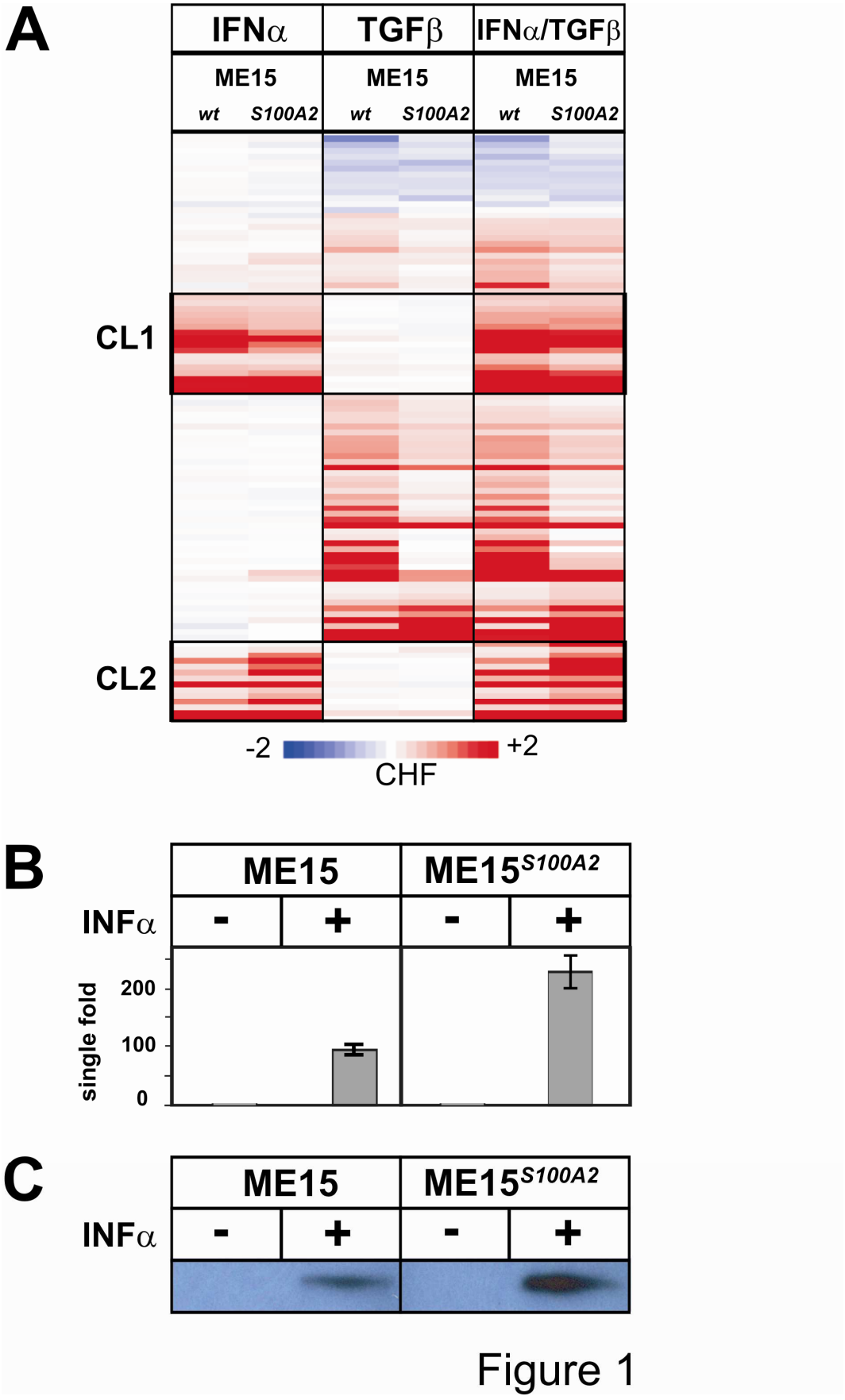
A
IFNα
TGFβ
IFNα/TGFβ
ME15
wt
S100A2
CL1
CL2
-2
+2
CHF
B
ME15
ME15S100A2
INFα
-
+
single fold
200
100
0
C
ME15
ME15S100A2
INFα
-
+

Figure 1

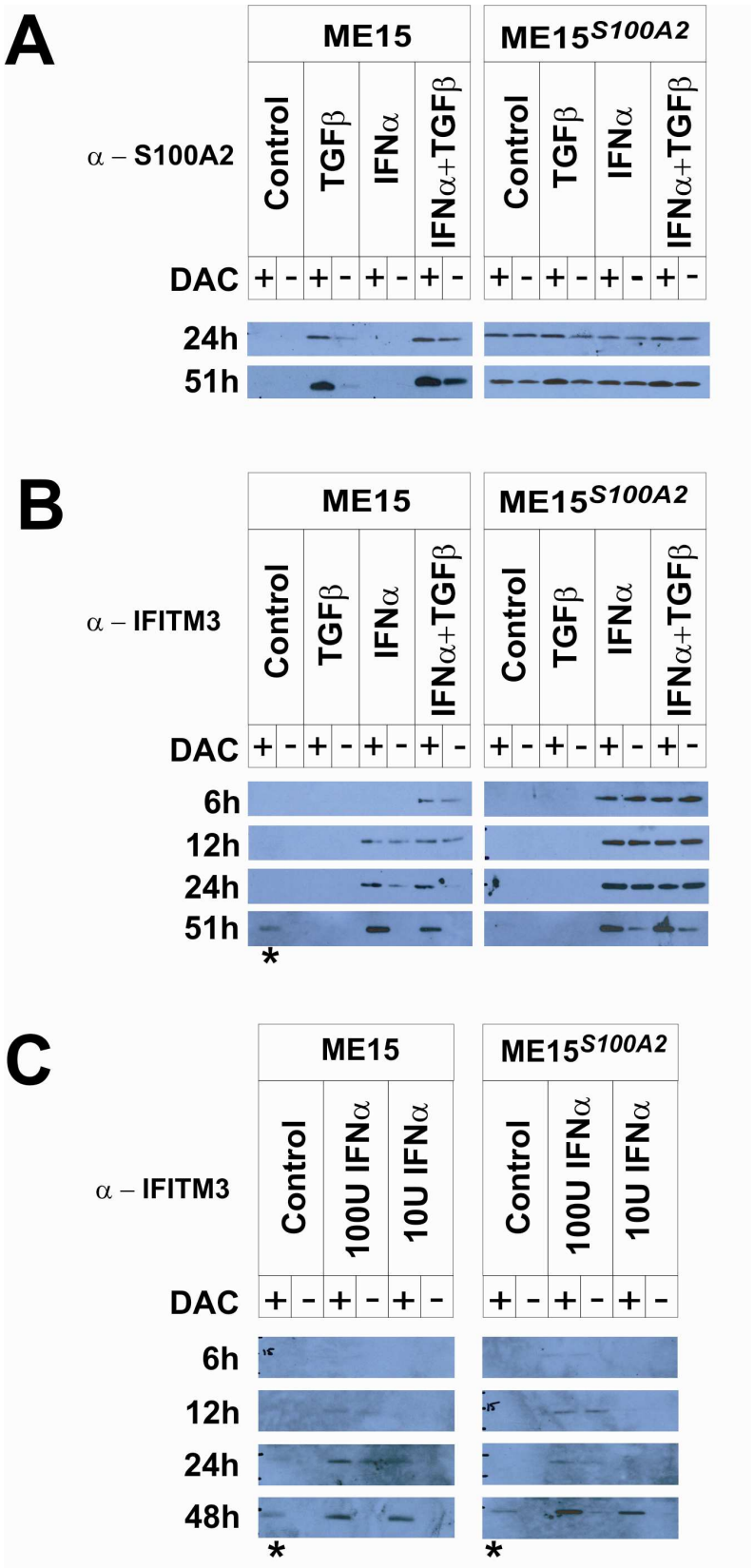
A
ME15
ME15S100A2
Control
TGFβ
IFNα
IFNα+TGFβ
α – S100A2
DAC
24h
51h
B
ME15
ME15S100A2
Control
TGFβ
IFNα
IFNα+TGFβ
α – IFITM3
DAC
6h
12h
24h
51h
*
C
ME15
ME15S100A2
Control
100U IFNα
10U IFNα
α – IFITM3
DAC
6h
12h
24h
48h
*
*

Figure 2

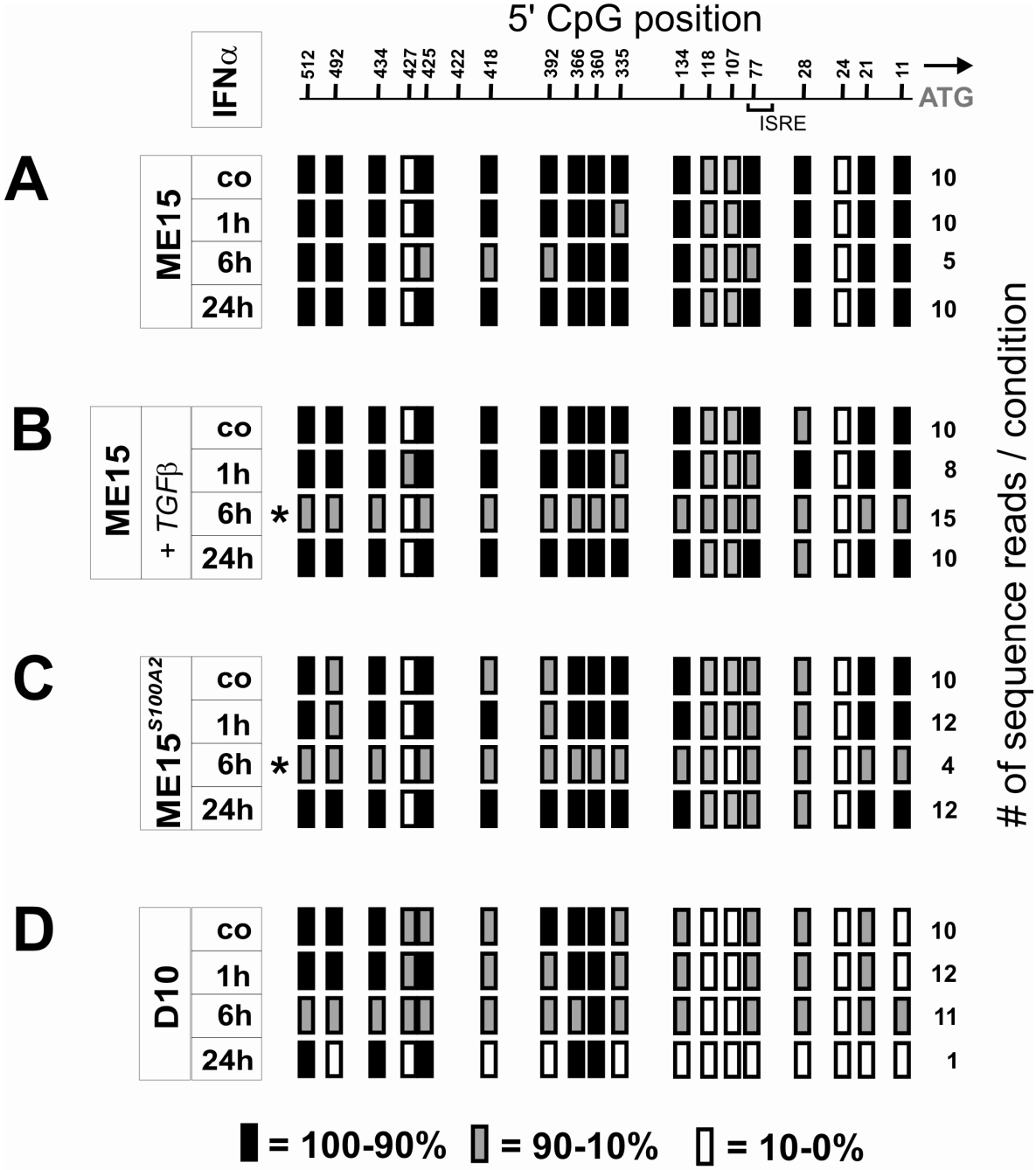
5' CpG position
IFNα
512
492
434
427
425
422
418
392
366
360
335
134
118
107
77
28
24
21
11
ATG
ISRE
A
ME15
co
1h
6h
24h
10
10
5
10
B
ME15
+ TGFβ
co
1h
6h
24h
*
10
8
15
10
C
ME15S100A2
co
1h
6h
24h
*
10
12
4
12
D
D10
co
1h
6h
24h
10
12
11
1
# of sequence reads / condition
= 100-90%
= 90-10%
= 10-0%

Figure 3

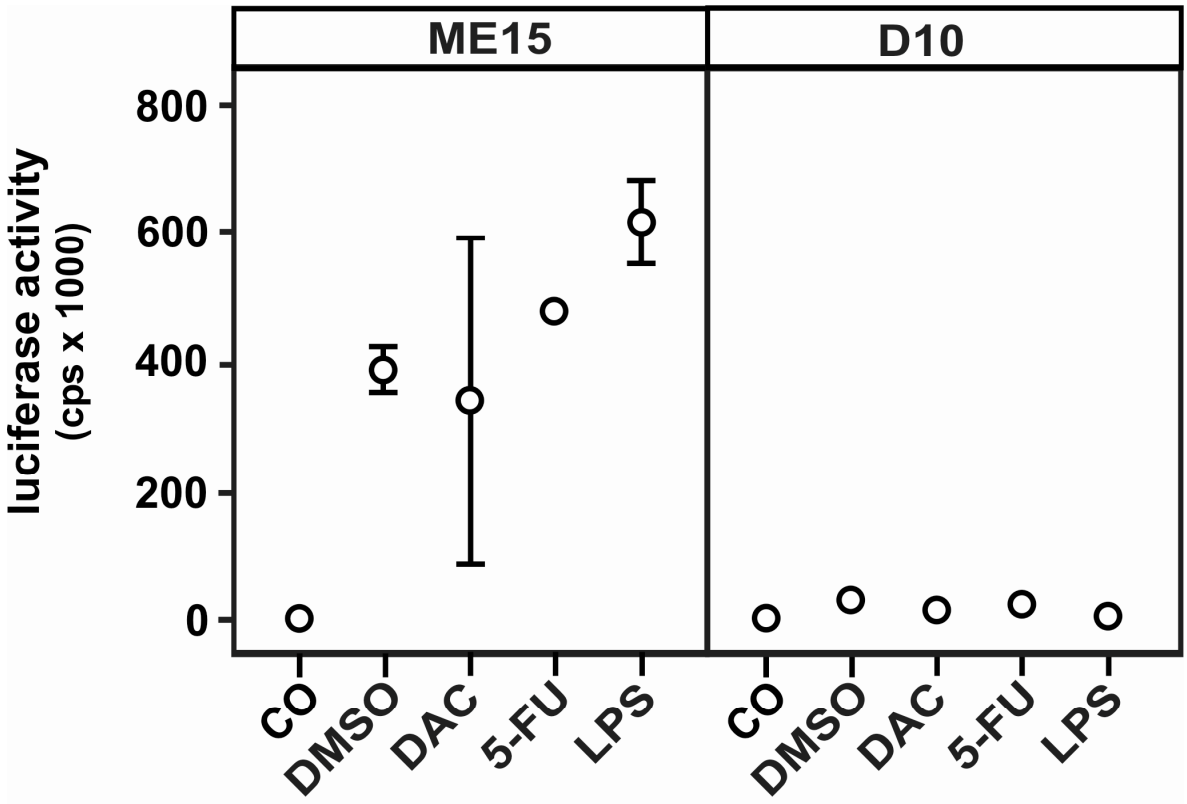
ME15
D10
luciferase activity
(cps x 1000)
800
600
400
200
0
CO
DMSO
DAC
5-FU
LPS
CO
DMSO
DAC
5-FU
LPS

Figure 4

10. CURRICULUM VITAE

Rachel Woodward Scott

For details on Rachel Woodward Scott's curriculum vitae please see hardcopies stored at the library of the University of Basel in Basel, Switzerland

---

Submitted Papers and Published Posters and Abstracts

R. Scott, F. Siegrist, S. Foser, U. Certa, Interferon-alpha promotes S100A2 dependant dynamic demethylation of the IFITM3 core promoter, submitted

R. Scott, F. Siegrist, Y. Burki, S. Foser, U. Certa, Methylation Status' Influence On Interferon-alpha Sensitivity In Human Melanoma Cells. 3rd Swiss Meeting on Genome Stability „DNA Dynamics and Epigenetics", October 3-5, 2007, Uetendorf, Switzerland.

R. Scott, H. L. Henry, M. Heim, J. E. Bishop**,** T. Pennimpede**, G.** Kampmann, W. Hunziker, P. Weber, A. W. Norman and I. Bendik. Comparison of intestinal gene expression of wild type and VDR KO-mice challenged with 1-α,25-Dihydroxy-Vitamin D3 and 24R,25-Dihydroxy-Vitamin D3. 12th Workshop on Vitamin D, July 6-10, 2003; Maastricht, The Netherlands.

M. Heim, T. Pennimpede, G. Kampmann, P. Fuchs, **R. Scott**, P. Weber, C. Riegger, W. Hunziker and I. Bendik. The estrogen receptor a pathway is the major route for genistein's bone promoting effects. 1st Joint Meeting of the International Bone and Mineral Society and the Japanese Society for Bone and Mineral Research, June 3-7, 2003; Osaka, Japan.

T. Pennimpede, S. Lorenzetti, M. Heim, G. Kampmann, **R. Scott**, P. Fuchs, F. Branca, P. Weber, W. Hunziker and I. Bendik. Human osteoclast estrogen receptor expression differs from that of osteoblasts. 30th European Symposium on Calcified Tissues, May 8-12, 2003; Rome, Italy.

S. Lorenzetti, T. Pennimpede, M. Heim, G. Kampmann, **R. Scott**, P. Fuchs, P. Weber, W. Hunziker, I. Bendik, and F. Branca. An ex-vivo human model of osteoclastogenesis to investigate the role of the phytoestrogen genistein. 30th European Symposium on Calcified Tissues, May 8-12, 2003; Rome, Italy.

T. Pennimpede, S. Lorenzetti, G. Kampmann, M. Heim, **R. Scott**, P. Fuchs, F. Branca, P. Weber, W. Hunziker and I. Bendik. Nuclear hormone receptor profiling in human osteoclasts. FASEB Journal, Volume 17, No. 4-5, p. Abstract No. 442.4, 2003. FASEB Meeting April 11 - April 15, 2003; San Diego, CA, USA.

S. Lorenzetti, T. Pennimpede, M. Heim, G. Kampmann, **R. Scott**, P. Fuchs, P. Weber, W. Hunziker, I. Bendik and F. Branca. The influence of the phytoestrogen genistein on osteoclast differentiation. FASEB Journal, Volume 17, No. 4-5, p. Abstract No. 442.3, 2003. FASEB Meeting April 11 - April 15, 2003; San Diego, CA, USA.